ORNL/TM-2022/2586
Revision 0

Radial Deconsolidation and Leach-Burn-Leach of AGR-3/4 Compacts 1-3, 4-3, 10-1, and 10-2

Grant W. Helmreich
John D. Hunn
Fred C. Montgomery
Darren J. Skitt

September 2022

Approved for public release.
Distribution is unlimited.

OAK RIDGE National Laboratory

ORNL IS MANAGED BY UT-BATTELLE LLC FOR THE US DEPARTMENT OF ENERGY

ORNL/TM-2022/2586

Nuclear Energy and Fuel Cycle Division

RADIAL DECONSOLIDATION AND LEACH-BURN-LEACH OF AGR/3/4 COMPACTS 1-3, 4-3, 10-1, AND 10-2

Grant W. Helmreich
John D. Hunn
Fred C. Montgomery
Darren J. Skitt

Revision 0

September 2022

Work sponsored by
US DEPARTMENT OF ENERGY
Office of Nuclear Energy—Advanced Reactor Technologies
under the
Advanced Gas Reactor Fuel Development and Qualification Program

Prepared by
OAK RIDGE NATIONAL LABORATORY
Oak Ridge, TN 37831
managed by
UT-BATTELLE LLC
for the
US DEPARTMENT OF ENERGY
under contract DE-AC05-00OR22725

CONTENTS

REVISION LOG

Revision	Date	Affected pages	Revision description
0		All	Initial issue

LIST OF FIGURES

LIST OF TABLES

ABBREVIATIONS

AGR	Advanced Gas Reactor (Fuel Development and Qualification Program)
AGR-1	first AGR program irradiation experiment
AGR-2	second AGR program irradiation experiment
AGR-3/4	third and fourth AGR program irradiation experiments
DLBL	deconsolidation and leach-burn-leach
DTF	designed-to-fail (fuel particle)
EOL	end of life
FACS	Fuel Accident Condition Simulator
FB-CVD	fluidized-bed chemical vapor deposition (coating system)
FIMA	fissions per initial metal atom
ID	identification
INL	Idaho National Laboratory
IMGA	Irradiated Microsphere Gamma Analyzer
LBL	leach-burn-leach
JMOCUP	Jim's MCNP-ORIGEN2 Coupled Utility Program
M/A	measured vs. average
M/C	measured vs. calculated
MCNP	Monte Carlo N-Particle Transport code
ORIGEN	Oak Ridge Isotope Generation and Depletion code
ORNL	Oak Ridge National Laboratory
PIE	post-irradiation examination
RS	randomly-selected (particles)
SD	standard deviation
SiC	silicon carbide (TRISO layer)
SP	special particle (abnormal particles typically identified with IMGA)
TA_{max}	time-average maximum (temperature)
TA_{min}	time-average minimum (temperature)
TAVA	time-average, volume-average (temperature)
TRISO	tristructural-isotropic (coated particles)
UCO	uranium carbide and uranium oxide (fuel kernels)

ACKNOWLEDGEMENTS

This work was sponsored by the US Department of Energy Office of Nuclear Energy Advanced Reactor Technologies as part of the Advanced Gas Reactor Fuel Development and Qualification Program. Thanks to the Irradiated Fuels Examination Laboratory Operations Group for overall support of hot cell operations and material transfers, and especially to Caleb Dryman who was the primary operator responsible for the complex in-cell manipulations required for the radial deconsolidation and leach-burn-leach (LBL) activities. Special thanks also go to the Radiological Materials Analytical Laboratory's chemists (Charles Watson for gamma spectrometry, Tamara Keever for mass spectrometry, Haley Wightman and Marc Chattin for sample preparation, radiochemistry, and ^{90}Sr analysis, and Wade Ivey for data review) and radiological technicians (Lisa Duncan and John Garan). The authors also want to acknowledge the invaluable support provided by our ORNL glassblowers Jason Craig and Carlos Rodrigues Flores who regularly craft the custom glassware used for LBL, as well as design and fabricate one-off solutions that have allowed us to overcome unexpected challenges and stay on schedule, such as a special deconsolidation tube that allowed us to complete the electrolytic deconsolidation of Compact 10-2 after the core segment detached from its carrier rod.

1. INTRODUCTION AND BACKGROUND*

The Advanced Gas Reactor (AGR) Fuel Development and Qualification Program's third and fourth irradiation experiments (AGR-3/4), originally planned as separate tests, were combined into one test train for irradiation in the Advanced Test Reactor at Idaho National Laboratory (INL). The irradiation test began on December 14, 2011 and ended on April 12, 2014 (Collin 2016). The originally planned AGR-3 and AGR-4 irradiation experiments were both focused on obtaining data on fission product transport to support modeling improvement. The AGR-3 experimental plan was focused on gaseous and metallic fission product release from the kernels and diffusion in the coatings during irradiation and post-irradiation safety testing. The AGR-4 experimental plan was focused on diffusivities and sorptivities in the compact matrix and reactor graphite (Petti et al. 2005). These two goals were combined in the AGR-3/4 irradiation, which consisted of twelve independently monitored capsules that each contained four AGR-3/4 compacts in a single stack surrounded by an inner ring of matrix or graphite and an outer ring of graphite. There were two capsule types: a standard capsule and a fuel body in which the outer graphite ring included a floor and cap that fully enclosed the fuel (Stempien et al. 2018a). The fuel body design supported post-irradiation safety testing of the intact fuel and ring assembly to provide data on fission product transport and release from matrix and graphite at accident temperatures (Demkowicz 2017).

The key feature of the AGR-3/4 compacts was the inclusion of 20 designed-to-fail (DTF) fuel particles distributed along the centerline of each compact. A summary of the AGR-3/4 irradiation test compact fabrication campaign has been published by Hunn et al. (2012). The DTF fuel particles and surrounding driver fuel particles were fabricated at Oak Ridge National Laboratory (ORNL) using a lab-scale fluidized-bed chemical vapor deposition (FB-CVD) coating system with a chamber inner diameter of 50 mm. Kernels came from a single composite (G73V-20-69303) manufactured by BWX Technologies, which was upgraded by manual sorting to remove debris and irregularly shaped kernels and was then renamed *LEU03*. The kernels contained both uranium carbide and uranium oxide phases (UCO) with an enrichment of 19.7%, and were similar to those used in the first AGR program irradiation experiment (AGR-1). Kernel diameter was nominally 350 μm, with a measured average value of 357.3 μm and a standard deviation of 1.6 μm (Kercher and Hunn 2006). The AGR-3/4 driver fuel particles were standard tristructural isotropic (TRISO)–coated particles similar to the TRISO particles used in the AGR-1 experiment (Lowden 2006). Four coater batches were upgraded and combined into one composite (LEU03-09T). The TRISO particle batches and composite were thoroughly characterized and found to pass all specifications (Hunn and Lowden 2007). The DTF particles were produced in a single batch (LEU03-07DTF) after an extensive development effort to ensure that the 20 μm pyrolytic carbon coating met the specified properties for a coating expected to fail during irradiation without failing prematurely during compact heat treatment up to 1800°C (Kercher et al. 2011). Overcoating and pressing of the AGR-3/4 DTF and driver fuel particles into the final cylindrical compact fuel form (nominally one half of an inch in both diameter and length) was accomplished using similar methods that were developed for the fabrication of compacts made for the second AGR program irradiation experiment (AGR-2), with the exception of new techniques for overcoating and distributing the DTF particles along the center line of the AGR-3/4 fuel compact. Overcoated DTF particles were imaged with x-ray radiography to verify that each overcoated particle contained exactly one DTF particle, and the overcoated particles were hand counted to ensure that each compact held exactly twenty DTF particles. Radiographs of 2.5 mm sections cut from the center of four AGR-3/4 compacts are shown in Figure 1-1, in which the compacts were sectioned so the radiography would show the DTF particles. The DTF particles were evenly distributed in the bottom three-quarters of the compact and within ~1.3 mm of the compact centerline. The partial collapse of the linear stack of overcoated DTF particles was likely a result of the overcoated DTF and surrounding driver fuel particles redistributing slightly after removal of the tube that was used to hold the overcoated DTF in position during addition of the overcoated driver fuel particles. Thorough characterization of AGR-3/4

* This introduction section is a revised version of a similar section in a previous AGR-3/4 PIE report (Hunn et al. 2020) and is included herein for contextual information and definition of common terminology used throughout this report.

fuel compact composite determined that it conformed to all specifications (Hunn, Trammell, and Montgomery 2011). In addition to 20 DTF particles, each AGR-3/4 compact held an average of 1,898 driver fuel particles based on a count of the particles deconsolidated from 18 randomly selected compacts.

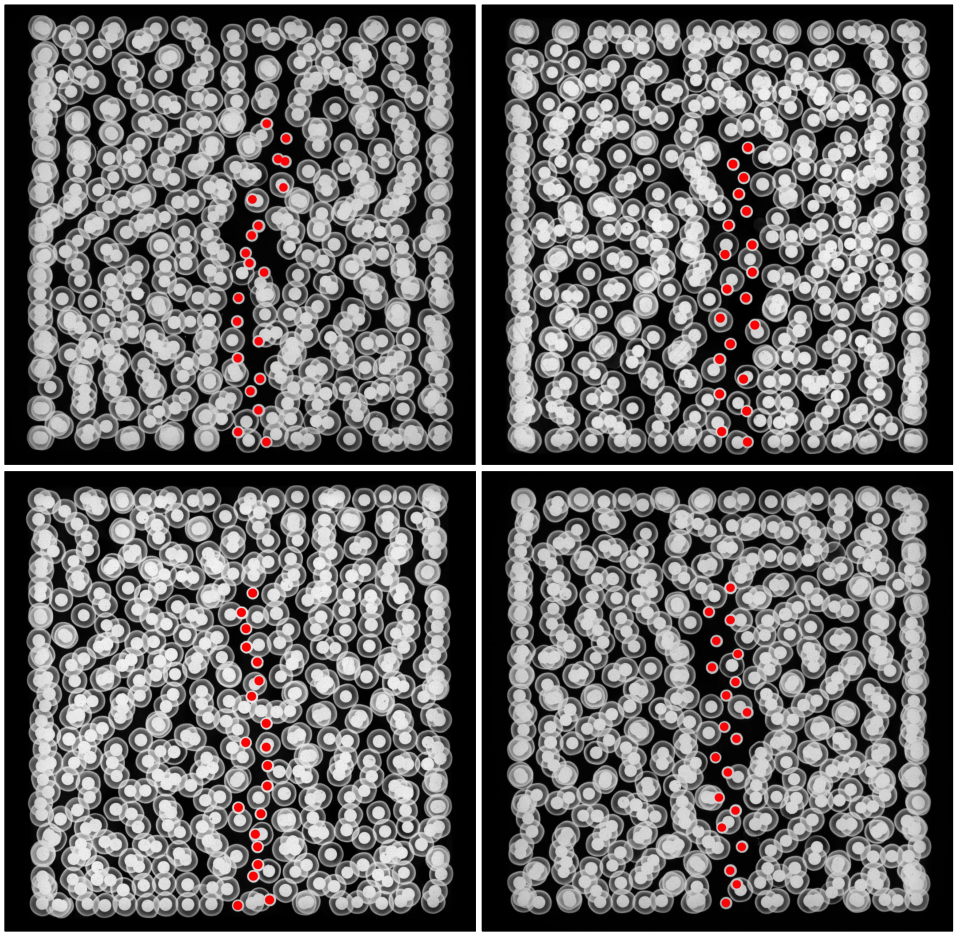

Figure 1-1. X-ray radiographs of 2.5 mm sections from four AGR-3/4 compacts, with DTF marked in red.

Ongoing post-irradiation examination (PIE) of the AGR-3/4 compacts includes radial deconsolidation of individual compacts to segment the compacts into separate collections of particles and matrix debris from concentric cylindrical volumes, each of which can be subjected to leach-burn-leach (LBL) analysis to quantify the presence of actinides and fission products released by the driver fuel and DTF particles. Typically, three cylindrical rings of driver fuel particles and matrix are removed, leaving a cylindrical core encompassing the DTF particles. The core section is then axially deconsolidated. Initial development and testing of the radial deconsolidation process were accomplished using unirradiated AGR-3/4 compacts (Helmreich, Montgomery, and Hunn 2015), and then the concept was modified for deconsolidation of irradiated AGR-3/4 compacts in the INL hot cells (Stempien 2017). Detailed information on the process and equipment can be obtained from the referenced reports.

Radial deconsolidation of irradiated AGR-3/4 compacts began at ORNL in 2020. Excess equipment from the development of the INL hot cell rig was shipped to ORNL and assembled for use at ORNL with minor modifications (Figure 1-2–Figure 1-4). Notably, a 20 mil shim (0.5 mm) was inserted between the sample holder and drive support bracket to reduce wobble of the compact and rod during rotation, and a slot was cut in the beaker opposite the spout, so the required level of the nitric acid was lower, which made it easier to pick up the beaker without spilling acid. Deconsolidation was performed using 6 mol/L nitric acid, and current was controlled at 0.8 A for the radial deconsolidation or 0.35 A for the axial deconsolidation (direct current voltage was typically around 5 V).

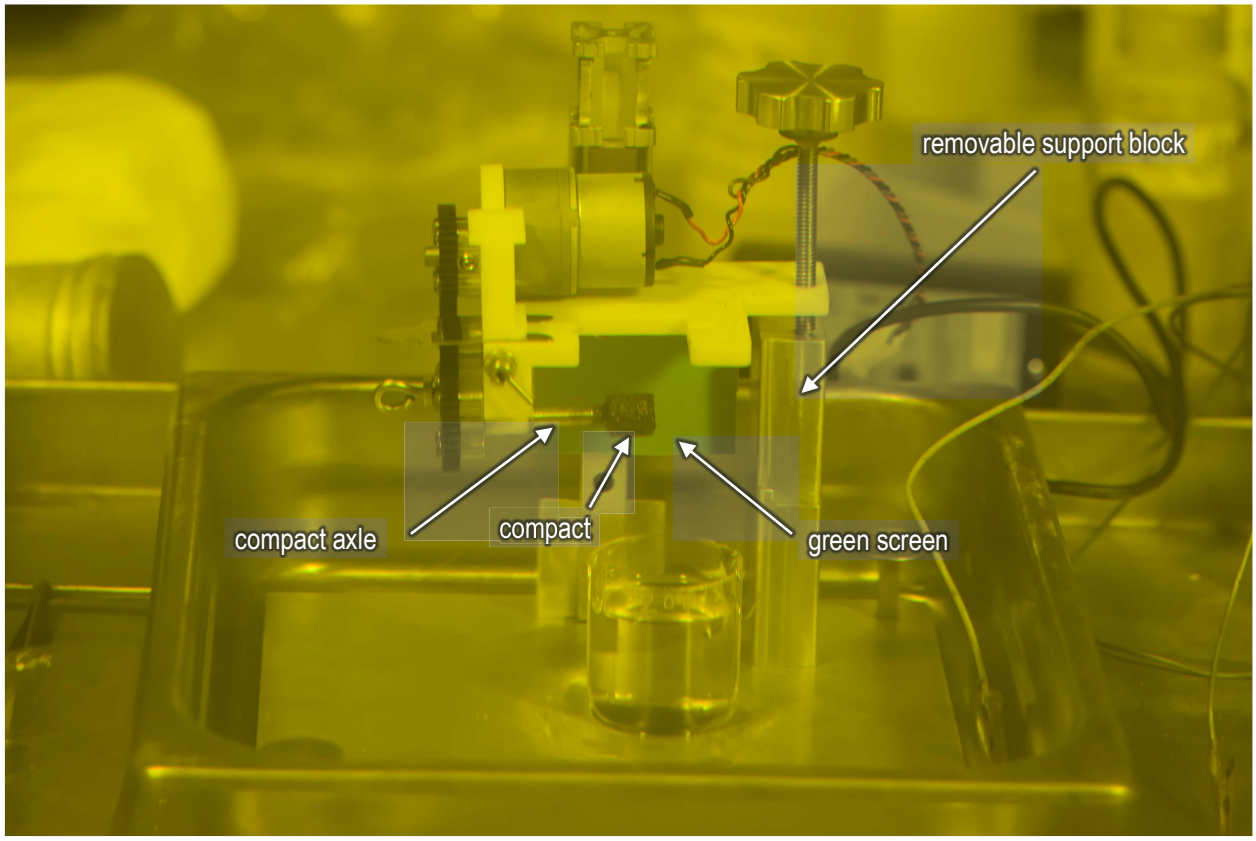

Figure 1-2. Radial deconsolidation rig in raised position for imaging and beaker exchange.

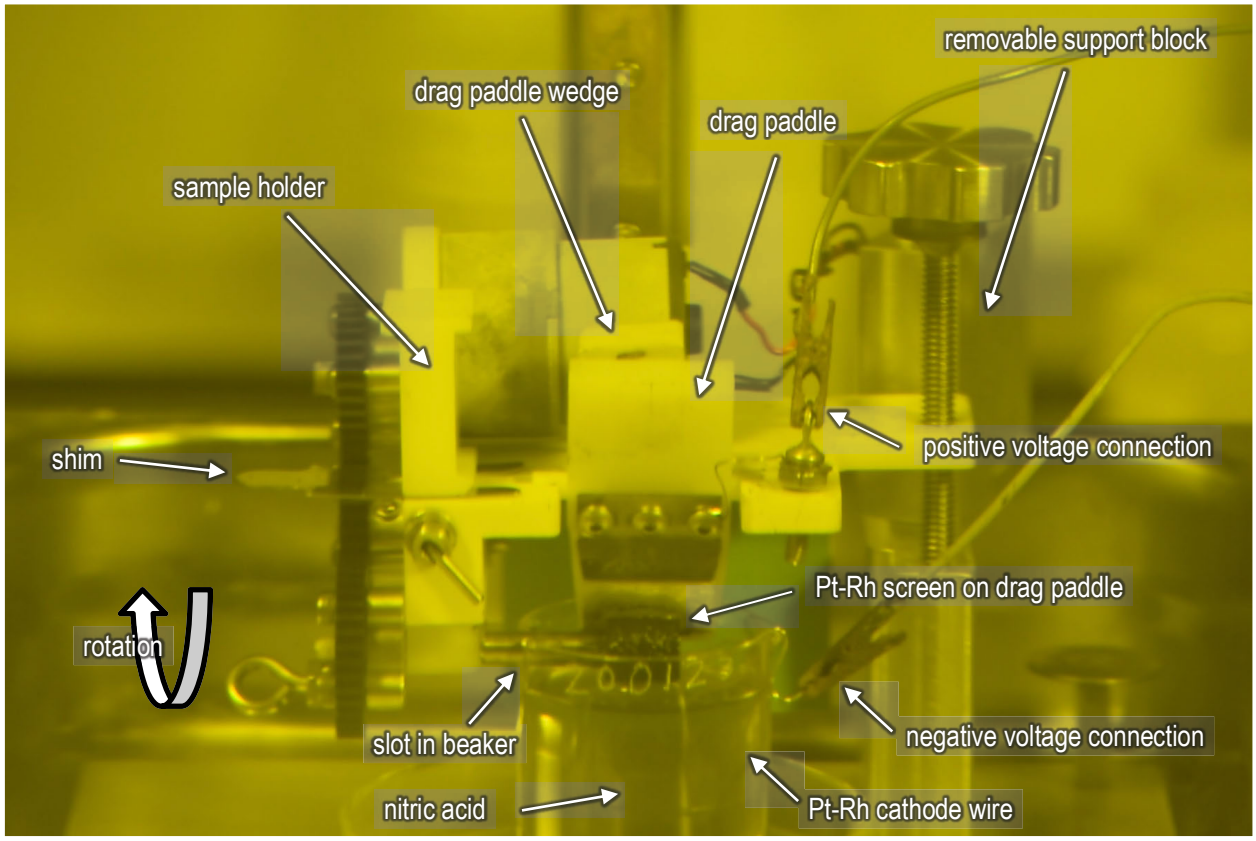

Figure 1-3. Radial deconsolidation in progress.

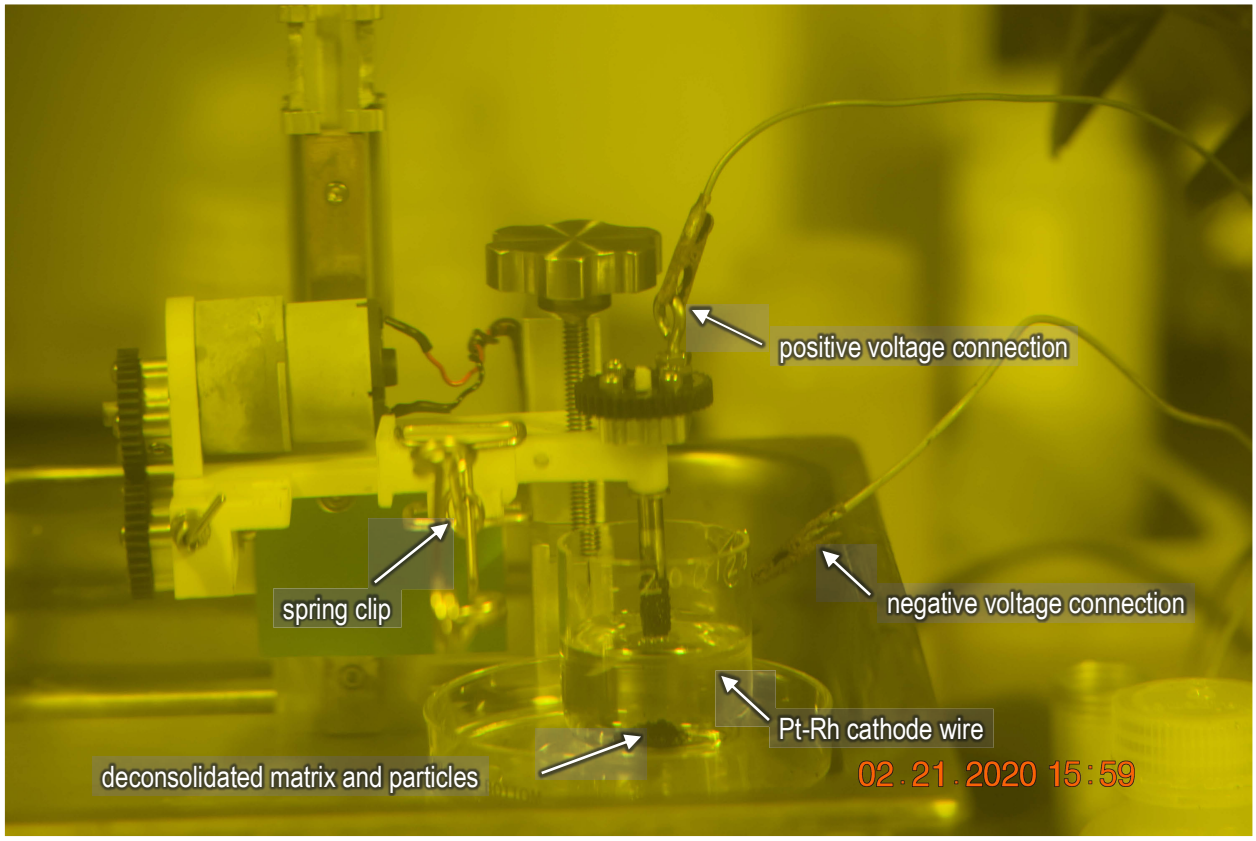

Figure 1-4. Axial deconsolidation in progress.

The AGR-3/4 compacts were irradiated to average calculated burnups of 4.85–15.27% fissions per initial metal atom (FIMA), and the average calculated fluences of fast neutrons with energies $E_n > 0.18$ MeV were $1.19–5.32\times10^{25}$ n/m^2 (Sterbentz 2015). The calculated time-average, volume-average (TAVA) compact temperatures ranged between 832°C–1376°C (Hawkes 2014). Table 1-1 shows the calculated irradiation conditions for the four compacts subjected to radial deconsolidation and LBL (DLBL) at ORNL and reported herein. Compact 1-3 experienced burnup and temperatures near the lower end of the ranges for compacts in the AGR-3/4. Compact 4-3 experienced burnup near the upper end of the range and temperature near the middle of the range. Compact 10-1 experienced burnup and temperature near the middle of the range. Compact 10-2 experienced burnup near the middle of the range and temperature near the upper end of the range. While Compact 1-3 was deconsolidated in the as-irradiated state, the other three compacts reported on herein were safety tested at temperatures between 1000°C–1400°C before radial deconsolidation, as listed in Table 1-1 (Stempien et al. 2018b, Stempien et al. 2021). Compact 4-3 and Compact 10-1 also experienced reirradiation (Stempien 2021, Stempien et al. 2021).

Table 1-1. Irradiation and safety test parameters for AGR-3/4 compacts analyzed in this study

Compact ID [a]	Fabrication ID number [b]	Safety test (°C)	Burnup [c] (% FIMA)	Fast fluence [c] (n/m^2)	Temperature [d] (°C)		
					TAVA	TA_{min}	TA_{max}
AGR-3/4 Compact 1-3	Z003	none	6.37	1.87×10^{25}	959	942	978
AGR-3/4 Compact 4-3	Z059	1000	14.29	4.89×10^{25}	1035	992	1084
AGR-3/4 Compact 10-1	Z133	1400	12.08	4.12×10^{25}	1172	1080	1238
AGR-3/4 Compact 10-2	Z134	1200	11.96	4.01×10^{25}	1213	1179	1249

[a] The compact identification (ID) denotes the compact's location in the irradiation test train: *capsule-level* (Collin 2015).
[b] Each compact in the fabrication lot (LEU03-10T-OP2/LEU03-07DTF-OP1)-Z had a unique compact ID number from 001–175, and physical properties data are available and referenced by compact ID number (Hunn, Trammell, and Montgomery 2011).
[c] Compact average burnups and fast neutron fluences ($E_n > 0.18$ MeV) are based on daily depletion calculations (Sterbentz 2015).
[d] Compact TAVA, time-average minimum (TA_{min}) and time-average maximum (TA_{max})temperatures are based on thermal calculations (Hawkes 2016).

2. RADIAL DECONSOLIDATION AND IMAGE ANALYSIS METHODS[†]

Each compact reported herein was radially deconsolidated in three stages to remove three cylindrical rings of driver fuel particles and matrix, leaving a cylindrical core encompassing the DTF particles, which was then axially deconsolidated. Four segments of equal volume were created for each compact, and radial deconsolidation was paused several times during each deconsolidation stage to obtain a photo, which was visually examined to evaluate progress toward the target diameter for the segment. At the end of each radial deconsolidation, the compact was raised to the imaging position (Figure 1-2), loose debris on the screen and compact were gently rinsed off into the deconsolidation beaker, the drag paddle was removed, and images of the compact were acquired to measure the residual diameter. At least 50 photos were acquired of the rotating compact. The number of photos was based on analysis of the distribution of rotations presented to the camera, in which a range of 40–50 images acquired at varying capture rates was determined to provide sufficient randomness in the compact orientation.

Example photos of one compact at each stage in the process are shown in Figure 2-1. Material removal for each compact was relatively uniform along the length and around the circumference of the compact with respect to the average driver fuel particles diameter of 0.819 mm (Hunn and Lowden 2007). The key to this uniform removal was the use of the Pt-Rh screen, which not only provided electrical contact for the electrolytic circuit, but also provided a gentle shear force that helped dislodge particles and matrix debris, as the matrix graphite was intercalated by the nitrate anions (Helmreich, Montgomery, and Hunn 2015). The nylon threaded rod shown in Figure 2-1 was inserted into the hollow axle tube as part of the mounting process. To bond the compact to the rod, conducting epoxy was packed into half of the axle, and the nylon threaded rod was inserted until it was in contact with the epoxy. A nylon nut on the rod prevented it from pressing on the epoxy. The axle was loaded into the hot cell, and the sample holder (axle, gear, and bracket) was assembled (Figure 1-3). The compact and axle were loaded into a mounting jig developed at INL to align the axle to the center of the compact (Stempien 2017). The axle was placed in contact with the compact to provide electrical connection during axial deconsolidation (Figure 1-4), and the nylon nut was backed off about one turn and pressed into the axle. This ejected an easily metered small volume of epoxy which squeezed through slots in the end of the axle and formed a small, tapered bead at the joining (Helmreich et al. 2015).

[†] This methods section is a revised version of a similar section in a previous AGR-3/4 PIE report (Hunn et al. 2020) and is included herein for contextual information and definition of common terminology used throughout this report.

The residual diameter of each compact after the radial deconsolidation of Segment 3 was close to the outer diameter of the stainless steel tube used as a drive axle for compact rotation. The axle diameter of 6 mm presented a practical limit to the outer diameter of the solid core segment. This diameter was more than sufficient to ensure that any residuals of the DTF particles that remained in their original location (<1.5 mm from the compact axis) were located within the core (Figure 1-1).

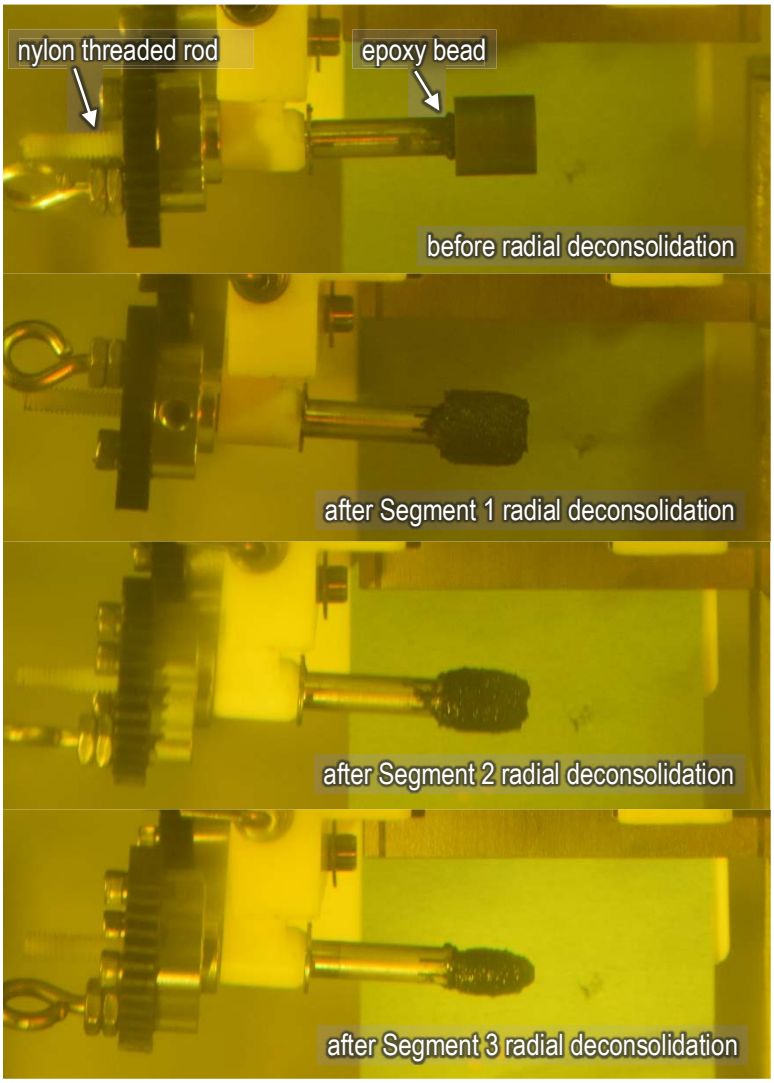

Figure 2-1. Compact 1-3 at each stage of radial deconsolidation.

Automated image analysis was accomplished using a custom MATLAB script designed to differentiate the boundary between the image of the compact and the green cardboard located behind the compact. The green cardboard provided a convenient monochromatic green screen background that could be digitally removed; however, insufficient lighting in the hot cell produced shadows that introduced some challenges to this aspect of the image analysis. The MATLAB script also included code to determine the axle boundary which could be used to apply a rotational correction to the image if the axle edges were not aligned to the image pixel array. This would also effectively square the compact edges to the image. This rotational correction could be applied to each image individually to account for wobble or precession of the rotating axle. As a result of careful camera alignment and the insertion of a shim to prevent wobble, only a minor variation between the axle and the horizontal image axis was observed in any of the photos or videos.

As shown in Figure 2-2, a steel calibration block was used to calibrate images of each compact. This calibration block was designed to sit close to the compact by sliding into the mounting bracket for the paddle (removed for measurement photographs). This position improved the quality and consistency of calibration by reducing the effects of camera tilt on the relative magnification of the compact and the calibration block and by ensuring that the face of the block was in the imaging plane of the compact if it were snugly pressed into the bracket. Both the inner and outer widths between the lines on the calibration block are known, so both were measured in the images, and the average of the two widths was used for calibration.

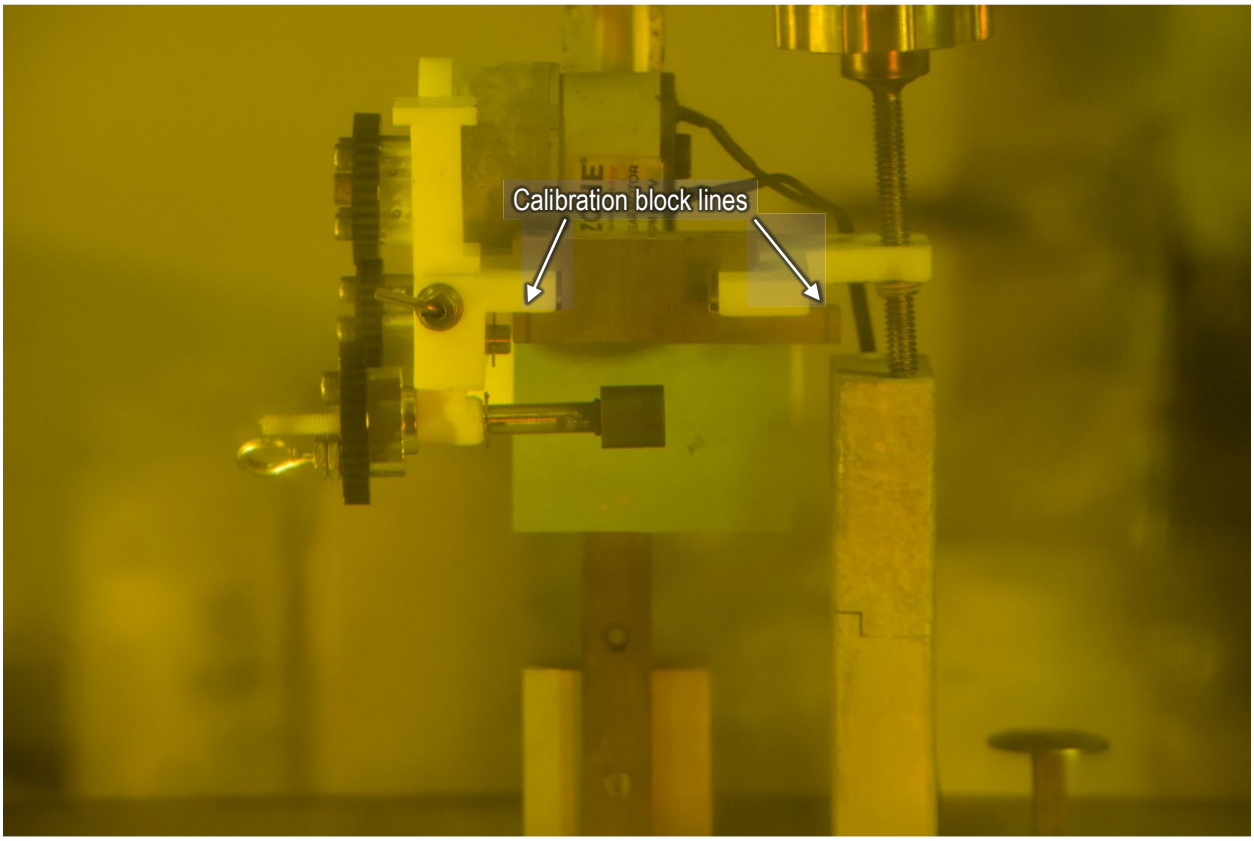

Figure 2-2. Compact 1-3 before radial deconsolidation with calibration block.

Figure 2-3 shows an example of the output images from the automated photo analyses for each stage of radial deconsolidation. The blue overlay shows what the image analysis identified as part of the compact. The left edge of the blue field is truncated based on a user-defined search area. The left side of the as-irradiated compact was intentionally omitted avoid problems caused by the shadow on the green screen. Analysis results were manually inspected, and flawed results were discarded.

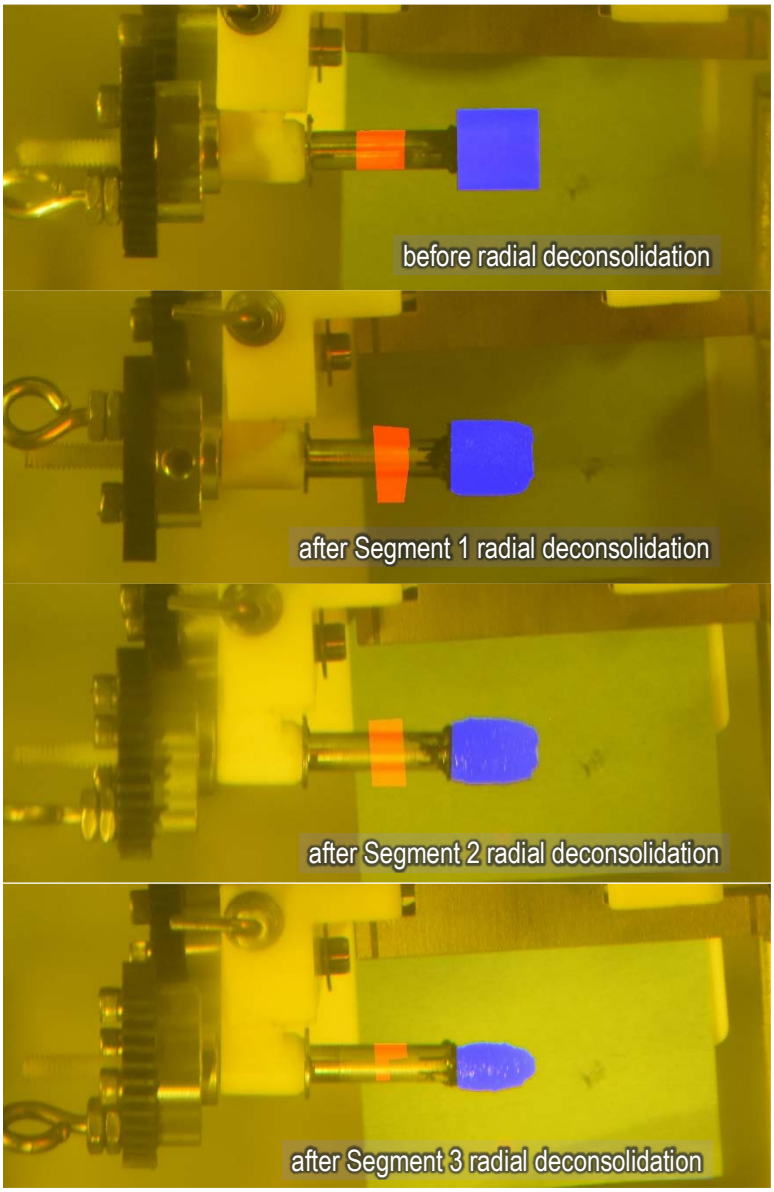

Figure 2-3. Examples of Compact 1-3 automated photo analysis at each stage of radial deconsolidation.

3. LBL METHODS‡

After radial deconsolidation, LBL and gamma scanning of individual particles were performed using the same methods that were developed for destructive PIE of as-irradiated AGR-1 compacts, and the details of the equipment and methods are reported in the literature (Hunn et al. 2013). Figure 3-1 is a flow diagram of the typical process for compact DLBL integrated with gamma survey of the particle inventory using the ORNL Irradiated Microsphere Gamma Analyzer (IMGA). Deconsolidation and leach solutions were analyzed by gamma and mass spectrometry, providing information about actinides and fission products that were not sealed inside retentive SiC layers. Results are expected to be dominated by actinides and fission products from the twenty DTF particles in each AGR-3/4 compact. However, actinides and fission products leached in the deconsolidation acid, preburn Soxhlet extractions of the particles and matrix, pot boil of the particles and matrix, and postburn pot leaches of the matrix may have

‡ This experimental methods section is a revised version of a similar section in a previous AGR-2 PIE report (Hunn et al. 2020) and is included herein for contextual information and definition of common terminology used throughout this report.

also come from (1) uranium outside the SiC in the as-fabricated compacts, (2) diffusion through the driver fuel SiC layers during irradiation or safety testing, and/or (3) exposed kernels in driver fuel particles with failed TRISO. In addition, actinides and fission products leached in the postburn Soxhlet extractions of the particles may have come from (1) exposed kernels in driver fuel particles with failed SiC and/or (2) diffusively released actinides and fission products that were not leached prior to the burn because they were previously sequestered in a pyrolytic carbon layer or in an insoluble chemical form.

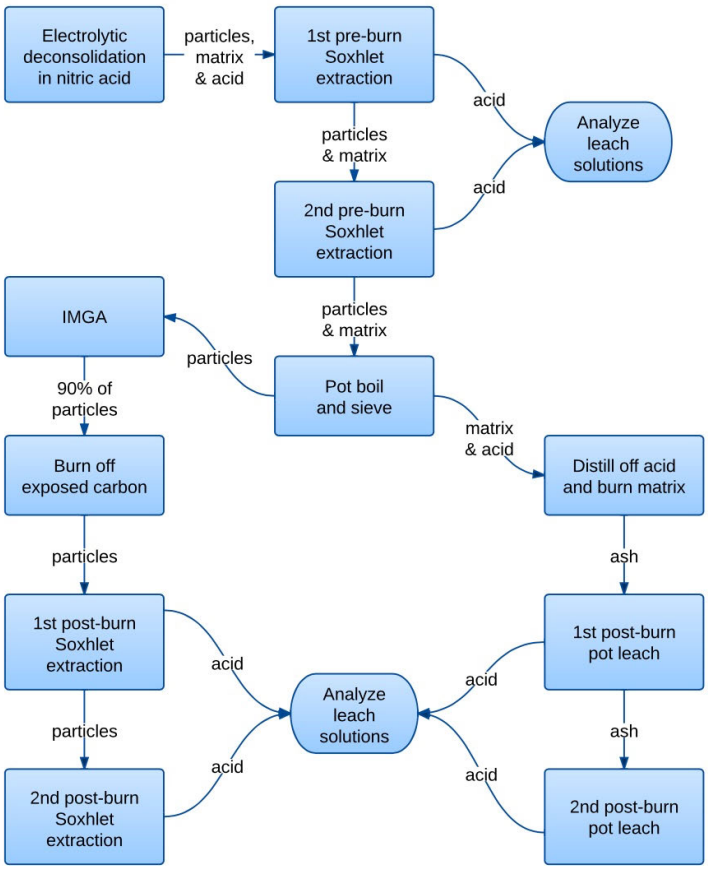

Figure 3-1. Process flow for DLBL and IMGA.

Actinide and fission product measurements were converted to fractions of the total compact inventory, or *compact fraction*, using the standard ORNL AGR PIE approach (Hunn et al. 2013), which involves dividing by the calculated inventory. The calculated total inventory of each nuclide was estimated using physics calculations (Sterbentz 2015) and reported at three specific times after the end of the irradiation, or the *end of life* (EOL): namely, one day after EOL, one year after EOL, and two years after EOL. Radionuclide quantities measured by gamma spectrometry (e.g., ^{106}Ru, ^{110m}Ag, ^{125}Sb, ^{134}Cs, ^{137}Cs, ^{144}Ce, ^{154}Eu, and ^{155}Eu), or chemical separation and beta spectrometry in the special case of ^{90}Sr, were decay-corrected to one day after EOL and divided by the calculated total inventory at that time to determine the compact fraction. For stable nuclides and actinides (e.g., ^{235}U, ^{236}U, ^{238}U, ^{239}Pu, and ^{240}Pu), the measured quantity was divided by the calculated total inventory at one year after EOL. This was done because radionuclide decay generated additional actinide and stable nuclides over the first year after the compacts were removed from the reactor, whereas any further increase in the calculated total inventories after one year was typically negligible. The mass spectrometry analysis was almost always performed after one year based on the time required for the test train to cool down and be disassembled. Results were also calculated and are often presented in terms of the equivalent particle inventory, or the number of *particle equivalents*, which is defined as the compact fraction multiplied by the average number of particles per compact: 1,918 for AGR-3/4 compacts (Hunn, Trammell, and Montgomery 2011).

4. AS-IRRADIATED AGR-3/4 COMPACT 1-3

4.1 RADIAL DECONSOLIDATION AND DIMENSIONAL ANALYSIS OF COMPACT 1-3

The segment plan to generate four segments of equal volume for Compact 1-3 is shown in Table 4-1, and the actual segment results based on image analysis of the compact are given in Table 4-2, along with the time that deconsolidation was active (power applied) for each radially deconsolidated segment.

Table 4-1. Equal volume segment plan for Compact 1-3

Quantity	Segment 1	Segment 2	Segment 3	Segment 4
Initial diameter (mm)	12.231	10.592	8.649	6.116
Target diameter (mm)	10.592	8.649	6.116	0
Segment thickness (mm)	0.820	0.972	1.267	solid
Segment volume (cm^3)	0.359	0.359	0.359	0.359

Note: The Average diameter of the irradiated compact was 12.231 mm with a standard deviation of 0.0093 mm, and the length from a single measurement was 12.395 mm (Stempien et al. 2016).

Table 4-2. Segment results for Compact 1-3 measured with automated photo analysis

Quantity	Segment 1	Segment 2	Segment 3	Segment 4
Initial diameter (mm)	12.231	11.305	9.377	7.357
Residual diameter (mm)	11.305	9.377	7.357	0
Segment thickness (mm)	0.463	0.964	1.010	solid
Segment volume (cm^3)	0.212	0.388	0.329	0.527
Deconsolidation time (min)	77	40	45	-

The radial deconsolidation of Compact 1-3 progressed smoothly until midway through Segment 3, when the epoxy bead at the junction of the mounting axle and the compact began to interfere with the paddle, breaking the electrical contact between the screen and compact. The deconsolidation process was paused while a special paddle with a cutout to one side was produced. Radial deconsolidation was then successfully resumed, with the new paddle with the cutout preventing contact between the epoxy bead and the paddle.

4.2 DLBL OF COMPACT 1-3

After radial deconsolidation of each segment was complete, the particles, matrix debris, and acid were transferred to a labeled storage vial. The beaker was rinsed several times, and the rinse was also added to the storage vial. The contents of each storage vial were sequentially analyzed using the process flow shown in Figure 3-1. The 6 mol/L nitric acid used for deconsolidation was decanted off for separate analysis, and concentrated (15.8 mol/L) nitric acid was used for the extractions and pot leaches. The details of the equipment and methods for Soxhlet extractor LBL are reported in the literature (Hunn et al. 2013, Hunn and Montgomery 2020). Appendix A contains the Compact 1-3 DLBL data from each primary leach solution for select actinides (Appendix Table A-1–Appendix Table A-4),beta/gamma emitting fission products (Appendix Table A-17–Appendix Table A-20) and stable nuclides (Appendix Table A-33–Appendix Table A-36). In some cases, stable and radioactive isotopes of the same element were reported.

The particle equivalents of ^{235}U in each DLBL solution are shown in Table 4-3. A total of 19.3 particle equivalents of ^{235}U was detected in all solutions, which is consistent with the presence of 20 DTF particles given the range in particle size and the uncertainty of the measurement. As shown in Figure 4-1, ^{235}U was mostly in the core of the compact with significant ^{235}U present in Segment 3 and progressively

lower inventories in the outer segments, which is consistent with limited diffusion from the DTF particles in the compact core radially outward.

Table 4-3. Particle equivalents of ^{235}U detected in Compact 1-3 DLBL solutions

DLBL Step	Segment 1	Segment 2	Segment 3	Segment 4	Total
Deconsolidation acid	(0.007)	(0.026)	(5.696)	(13.249)	(18.978)
Preburn leach 1	(0.0007)	(0.0083)	(0.021)	(0.178)	(0.207)
Preburn leach 2	(0.0004)	(0.0008)	(0.0006)	(0.022)	(0.023)
Postburn leach 1	(0.0009)	(0.0045)	(0.0015)	(0.062)	(0.069)
Postburn leach 2	(0.0006)	(0.0005)	(0.0001)	(0.0007)	(0.0019)
Total	(0.0096)	(0.041)	(5.719)	(13.511)	(19.280)

*Less than values were not included in the totals.

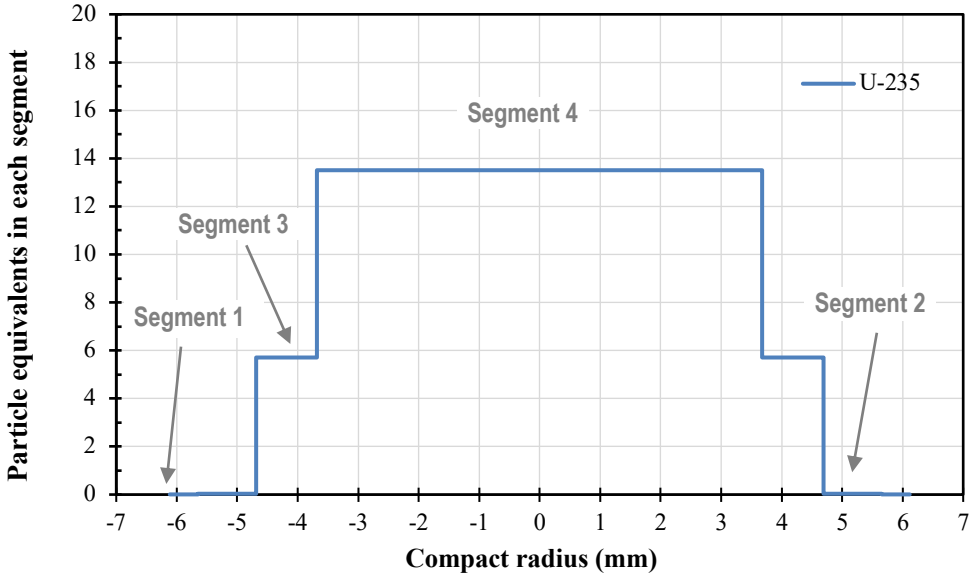

Figure 4-1. Distribution of ^{235}U from DTF particles in Compact 1-3.

Appendix Table A-49 contains concentration values for select actinides, beta/gamma emitting fission products, and stable fission products calculated from the total quantities detected in each Compact 1-3 segment divided by the segment volumes given in Table 4-2 that were determined by the automated photo analysis. Figure 4-2 shows the ^{235}U data from Figure 4-1 in terms of particle equivalent concentration plotted on a logarithmic scale. Figure 4-3 provides a comparison of the ^{144}Ce, ^{235}U, and ^{239}Pu concentration profiles. Variations in the total inventory of each radionuclide and uncertainties in the relatively low concentrations present in the outer two segments present a challenge to comparison of apparent diffusion rates between radionuclides. Figure 4-4 indicates there was more active diffusion of ^{154}Eu and ^{137}Cs than ^{235}U and ^{90}Sr given the higher relative fractions of ^{154}Eu and ^{137}Cs measured in segments outside the core. Table 4-4 shows the particle equivalents of all six of these nuclides as measured with DLBL in each segment. The total inventory of ^{154}Eu (18.7 particle equivalents) was slightly below the DTF inventory of 20 particle equivalents, which indicates that some may have been released from the compact. The slightly high total inventory of ^{90}Sr (24.0 particle equivalents) indicates the potential for diffusional release from driver fuel particles. If strontium was coming out of intact driver fuel, it is likely that europium was as well, which suggests ^{154}Eu release from the compact may have been higher then evident from the total inventory alone. Further evidence for ^{154}Eu release from the compact comes from the relatively high inventory of 0.61 particle equivalents found in the outermost 0.8 mm of the compact.

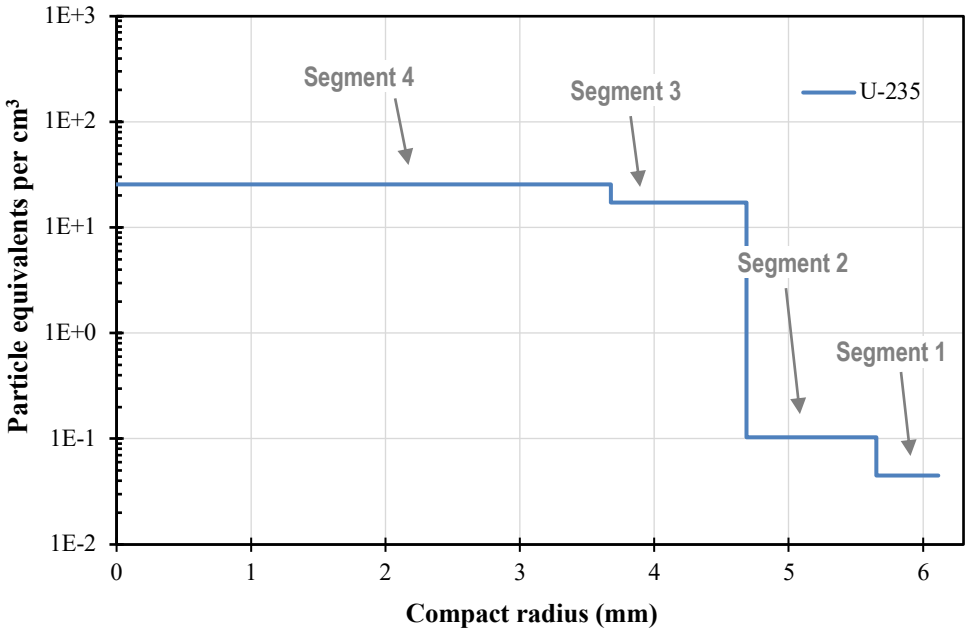

Figure 4-2. Concentration gradient of ^{235}U from DTF particles in Compact 1-3.

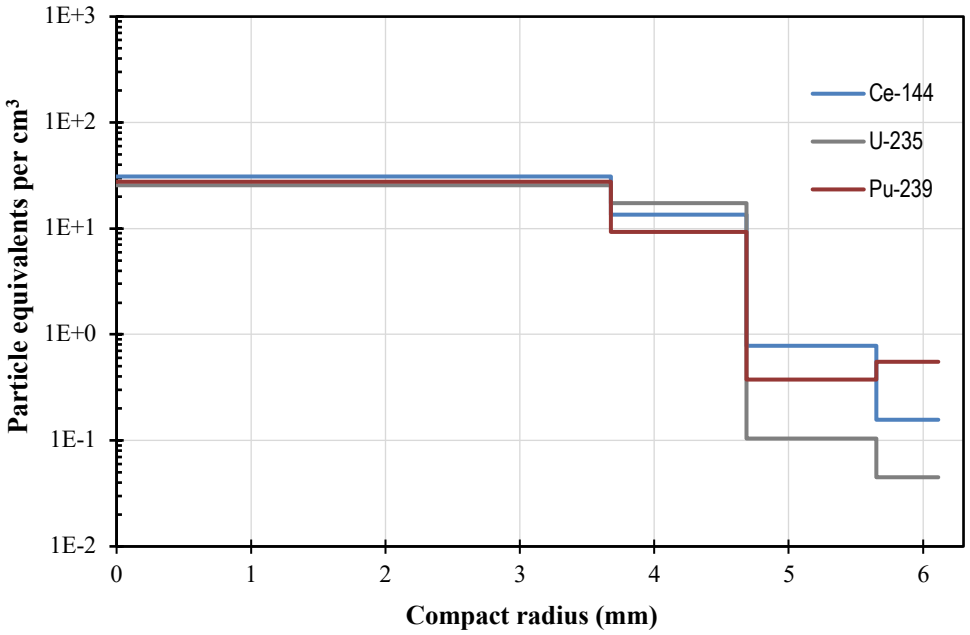

Figure 4-3. Comparison of ^{144}Ce, ^{235}U, and ^{239}Pu diffusion from DTF particles in Compact 1-3.

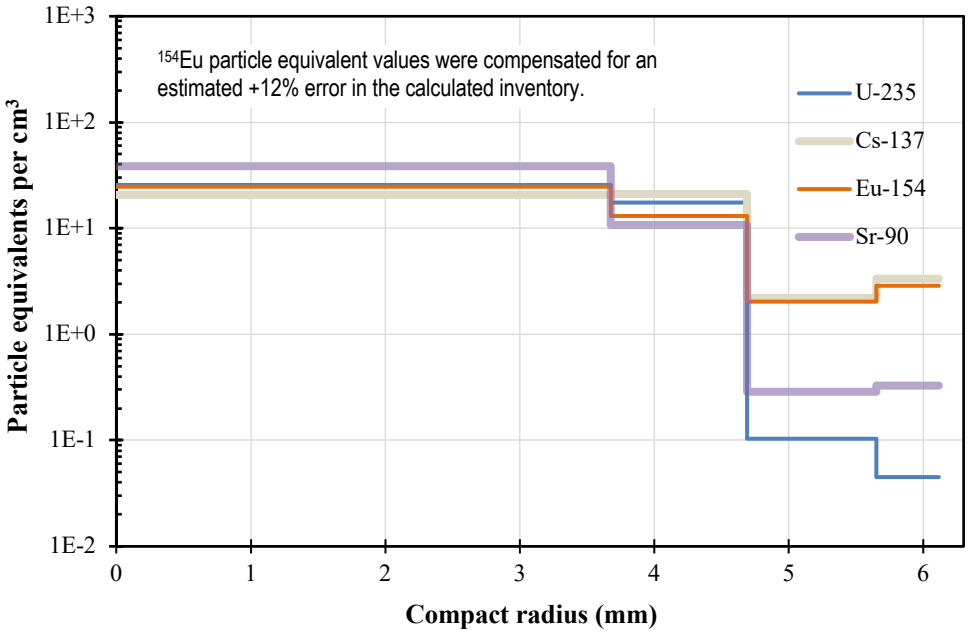

Figure 4-4. Comparison of ^{235}U, ^{137}Cs, ^{154}Eu, and ^{90}Sr diffusion from DTF particles in Compact 1-3.

Table 4-4. Comparison of particle equivalents of select nuclides in Compact 1-3 segments

Nuclide	Segment 1	Segment 2	Segment 3	Segment 4	Total
^{235}U	(0.0096)	(0.041)	(5.719)	(13.511)	(19.281)
^{239}Pu	(0.117)	(0.146)	(3.079)	(14.597)	(17.939)
^{144}Ce	(0.033)	(0.306)	(4.459)	(16.348)	(21.146)
^{137}Cs	(0.707)	(0.855)	(6.927)	(10.856)	(19.345)
^{90}Sr	(0.070)	(0.111)	(3.534)	(20.287)	(24.002)
^{154}Eu [a]	(0.608)	(0.790)	(4.324)	(13.002)	(18.722)

[a] Values for ^{154}Eu were adjusted for offset in calculated inventory by dividing by the average measured vs. calculated (M/C) ratio (0.89) for particles from Compacts 1-4, 10-4, and 7-4 which were gamma counted using IMGA.

5. REIRRADIATED AND 1000°C SAFETY-TESTED AGR-3/4 COMPACT 4-3

5.1 RADIAL DECONSOLIDATION AND DIMENSIONAL ANALYSIS OF COMPACT 4-3

The segment plan to generate four segments of equal volume for Compact 4-3 is shown in Table 5-1, and the actual segment results based on image analysis of the compact are given in Table 5-2, along with the time that deconsolidation was active (power applied) for each radially deconsolidated segment.

Table 5-1. Equal volume segment plan for Compact 4-3

Quantity	Segment 1	Segment 2	Segment 3	Segment 4
Initial diameter (mm)	12.175	10.544	8.609	6.088
Target diameter (mm)	10.544	8.609	6.088	0
Segment thickness (mm)	0.816	0.967	1.261	solid
Segment volume (cm^3)	0.365	0.365	0.365	0.365

Note: The average diameter of the irradiated compact was 12.175 mm with a standard deviation of 0.0118 mm, and the length from a single measurement was 12.535 mm (Stempien et al. 2016).

Table 5-2. Segment results for Compact 4-3 measured with automated photo analysis

Quantity	Segment 1	Segment 2	Segment 3	Segment 4
Initial diameter (mm)	12.175	10.842	8.808	7.357
Residual diameter (mm)	10.842	8.808	6.510	0
Segment thickness (mm)	0.667	1.017	1.149	solid
Segment volume (cm^3)	0.302	0.394	0.347	0.417
Deconsolidation time (min)	44	20	20	

During the second radial deconsolidation step, the bulk of the compact broke away from the mounting rod, leaving some particles attached to the residual portion of the compact that was still attached to the rod. The compact was remounted to another rod on the remaining face, and the remainder of the radial deconsolidation process continued without incident.

5.2 DLBL OF COMPACT 4-3

After the radial deconsolidation of each segment was complete, deconsolidated material from each segment was collected and subjected to LBL as described in Section 4.2. Appendix A contains DLBL data in terms of compact fraction and particle equivalents for select actinides (Appendix Table A-5–Appendix Table A-9), beta/gamma emitting fission products (Appendix Table A-21–Appendix Table A-24), and stable fission products (Appendix Table A-37–Appendix Table A-40).

The particle equivalents of ^{235}U in each DLBL solution are shown in Table 5-3. A total of 32.7 particle equivalents of ^{235}U was detected in all solutions, which is substantially higher than would be expected for 20 DTF particles. As shown in Figure 5-1, large amounts of ^{235}U were found in the core of the compact and in the second segment. The 7.98 particle equivalents of ^{235}U in the second segment were likely a result of particles broken by the shearing of the compact from the mounting rod during the second segment deconsolidation. As previously noted, the compact did not separate cleanly from the rod, but fractured through the compact body, which may have led to fracture or damage of driver fuel particles. This conclusion is supported by the elevated concentrations of other nuclides in the second segment. The 4.41 particle equivalents in the third segment may have also included contributions from broken driver fuel particles as well as uranium that diffused from the core as observed in Compact 1-3 (Figure 4-1). In addition, all of these segments may have included some uranium released by intact driver fuel.

Table 5-3. Particle equivalents of ^{235}U detected in Compact 4-3 DLBL solutions

DLBL Step	Segment 1	Segment 2	Segment 3	Segment 4	Total
Deconsolidation acid	(0.496)	(7.855)	(2.836)	(18.110)	(29.296)
Preburn leach 1	(0.039)	(0.091)	(0.079)	(0.234)	(0.443)
Preburn leach 2	(0.0018)	(0.0018)	(0.0024)	(0.012)	(0.018)
Postburn leach 1	(0.015)	(0.032)	(1.482)	(1.406)	(2.935)
Postburn leach 2	(0.0029)	(0.0008)	(0.0084)	(0.0067)	(0.019)
Total	(0.554)	(7.980)	(4.408)	(19.768)	(32.711)

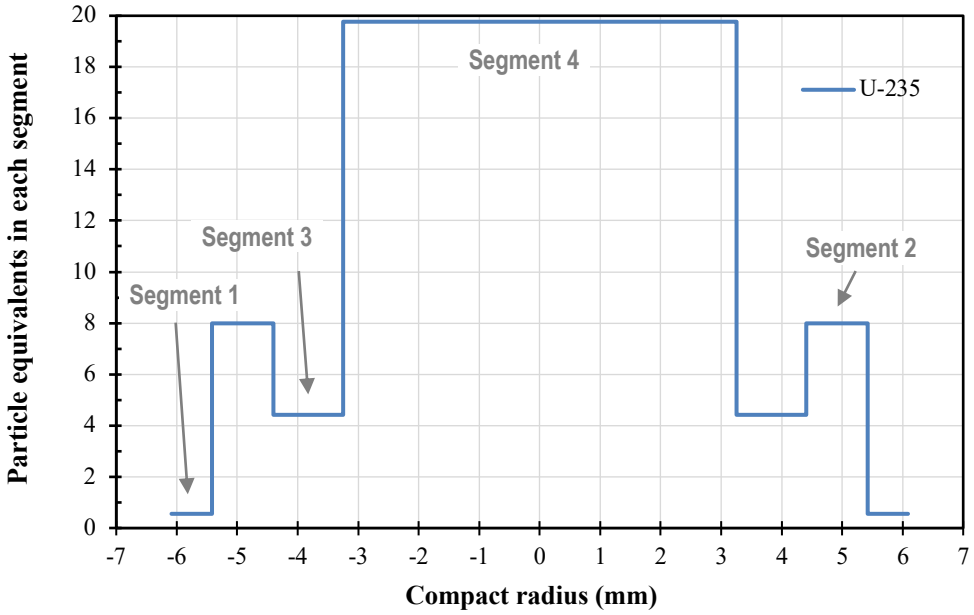

Figure 5-1. Distribution of ^{235}U from DTF particles and broken driver fuel particles, in Compact 4-3.

Appendix Table A-50 contains concentration values calculated from the total quantities detected in each Compact 4-3 segment divided by the segment volumes given in Table 5-2. Figure 5-2 shows the ^{235}U concentration data and Figure 5-3 provides a comparison of the ^{144}Ce, ^{235}U, and ^{239}Pu concentration profiles. Analysis of this data is difficult because of the probable release of nuclides from damaged driver fuel particles in Segments 2 and 3 as well as complications from generation of additional fission products during reirradiation of Compact 4-3 that will need to be deconvoluted. Reirradiation contributions were most evident for ^{144}Ce, which was measured in Segment 4 at a level of 34.1 particle equivalents (Appendix Table A-24). This reirradiation contribution elevated the ^{144}Ce profile plotted in Figure 5-3.

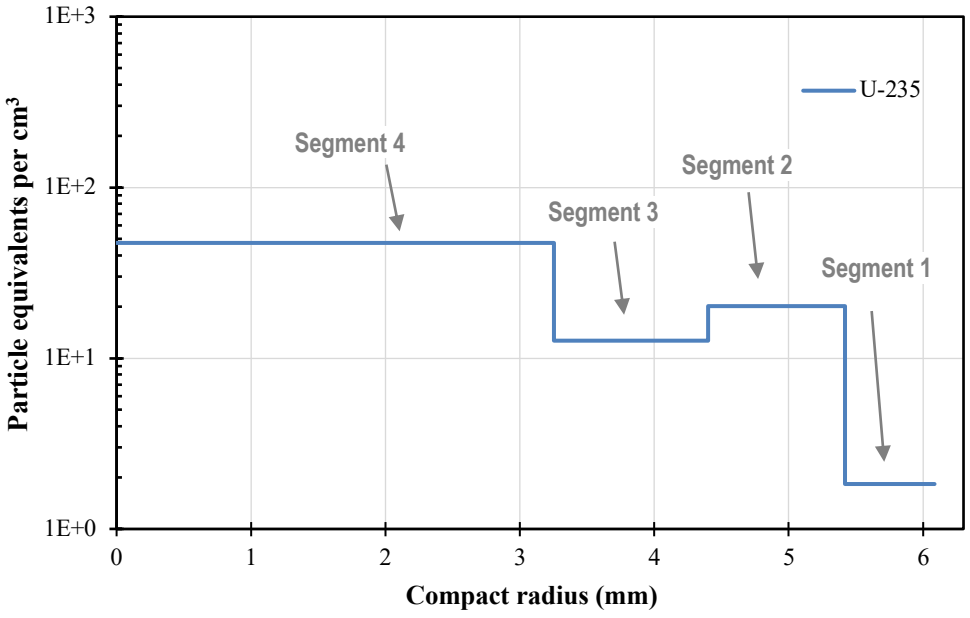

Figure 5-2. Concentration gradient of ^{235}U from DTF particles and broken driver fuel particles in Compact 4-3.

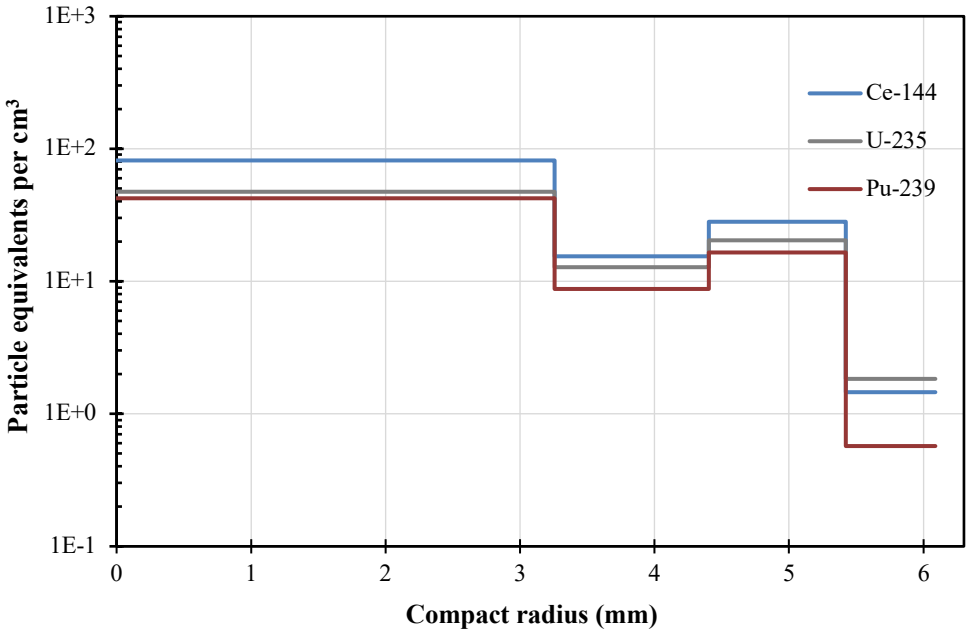

Figure 5-3. Comparison of ^{144}Ce, ^{235}U, and ^{239}Pu diffusion from DTF particles and broken driver fuel particles in Compact 4-3.

Figure 5-4 provides a comparison of the ^{235}U, ^{137}Cs, ^{154}Eu, and ^{90}Sr profiles. Again, release from damaged driver fuel particles in Segment 2 and reirradiation contributions present a challenge to analysis. The relatively flat profile and low total inventory of ^{137}Cs indicates substantial diffusion from the core and out of the compact. The profile of ^{154}Eu was more concentrated in the core, but it still indicated significant diffusion and probable release of some inventory from the compact after discounting some of the inventory measured in Segment 2.Table 5-4 shows the measured particle equivalents for all six of these nuclides as measured with DLBL in each segment.

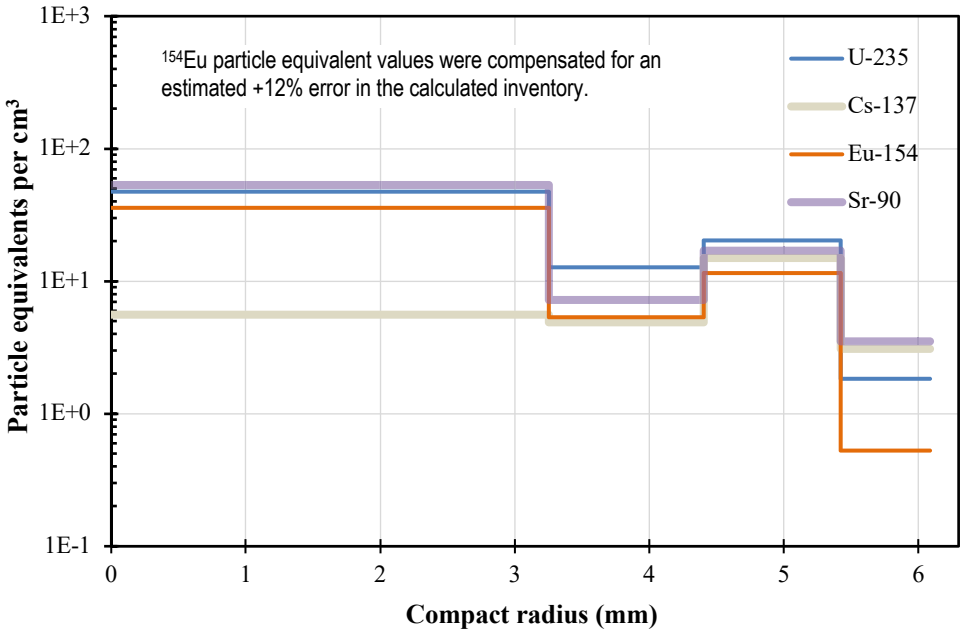

Figure 5-4. Comparison of ^{235}U, ^{137}Cs, ^{154}Eu, and ^{90}Sr diffusion from DTF particles and broken driver fuel particles in Compact 4-3.

Table 5-4. Comparison of particle equivalents of select nuclides in Compact 4-3 segments

Nuclide	Segment 1	Segment 2	Segment 3	Segment 4	Total
^{235}U	(0.554)	(7.980)	(4.408)	(19.768)	(32.710)
^{239}Pu	(0.172)	(6.526)	(3.018)	(17.647)	(27.363)
^{144}Ce	(0.440)	(11.052)	(5.325)	(34.059)	(50.876)
^{137}Cs	(0.932)	(5.885)	(1.700)	(2.337)	(10.854)
^{90}Sr	(1.062)	(6.722)	(2.506)	(22.205)	(32.495)
^{154}Eu [a]	(0.159)	(4.509)	(1.847)	(14.929)	(21.444)

[a] Values for ^{154}Eu were adjusted for offset in calculated inventory by dividing by the average M/C ratio (0.89) for particles from Compacts 1-4, 10-4, and 7-4 which were gamma counted using IMGA.

6. REIRRADIATED AND 1400°C SAFETY-TESTED AGR-3/4 COMPACT 10-1

6.1 RADIAL DECONSOLIDATION AND DIMENSIONAL ANALYSIS OF COMPACT 10-1

The segment plan to generate four segments of equal volume for Compact 10-1 is shown in Table 6-1, and the actual segment results based on image analysis of the compact are given in Table 6-2, along with the time that deconsolidation was active (power applied) for each radially deconsolidated segment.

Table 6-1. Equal volume segment plan for Compact 10-1

Quantity	Segment 1	Segment 2	Segment 3	Segment 4
Initial diameter (mm)	12.139	10.513	8.584	6.070
Target diameter (mm)	10.513	8.584	6.070	0
Segment thickness (mm)	0.813	0.965	1.257	solid
Segment volume (cm^3)	0.359	0.359	0.359	0.359

Note: The average diameter of the irradiated compact was 12.139 mm with a standard deviation of 0.0050 mm, and the length from a single measurement was 12.3952 mm (Stempien et al. 2016).

Table 6-2. Segment results for Compact 10-1 measured with automated photo analysis

Quantity	Segment 1	Segment 2	Segment 3	Segment 4
Initial diameter (mm)	12.139	10.387	8.158	6.496
Residual diameter (mm)	10.387	8.158	6.496	0
Segment thickness (mm)	0.876	1.13	0.816	Solid
Segment volume (cm^3)	0.384	0.407	0.232	0.411
Deconsolidation time (min)	30	40	45	

6.2 DLBL OF COMPACT 10-1

After the radial deconsolidation of each segment was complete, deconsolidated material from each segment was collected and subjected to LBL as described in Section 4.2. Appendix A contains DLBL data for select actinides (Appendix Table A-9–Appendix Table A-12), beta/gamma emitting fission products (Appendix Table A-25–Appendix Table A-28), and stable fission products (Appendix Table A-41–Appendix Table A-44).

The particle equivalents of ^{235}U in each DLBL solution are shown in Table 6-3. A total of 20.0 particle equivalents of ^{235}U was detected in all solutions, which is what would be expected for 20 DTF particles. As shown in Figure 6-1, ^{235}U was concentrated in the core of the compact.

Table 6-3. Particle equivalents of ^{235}U detected in Compact 10-1 DLBL solutions

DLBL Step	Segment 1	Segment 2	Segment 3	Segment 4	Total
Deconsolidation acid	(0.045)	(0.786)	(0.648)	(17.455)	(18.935)
Preburn leach 1	(0.0013)	(0.010)	(0.026)	(0.504)	(0.541)
Preburn leach 2	(0.0007)	(0.0003)	(0.0003)	(0.0088)	(0.010)
Postburn leach 1	(0.025)	(0.024)	(0.020)	(0.452)	(0.522)
Postburn leach 2	(0.0005)	(0.0003)	(0.0054)	(0.0066)	(0.013)
Total	(0.073)	(0.821)	(0.701)	(18.426)	(20.020)

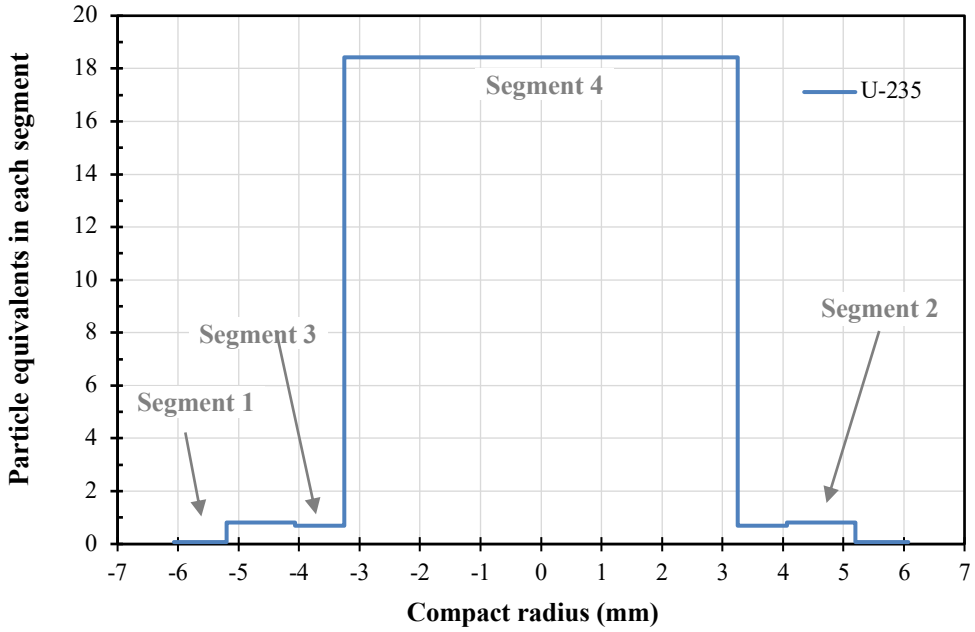

Figure 6-1. Distribution of ^{235}U from DTF particles in Compact 10-1.

Appendix Table A-51 contains concentration values for select actinides, beta/gamma emitting fission products, and stable fission products calculated from the total quantities detected in each Compact 10-1 segment divided by the segment volumes given in Table 6-2. Figure 6-2 shows the ^{235}U concentration data. Figure 6-3 provides a comparison of the ^{144}Ce, ^{235}U, and ^{239}Pu profiles. As with Compact 4-3, the ^{144}Ce in the core was noticeably elevated due to contributions from reirradiation of the compact. There were 34.5 particle equivalents of ^{144}Ce in Segment 4 of Compact 10-1 (Appendix Table A-28). Excepting the spike in ^{144}Ce in the core, ^{144}Ce, ^{235}U, and ^{239}Pu had similar profiles. Figure 6-4 shows that ^{154}Eu and ^{90}Sr exhibited more active diffusion based on the relatively even distribution of their concentrations across all four segments, compared with the other compacts not heated to 1400°C. In comparison, ^{137}Cs showed a significantly lower but nontrivial concentration in the core and substantially lower concentration in the outer segments. The total inventory of ^{137}Cs in Compact 10-1 was only 1.5 particle equivalents. Taken together, this indicates that a significant fraction of the ^{137}Cs inventory was released during safety testing at 1400°C and the residual diffusion curve may have resulted from slower release of ^{137}Cs still retained in the DTF kernels. Table 6-4 shows the particle equivalents of all six of these nuclides as measured with DLBL in each segment.

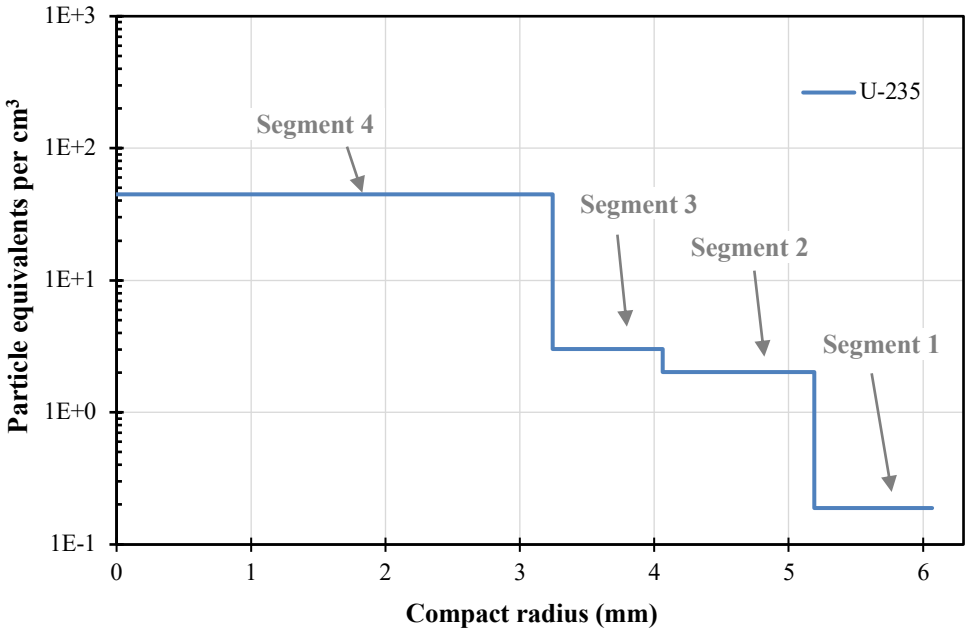

Figure 6-2. Concentration gradient of ^{235}U from DTF particles in Compact 10-1.

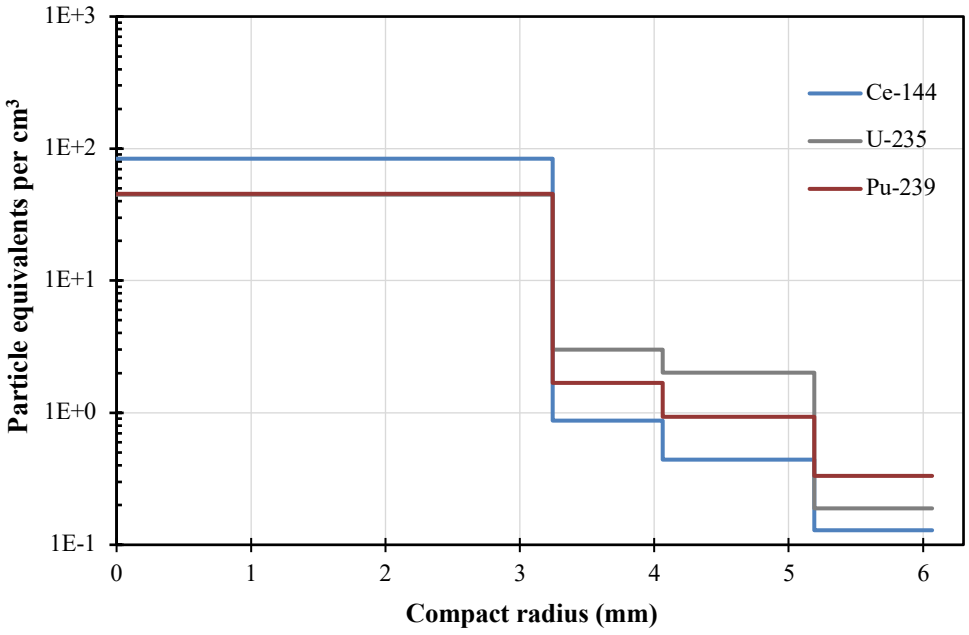

Figure 6-3. Comparison of ^{144}Ce, ^{235}U, and ^{239}Pu diffusion from DTF particles in Compact 10-1.

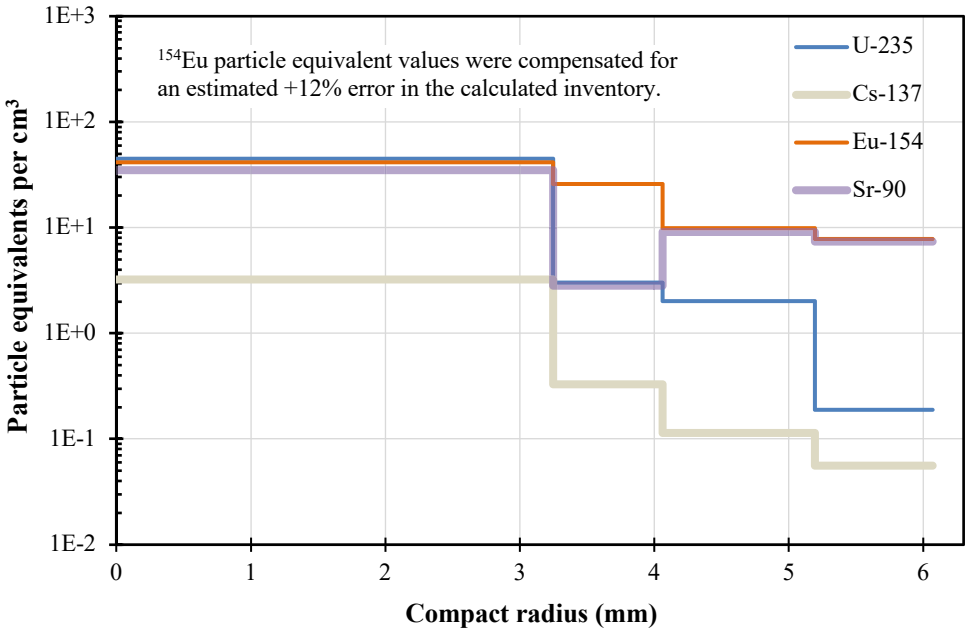

Figure 6-4. Comparison of ^{235}U, ^{137}Cs, ^{154}Eu, and ^{90}Sr diffusion from DTF particles in Compact 10-1.

Table 6-4. Comparison of particle equivalents of select nuclides in Compact 10-1 segments

Nuclide	Segment 1	Segment 2	Segment 3	Segment 4	Total
^{235}U	(0.073)	(0.821)	(0.701)	(18.426)	(20.021)
^{239}Pu	(0.128)	(0.380)	(0.391)	(18.707)	(19.606)
^{144}Ce	(0.050)	(0.181)	(0.203)	(34.498)	(34.932)
^{137}Cs	(0.022)	(0.047)	(0.077)	(1.327)	(1.473)
^{90}Sr	(2.847)	(3.683)	(0.655)	(14.359)	(21.544)
^{154}Eu [a]	(2.672)	(3.569)	(5.310)	(15.169)	(26.720)

[a] Values for ^{154}Eu were adjusted for offset in calculated inventory by dividing by the average M/C ratio (0.89) for particles from Compacts 1-4, 10-4, and 7-4 which were gamma counted using IMGA.

7. 1200°C SAFETY-TESTED AGR-3/4 COMPACT 10-2

7.1 RADIAL DECONSOLIDATION AND DIMENSIONAL ANALYSIS OF COMPACT 10-2

The segment plan to generate four segments of equal volume for Compact 10-2 is shown in Table 7-1 and the actual segment results based on image analysis of the compact are given in Table 7-2, along with the time that deconsolidation was active (power applied) for each radially deconsolidated segment.

Table 7-1. Equal volume segment plan for Compact 10-2

Quantity	Segment 1	Segment 2	Segment 3	Segment 4
Initial diameter (mm)	12.231	10.592	8.649	6.116
Target diameter (mm)	10.592	8.649	6.116	0
Segment thickness (mm)	0.820	0.972	1.267	solid
Segment volume (cm^3)	0.359	0.359	0.359	0.359

Note: The average diameter of the irradiated compact was 12.141 mm with a standard deviation of 0.0000 mm, and the length from a single measurement was 12.433 mm (Stempien et al. 2016).

Table 7-2. Segment results for Compact 10-2 measured with automated photo analysis

Quantity	Segment 1	Segment 2	Segment 3	Segment 4
Initial diameter (mm)	12.141	10.700	8.588	6.444
Residual diameter (mm)	10.700	8.588	6.444	0
Segment thickness (mm)	0.720	1.056	1.072	solid
Segment volume (cm^3)	0.321	0.398	0.315	0.406
Deconsolidation time (min)	55	14.5	20	

It was necessary to pause the radial deconsolidation of Compact 10-2 two times because the compact fell off the axle during radial deconsolidation. The compact first detached from the axle in the middle of the second deconsolidation segment. The compact diameter was estimated from photographs, and a custom vee-block was fabricated to reattach the axle to the other end of the compact. Based on visual inspection of the rotating compact, this reattachment was successful in keeping the compact centered on the axle. The compact detached from the axle a second time at the end of the third segment, at which point it was decided to end the segment and proceed with axial deconsolidation of the final segment.

It was later determined that compact detachment from the axle was due to excessive soaking of the epoxy connecting the axle to the compact in the nitric acid that must contact the surface of the compact during electrolytic deconsolidation. The degree of exposure of the epoxy to the acid was dependent both on the immersion depth of the compact and the tilt of the axle relative to the surface of the nitric acid. Analysis of pictures from various radial deconsolidation experiments showed that the axle mounting angle had gradually shifted over time such that the epoxy spent much longer in contact with the nitric acid. This issue was resolved by inserting stepped shims under one side of the base of the deconsolidation apparatus to tilt the surface of the nitric acid within the collection beaker to match the tilt of the axle. Subsequent radial deconsolidations using this approach did not exhibit deleterious degradation of the epoxy bond.

7.2 DLBL OF COMPACT 10-2

After the radial deconsolidation of each segment was complete, deconsolidated material from each segment was collected and subjected to LBL as described in Section 4.2. Appendix A contains DLBL data for select actinides (Appendix Table A-13–Appendix Table A-16), beta/gamma emitting fission products (Appendix Table A-29–Appendix Table A-32), and stable fission products (Appendix Table A-45–Appendix Table A-48).

The particle equivalents of ^{235}U in each DLBL solution are shown in Table 7-3. A total of 19.8 particle equivalents of ^{235}U was detected in all solutions, which is close to the expected inventory from 20 DTF particles. As shown in Figure 7-1, ^{235}U was concentrated in the core of the compact with progressively lower inventories in the outer segments, which is consistent with diffusion from the DTF particles in the compact core. The distribution of ^{235}U does not indicate substantial diffusive release from driver fuel particles, and the total inventory of actinide isotopes indicates that no driver fuel particles were broken when the compact detached from the axle.

Table 7-3. Particle equivalents of ^{235}U detected in Compact 10-2 DLBL solutions

DLBL Step	Segment 1	Segment 2	Segment 3	Segment 4	Total
Deconsolidation acid	(0.012)	(0.116)	(4.535)	(14.824)	(19.487)
Preburn leach 1	(0.0012)	(0.0018)	(0.031)	(0.132)	(0.166)
Preburn leach 2	(0.0004)	(0.0002)	(0.0019)	(0.0046)	(0.0072)
Postburn leach 1	(0.017)	(0.034)	(0.020)	(0.091)	(0.161)
Postburn leach 2	(0.0004)	(0.0002)	(0.0005)	(0.0013)	(0.0024)
Total	(0.031)	(0.152)	(4.588)	(15.053)	(19.824)

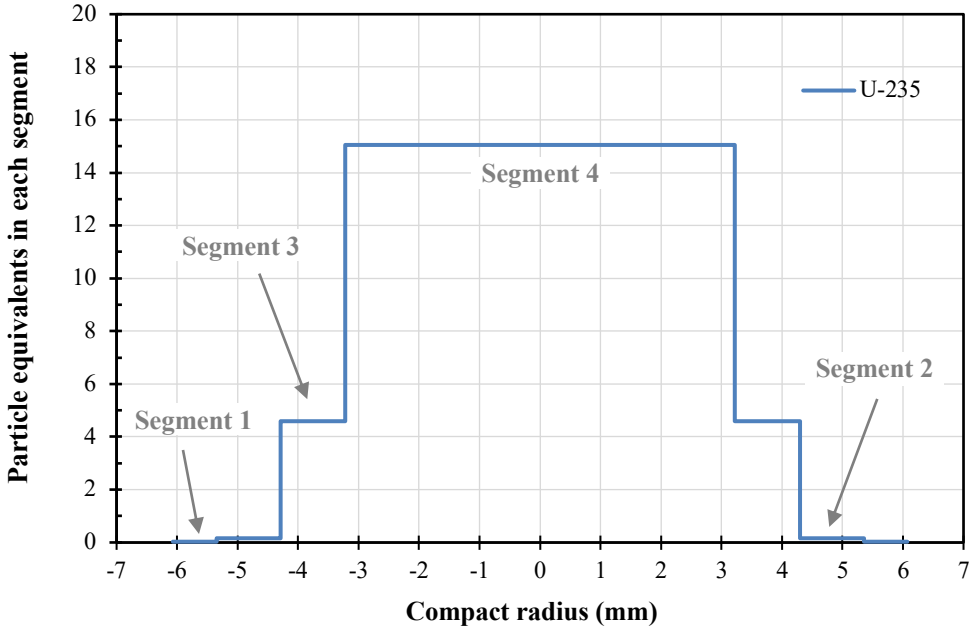

Figure 7-1. Distribution of ^{235}U from DTF particles in Compact 10-2.

Appendix Table A-52 contains concentration values for select actinides, beta/gamma emitting fission products, and stable fission products calculated from the total quantities detected in each Compact 10-2 segment divided by the segment volumes given in Table 7-2 that were determined by the automated photo analysis. Figure 7-2 shows the ^{235}U concentration data. Figure 7-3 provides a comparison of the ^{144}Ce, ^{235}U, and ^{239}Pu profiles. Figure 7-4 provides a comparison of the ^{154}Eu, ^{90}Sr, ^{137}Cs, and ^{235}U profiles. Both ^{154}Eu and ^{90}Sr show signs of active diffusion out of the center of the compact as well as diffusive release from driver fuel particles (as indicated by total retained inventories greater than 20 particle equivalents), whereas ^{137}Cs had been depleted from the compact during irradiation and safety testing. Diffusive release of ^{137}Cs from driver fuel particles is not expected in the absence of SiC failure. Table 7-4 shows the particle equivalents of all six of these nuclides as measured with DLBL in each segment.

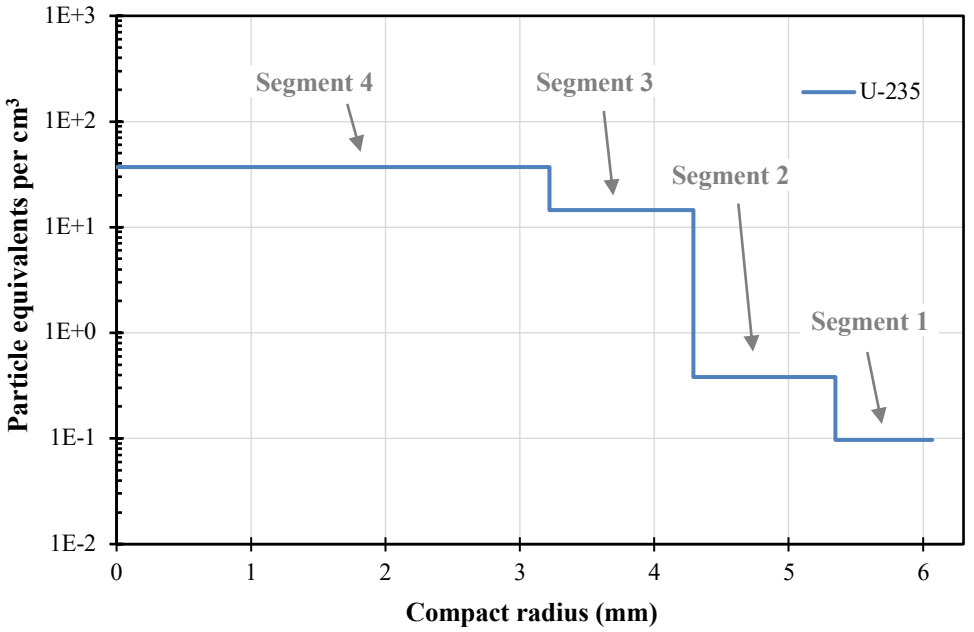

Figure 7-2. Concentration gradient of ^{235}U from DTF particles in Compact 10-2.

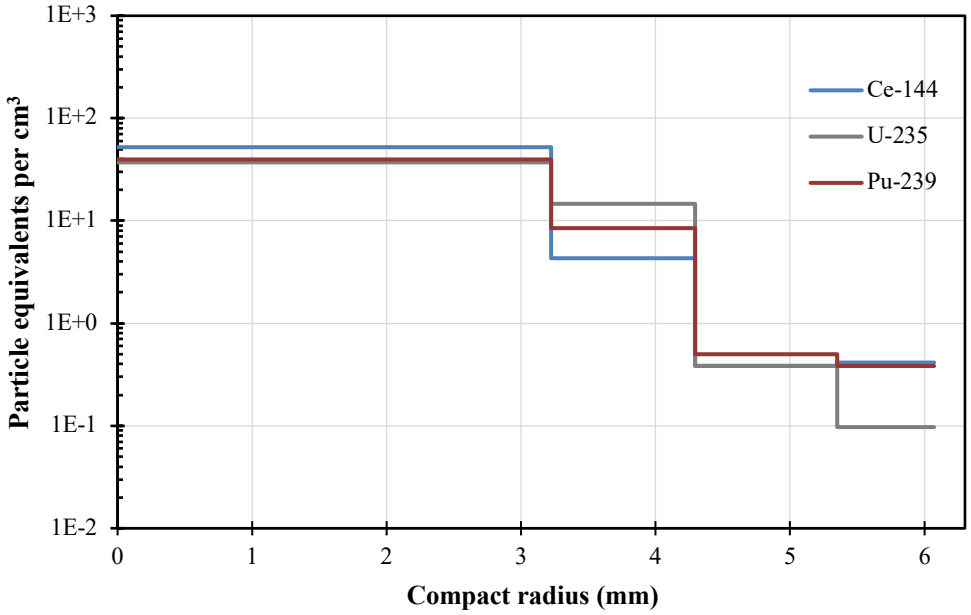

Figure 7-3. Comparison of ^{144}Ce, ^{235}U, and ^{239}Pu diffusion from DTF particles in Compact 10-2.

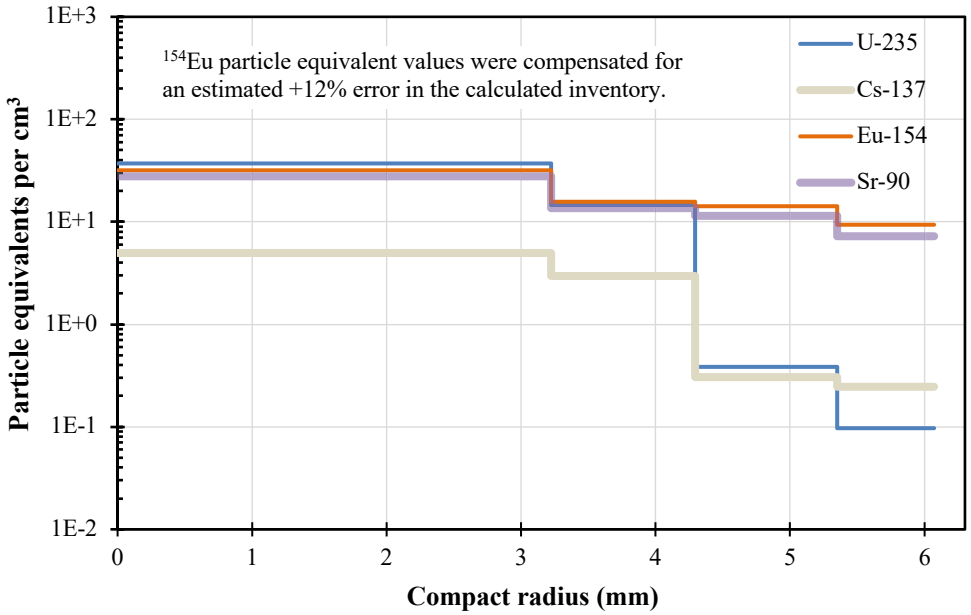

Figure 7-4. Comparison of ^{235}U, ^{137}Cs, ^{154}Eu, and ^{90}Sr diffusion from DTF particles in Compact 10-2.

Table 7-4. Comparison of particle equivalents of select nuclides in Compact 10-2 segments

Nuclide	Segment 1	Segment 2	Segment 3	Segment 4	Total
^{235}U	(0.031)	(0.152)	(4.588)	(15.053)	(19.824)
^{239}Pu	(0.123)	(0.198)	(2.662)	(16.083)	(19.066)
^{144}Ce	(0.132)	(0.152)	(1.348)	(21.181)	(22.813)
^{137}Cs	(0.079)	(0.122)	(0.928)	(2.014)	(3.143)
^{90}Sr	(2.325)	(4.542)	(4.288)	(11.272)	(22.427)
^{154}Eu [a]	(3.011)	(5.657)	(4.975)	(12.898)	(26.541)

[a] Values for ^{154}Eu were adjusted for offset in calculated inventory by dividing by the average M/C ratio (0.89) for particles from Compacts 1-4, 10-4, and 7-4 which were gamma counted using IMGA.

8. COMPARISON OF NUCLIDE PROFILES ACROSS COMPACTS

The data presented in this report, combined with previously reported data from Helmreich (Helmreich et al. 2021) and Hunn (Hunn et al. 2020) present nuclide behavior as measured by radial deconsolidation across a range of compact irradiation conditions. A summary of those irradiation conditions is provided in Table 8-1 in order of ascending irradiation temperature. Some observations for key nuclides of interest are presented herein using data from each of those sources. As noted in Table 8-1, several of the compacts considered were safety tested after irradiation at temperatures of 1000°C–1400°C (Stempien et al. 2018b, Stempien et al. 2021). Compact 4-3 and Compact 10-1 were also reirradiated prior to safety testing (Stempien 2021, Stempien et al. 2021). In addition to complications associated with reirradiation, Compact 4-3 experienced significant driver fuel particle failure due to compact fracture, as discussed in Section 5.2. Therefore, Compact 4-3 is excluded from the comparison discussion in this section. Compact 10-1 is included in most comparisons, with the exception of ^{144}Ce, due to the larger impact of the reirradiation on the ^{144}Ce inventory.

Table 8-1. Irradiation and safety test parameters for AGR-3/4 compacts radially deconsolidated at ORNL

Compact ID [a]	Fabrication ID number [b]	Safety test (°C)	Burnup [c] (% FIMA)	Fast fluence [c] (n/m^2)	Temperature [d] (°C)		
					TAVA	TA_{min}	TA_{max}
AGR-3/4 Compact 1-4	Z012	none	6.85	2.10×10^{25}	929	866	972
AGR-3/4 Compact 1-3	Z003	none	6.37	1.87×10^{25}	959	942	978
AGR-3/4 Compact 4-3	Z059	1,000	14.29	4.89×10^{25}	1035	992	1084
AGR-3/4 Compact 8-4	Z120	none	14.43	5.02×10^{25}	1169	1068	1242
AGR-3/4 Compact 10-4	Z140	1,400	11.43	3.75×10^{25}	1168	1079	1231
AGR-3/4 Compact 10-1	Z133	1,400	12.08	4.12×10^{25}	1172	1080	1238
AGR-3/4 Compact 10-2	Z134	1,200	11.96	4.01×10^{25}	1213	1179	1249
AGR-3/4 Compact 7-4	Z111	none	14.90	5.24×10^{25}	1319	1206	1397

[a] The compact identification (ID) denotes the compact's location in the irradiation test train: *capsule-level* (Collin 2015).

[b] Each compact in the fabrication lot (LEU03-10T-OP2/LEU03-07DTF-OP1)-Z had a unique compact ID number in the range of 001–175, and physical properties data are available and referenced by compact ID number (Hunn, Trammell, and Montgomery, 2011).

[c] Compact average burnups and fast neutron fluences ($E_n > 0.18$ MeV) are based on daily depletion calculations (Sterbentz 2015).

[d] Compact TAVA, time-average minimum (TA_{min}) and time-average maximum (TA_{max}) temperatures are based on thermal calculations (Hawkes 2016).

8.1 BEHAVIOR OF ^{144}Ce

The behavior of ^{144}Ce was generally consistent across all the compacts considered except for the two reirradiated compacts (Compacts 4-3 and 10-1). Compact 4-3 also experienced driver fuel particle failure due to compact fracture. Excluding Compacts 4-3 and 10-1, an average of 20.1 particle equivalents of ^{144}Ce was measured in the compacts, with a standard error of 0.8 particle equivalents, and the total inventory did not indicate any dependence on irradiation temperature or burnup. A comparison of the observed concentration profiles for ^{144}Ce is shown in Figure 8-1 for the compacts that were not reirradiated. Overarching observations on the diffusive behavior of ^{144}Ce are difficult to make because of the scattered nature of the data.

Overall, Compact 7-4 had the lowest retained inventory in the core, which indicated the most diffusion from the core, as would be expected for the compact in the comparison with the highest irradiation temperature. Considering ^{144}Ce concentration in the outermost segment, Compacts 7-4 and 8-4 appear to show the highest diffusion into this region, which could be related to their higher irradiation temperatures compared with the other compacts that were not safety tested. Compact 10-4 was irradiated at similar temperatures to Compact 8-4, but had the least ^{144}Ce in the outermost segment, which was likely due to the compact being safety tested at 1400°C after irradiation. Compact 10-2 had a TAVA temperature in between Compacts 7-4 and 8-4, and appeared to have the same flat profile in the outer two segments. However, the concentration was shifted down, which was probably a result of transport of cerium out of the compact during safety testing at 1200°C. Compact 10-2 did not share the extremely low ^{144}Ce concentration in the outermost segment observed in Compact 10-4, suggesting significant difference in cerium behavior at 1200°C vs. 1400°C.

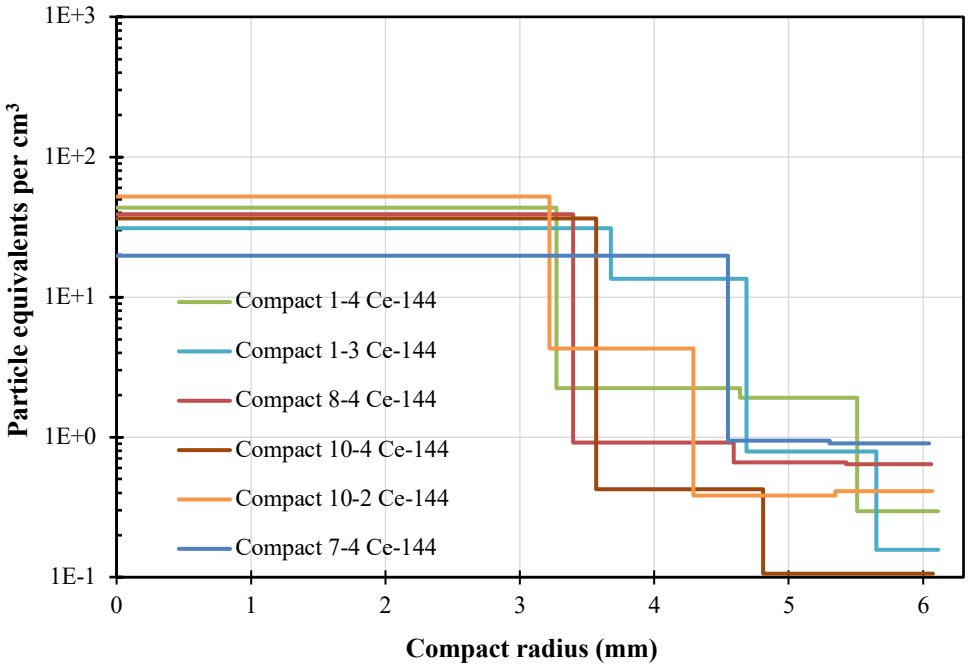

Figure 8-1. Comparison of ^{144}Ce concentration profiles in various AGR-3/4 compacts.

8.2 BEHAVIOR OF ^{235}U AND ^{239}Pu

Considering the total inventory of ^{235}U and ^{239}Pu in each compact suggests a possible dependence on compact burnup. The low burnup compacts from Capsule 1 and the moderate burnup compacts from Capsule 10 had close to the expected 20 particle equivalents of total inventory for both ^{235}U (20.2±0.3) and ^{239}Pu (18.5±0.4). In contrast, the higher burnup Compacts 8-4 and 7-4 had lower total inventories for both ^{235}U (16.7±0.6) and ^{239}Pu (16.5±0.2). As shown in Figure 8-2 and Figure 8-3, Compacts 8-4 and 7-4 also had the highest ^{235}U and ^{239}Pu inventories in the outermost segment and flattest concentration profiles for ^{235}U and ^{239}Pu in the outer two segments, which suggest more active release from these two high burnup compacts. Higher release of ^{235}U and ^{239}Pu might be expected for Compact 7-4, because it had the highest irradiation temperature of the compacts considered. However, the results for Compact 8-4 cannot be explained by irradiation temperature alone, in lieu of the apparently higher retention exhibited by the Capsule 10 compacts.

No substantial impact from post-irradiation safety testing was observed in the concentration profiles of either ^{235}U or ^{239}Pu.

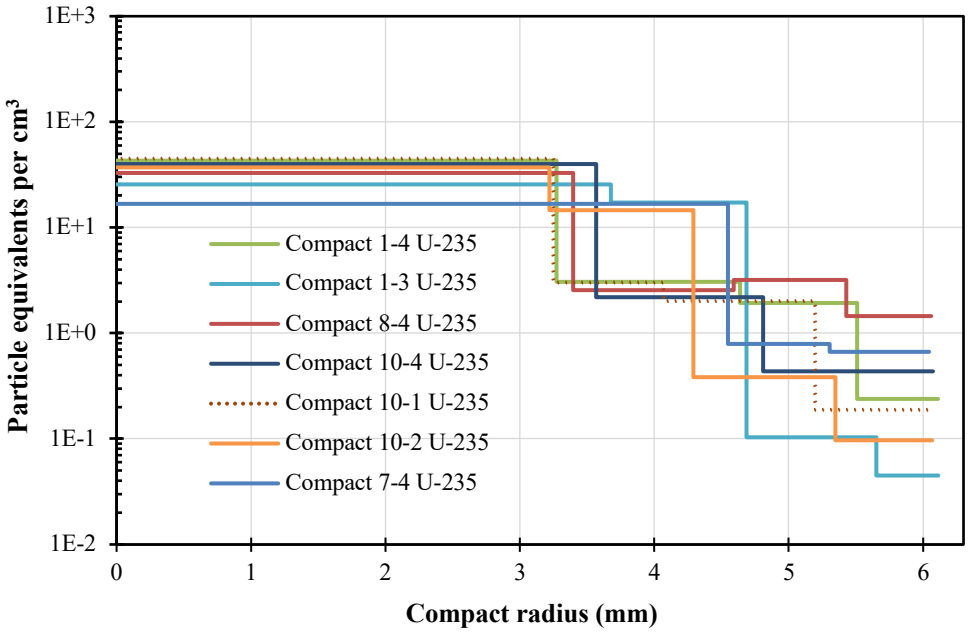

Figure 8-2. Comparison of ^{235}U concentration profiles in various AGR-3/4 compacts.

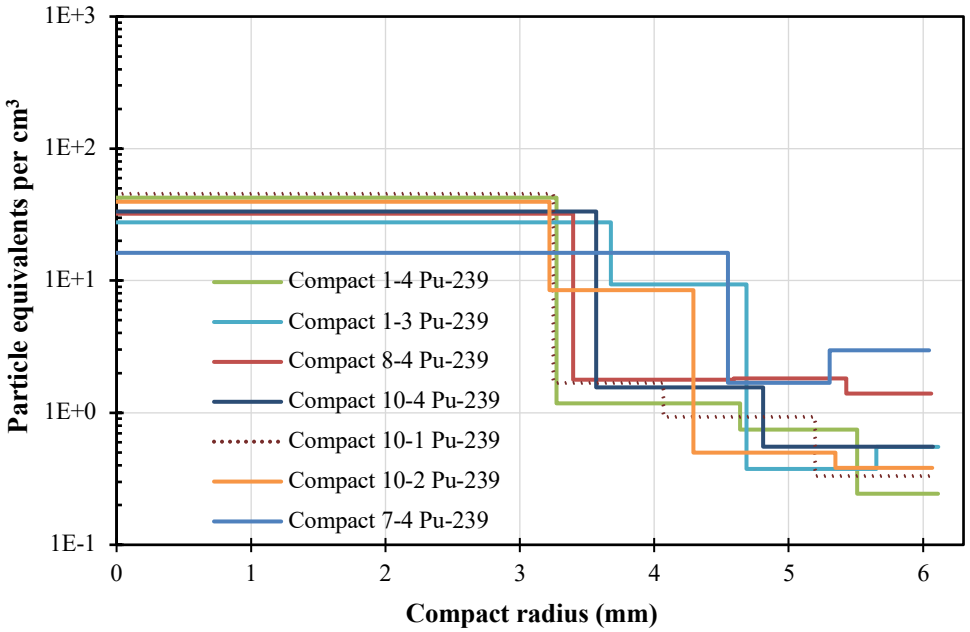

Figure 8-3. Comparison of ^{239}Pu concentration profiles in various AGR-3/4 compacts.

8.3 BEHAVIOR OF ^{137}Cs

The total inventory of ^{137}Cs in each compact decreased significantly with increasing irradiation temperature. As shown in Figure 8-4, which compares ^{137}Cs inventories to the much more stable ^{235}U inventories, the amount of ^{137}Cs from DTF particles retained by the compact was near the expected 20 particle equivalents for irradiation temperatures near 950°C, but it dropped to approximately 5 particle equivalents for irradiation temperatures above 1150°C. This shift in behavior for ^{137}Cs was also observed in the concentration profiles for each compact, as shown in Figure 8-5, in which the compacts that were irradiated at higher temperature all had lower concentrations of ^{137}Cs in the core as well as the outer segments. Whereas higher inventory in the outermost segment accompanied the apparently elevated diffusion of ^{144}Ce, ^{235}U, and ^{239}Pu discussed above, the opposite observation of relatively lower

concentrations of ^{137}Cs near the surface does not contradict higher diffusion through the compact because cesium is much more volatile and will not be retained in the compact matrix as strongly as cerium uranium, and plutonium. The diffusive depletion of ^{137}Cs from high-temperature compacts during the irradiation is supported by measurements of the inventory in the capsule rings and hardware for the capsules (Stempien et al. 2018a).

It is expected that safety testing did not significantly impact the DLBL-measured inventories and concentration profiles of ^{137}Cs, as safety test releases of ^{134}Cs observed by Stempien et al. (2018b) were minimal during 1200°C safety testing of Compact 10-2 (0.032 particle equivalents) and 1400°C safety testing of Compact 10-4 (0.14 particle equivalents). Compacts 10-1 and 10-4 were irradiated at nearly identical temperatures and experienced the same safety testing at 1400°C. However, DLBL measured less ^{137}Cs in Compact 10-1 than Compact 10-4, even though reirradiation of Compact 10-1 generated additional ^{137}Cs. It is possible that the variabilty in the DLBL measurements for the compacts with low ^{137}Cs inventory was due to significant contributions from hot cell contamination.

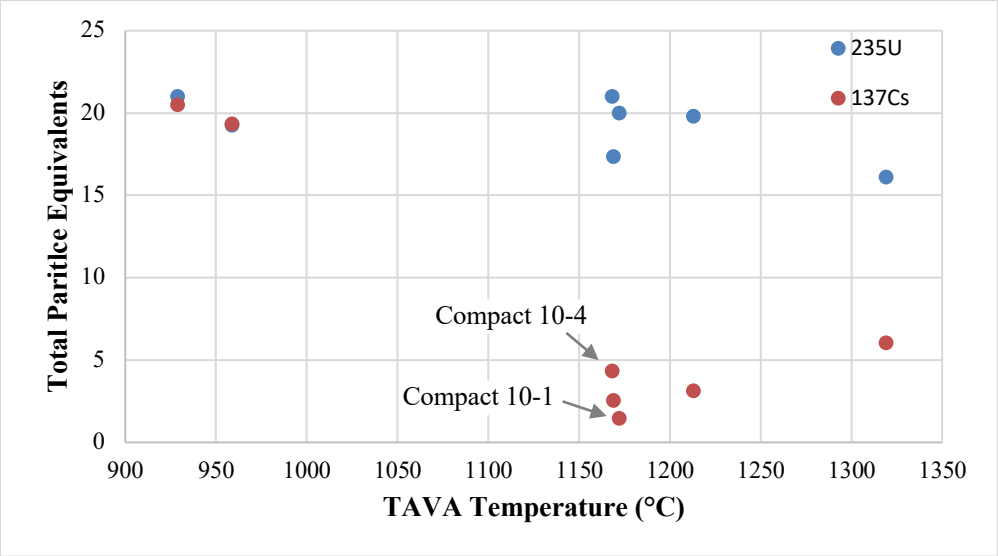

Figure 8-4. Comparison of ^{235}U and ^{137}Cs total inventories as a function of compact irradiation temperature.

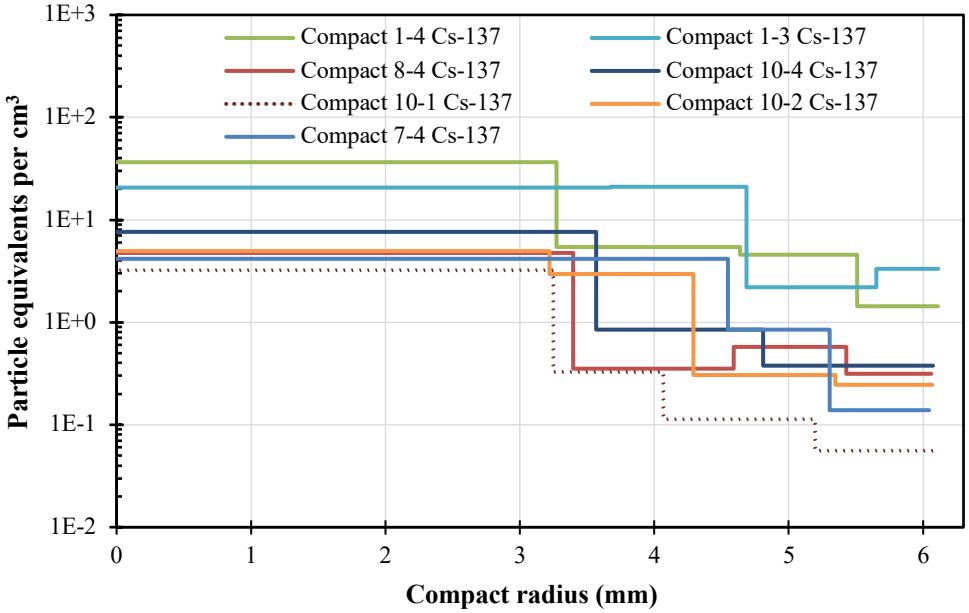

Figure 8-5. Comparison of ^{137}Cs concentration profiles in various AGR-3/4 compacts.

8.4 BEHAVIOR OF ^{90}Sr AND ^{154}Eu

^{90}Sr and ^{154}Eu show similar behavior across the compacts considered, with a combination of diffusive release from driver fuel particles, as well as diffusion out of the compact dependent on irradiation temperature and possibly burnup. As shown in Figure 8-6, the two compacts irradiated at lower temperatures (~950°C) had total inventories close to the expected 20 particle equivalents for ^{154}Eu, while the ^{90}Sr inventory was somewhat higher, suggesting some diffusive release from driver fuel particles. The concentration profiles for ^{90}Sr (Figure 8-7) and ^{154}Eu (Figure 8-8) in this temperature range show a strong peak in the core of the compact where the DTF particles were located and had the lowest inventories in the outer two segments, indicating little had diffused that far outward from the compact centerline.

The ^{90}Sr and ^{154}Eu inventories in Compact 10-1 were distinctly different than in Compact 10-4, which experienced very similar irradiation conditions and identical safety testing at 1400°C. This difference is assumed to have been caused by the reirradiation of Compact 10-1 elevating the ^{90}Sr and ^{154}Eu inventories.

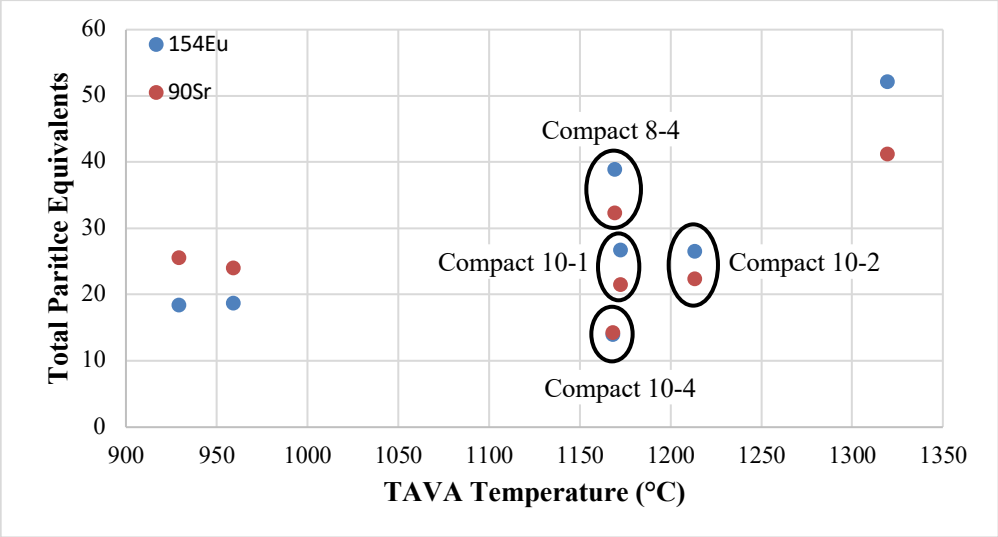

Figure 8-6. Comparison of ^{90}Sr and ^{154}Eu total inventories as a function of compact irradiation temperature.

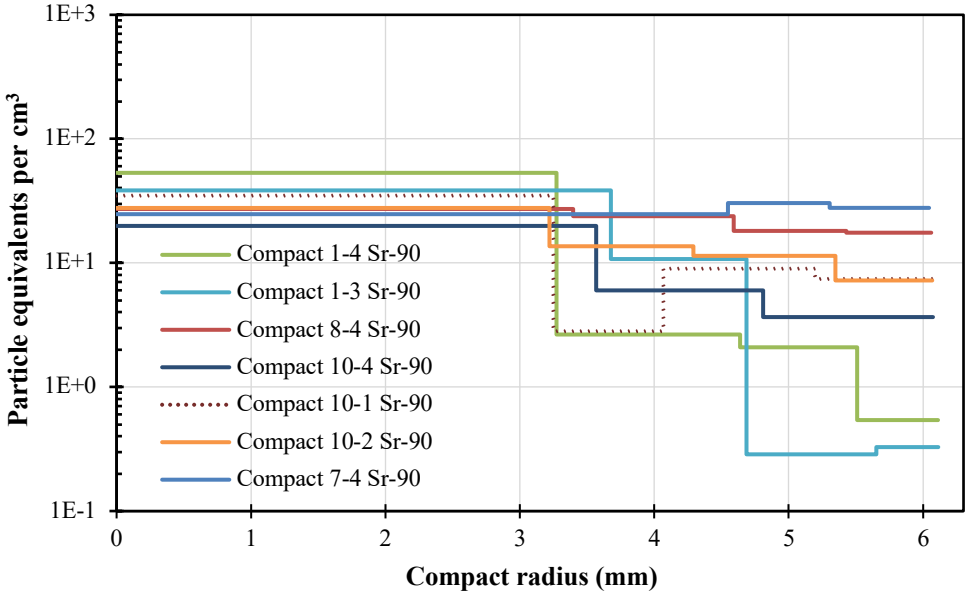

Figure 8-7. Comparison of ^{90}Sr concentration profiles in various AGR-3/4 compacts.

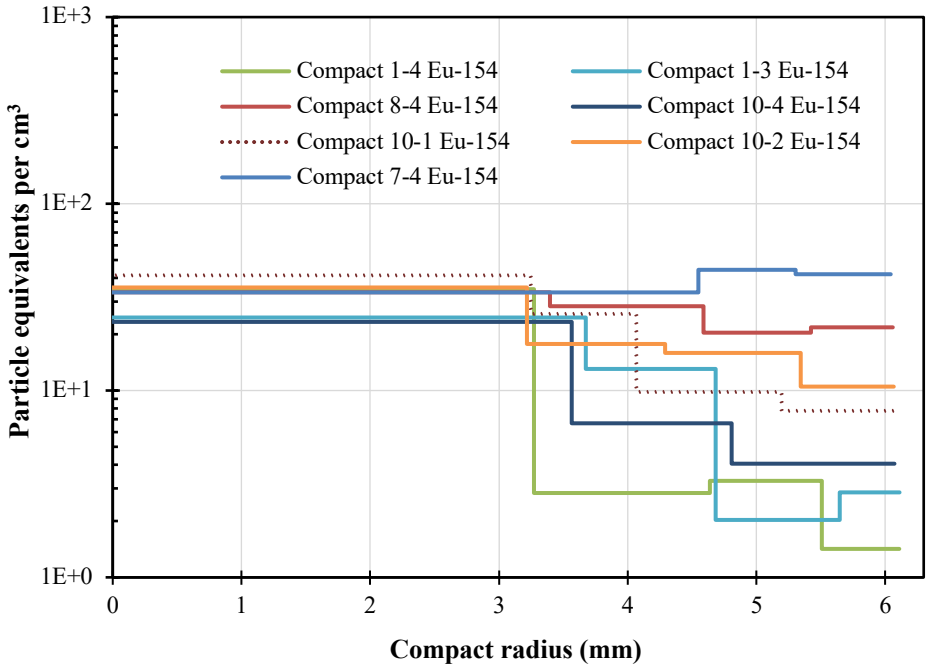

Figure 8-8. Comparison of ^{154}Eu concentration profiles in various AGR-3/4 compacts.

As shown in Figure 8-6, with increasing irradiation temperature, the total exposed inventory of ^{90}Sr and ^{154}Eu as measured by DLBL generally increased as a result of increasing diffusive release from driver fuel particles. Comparing only the four compacts not subjected to safety testing, the trend as a function of irradiation temperature is clear. In the highest temperature compact (Compact 7-4) the concentration profile for both ^{90}Sr and ^{154}Eu was slightly higher in the outer two segments as a significant fraction of the innermost segment concentration associated with DTF particles had diffused outward and significant release from intact driver fuel particles contributed to the measured concentration across the whole compact. In the middle temperature compact (Compact 8-4) the concentration profiles for both ^{90}Sr and ^{154}Eu step down slightly from the center of the compact as some contribution from the DTF particles source is still evident indicating slower diffusion than in Compact 7-4 and more moderate release from driver fuel particles. Finally, in the low temperature compacts (Compacts 1-3 and 1-4), the concentration profiles are dominated by diffusion from the DTF particle source in the center of the compacts, and this diffusion was significantly slower than the two higher temperature compacts.

An interesting difference in the total inventory of these isotopes was observed in Compact 8-4 compared with the two compacts from Capsule 10 not subjected to reirradiation. These compacts were irradiated at similar temperatures; however, Compact 8-4 was irradiated to a significantly higher fluence while Compacts 10-2 and 10-4 were safety tested at 1200°C and 1400°C respectively. The difference in behavior between them may be due to depletion of these isotopes from the Capsule 10 compacts during safety testing and/or increased release of ^{154}Eu and ^{90}Sr from driver fuel particles in Compact 8-4 due to higher fluence.

Stempien et al. (2018b) reported low cumulative releases of ^{90}Sr and ^{154}Eu were measured with the INL Fuel Accident Condition Simulator (FACS) for the 1200°C safety test of Compact 10-2 (0.0036 particle equivalents of ^{90}Sr and <0.0087 particle equivalents of ^{154}Eu) and 1400°C safety test of Compact 10-4 (0.080 particle equivalents of ^{90}Sr and 0.029 particle equivalents of ^{154}Eu). It was noted that these values likely underestimated the true compact releases because the condensation plate collection efficiencies in the FACS furnace at 1200°C and 1400°C are expected to be lower than the 1600°C collection efficiencies used to calculate the reported values. However, the actual efficiencies would have had to been two to three orders of magnitude lower than the 1600°C efficiencies to account for the differences in the DLBL data for Compacts 8-4, 10-2, and 10-4 with safety testing alone. For instance, assuming that

Compacts 10-2 and 10-4 started with exposed inventories equal to what were measured in Compact 8-4 by DLBL and only these inventories were impacted by the safety testing, then the safety test releases would have been 9.9 particle equivalents of ^{90}Sr and 12.4 particle equivalents of ^{154}Eu from Compact 10-2 at 1200°C and 18 particle equivalents of ^{90}Sr and 25 particle equivalents of ^{154}Eu from Compact 10-4 at 1400°C.

It is possible that the differences in the actual efficiencies and the 1600°C efficiencies for the FACS furnace were less than the two to three orders of magnitude necessary to explain the significantly higher inventories in Compact 8-4 compared with the safety tested Compacts 10-2 and 10-4. If this is the case, it suggests that the source of higher ^{90}Sr and ^{154}Eu in Compact 8-4 may have been the ~20% higher fluence to which it was irradiated. While irradiation temperature is known to be the dominant factor in diffusion of these isotopes, both within the compact and from intact driver fuel particles, increasing fluence may have played a secondary role.

As with ^{137}Cs, substantial inventories of ^{154}Eu and ^{90}Sr were measured in the capsule rings and hardware, supporting the conclusion of diffusive release from the compacts at high temperatures (Stempien et al. 2018a). The temperature-dependent diffusive release of ^{154}Eu and ^{90}Sr through intact SiC in the driver fuel particles is consistent with observations from AGR-1 and AGR-2 PIE and safety testing, in which releases of these elements tend to track together as a function of temperature (Demkowicz et al. 2015, Stempien et al. 2021). This similarity has been related to the fact that these elements both form carbides in the UCO fuel system.

9. CONCLUSIONS

Four compacts from the AGR-3/4 irradiation were subjected to radial DLBL to measure concentration profiles of key nuclides. Radial deconsolidation was successfully executed on all four compacts, regardless of some challenges caused by compacts detaching from the mounting rod and excess epoxy breaking the electrolytic circuit. Radial uniformity across each compact was excellent, and the previously developed automated image analysis method was applied to photos of the rotating residual compact after completion of each radial deconsolidation segment.

Leach-burn-leach analysis of the particles and matrix debris was performed using a well-tested and refined Soxhlet extraction method developed prior to the start of AGR-1 PIE. No issues were experienced with the extraction. Results of the DLBL were consistent with the presence of actinides and fission products from 20 DTF particles in three of the compacts; however, Compact 4-3 showed evidence of driver fuel particle fracture during compact detachment from the mounting rod, creating substantial difficulties in analyzing that data.

Comparison of the data reported herein with previously published data on AGR-3/4 compacts radially deconsolidated at ORNL provides a more complete picture of the behavior of key nuclides as a function of irradiation conditions. ^{144}Ce, ^{235}U, and ^{239}Pu were generally well retained within the compacts, with most of the compact inventory located within the core where the DTF particles were located and approximately exponential diffusion curves to the outer segments. At elevated irradiation temperature and fluence, there was some indication of diffusive release of ^{235}U and ^{239}Pu, with flatter concentration profiles near the compact surface and total compact inventories somewhat less than the expected 20 particle equivalents. Comparison of ^{137}Cs inventories and concentration profiles across compacts showed progressively more release due to increased diffusion with increasing irradiation temperature. The behaviors of ^{90}Sr and ^{154}Eu were more complex, with both diffusion of nuclides within the compacts and diffusive release from driver fuel particles increasing with irradiation temperature and possibly fluence.

10. REFERENCES

Collin, Blaise P. 2015. *AGR-3/4 Irradiation Experimental Plan.* INL/PLN-3867, Revision 1. Idaho Falls: Idaho National Laboratory.

Collin, Blaise P. 2016. *AGR-3/4 Irradiation Test Final As-Run Report.* INL/EXT-15-35550, Revision 1. Idaho Falls: Idaho National Laboratory.

Croff, Allen G. 1983. "ORIGEN2: A Versatile Computer Code for Calculating the Nuclide Compositions and Characteristics of Nuclear Materials." *Nucl. Tech.* 62: 335–352.

Demkowicz, Paul A., John D. Hunn, David A. Petti, and Robert N. Morris. 2016. "Key Results from Irradiation and Post-Irradiation Examination of AGR-1 UCO TRISO fuel." *Proc. 8th International Topical Meeting on High Temperature Reactor Technology (HTR-2016)*. Las Vegas, November 6–10, 2016. Also published in *Nucl. Eng. Des*. 329: 102–109.

Demkowicz, Paul A. 2017. *AGR-3/4 Phase 2 Post-Irradiation Examination Plan.* INL/PLN-5382, Revision 0. Idaho Falls: Idaho National Laboratory.

Hawkes, Grant L. 2016. *AGR-3/4 Daily As-Run Thermal Analyses.* INL/ECAR-2807, Revision 1. Idaho Falls: Idaho National Laboratory.

Helmreich, Grant W., Fred C. Montgomery, and John D. Hunn. 2015. *Development of a Radial Deconsolidation Method*. ORNL/TM-2015/699, Revision 0. Oak Ridge: Oak Ridge National Laboratory.

Helmreich, Grant W., John D. Hunn, Daniel R. Brown, and Brandon J. Blamer. 2018. "New Method for Analysis of X-ray Computed Tomography Scans of TRISO Fuel Forms." *Proc. 9th International Topical Meeting on High Temperature Reactor Technology (HTR-2018)*. Warsaw, October 8–10, 2018. Also published in *Nucl. Eng. Des.* 357: 110418.

Hunn, John D., and Richard A. Lowden. 2007. *Data Compilation for AGR-3/4 Driver Coated Particle Composite LEU03-09T*. ORNL/TM-2007/019, Revision 0. Oak Ridge: Oak Ridge National Laboratory.

Hunn, John D., Michael P. Trammell, and Fred C. Montgomery. 2011. *Data Compilation for AGR-3/4 Designed-to-Fail (DTF) Fuel Compact Lot (LEU03-10T-OP2/LEU03-07DTF-OP1)-Z*. ORNL/TM-2011/124, Revision 0. Oak Ridge: Oak Ridge National Laboratory.

Hunn, John D., Richard A. Lowden, James H. Miller, Brian C. Jolly, Michael P. Trammell, Andrew K. Kercher, Fred C. Montgomery, and Chinthaka M. Silva. 2012. "Fabrication and Characterization of Driver Fuel Particles, Designed-to-Fail Fuel Particles, and Fuel Compacts for the US AGR-3/4 Irradiation Test." *Proc. 6th International Topical Meeting on High Temperature Reactor Technology (HTR-2012)*. Tokyo, October 28–November 1, 2012. Also published in *Nucl. Eng. Des.* 271: 123–130.

Hunn, John D., Robert N. Morris, Charles A. Baldwin, Fred C. Montgomery, Chinthaka M. Silva, and Tyler J. Gerczak. 2012. *AGR-1 Irradiated Compact 6-1-1 PIE Report: Evaluation of As-Irradiated Fuel Performance Using Leach Burn Leach, IMGA, Materialography, and X-ray Tomography*. ORNL/TM-2012/233, Revision 0. Oak Ridge: Oak Ridge National Laboratory.

Hunn, John D., Robert N. Morris, Charles A. Baldwin, Fred C. Montgomery, Chinthaka M. Silva, and Tyler J. Gerczak. 2013. *AGR-1 Irradiated Compact 4-4-2 PIE Report: Evaluation of As-Irradiated Fuel Performance with Leach Burn Leach, IMGA, Materialography, and X-ray Tomography*. ORNL/TM-2013/236, Revision 0. Oak Ridge: Oak Ridge National Laboratory.

Hunn, John D., Robert N. Morris, Fred C. Montgomery, Tyler J. Gerczak, Darren J. Skitt, Charles A. Baldwin, John A. Dyer, Grant W. Helmreich, Brian D. Eckhart, Zachary M. Burns, Paul A. Demkowicz, and John D. Stempien. 2018. "Post-Irradiation Examination and Safety Testing of US

AGR-2 Irradiation Test Compacts." *Proc. 9th International Topical Meeting on High Temperature Reactor Technology (HTR-2018)*. Warsaw, October 8–10, 2018.

Hunn, John D., and Fred C. Montgomery. 2020. *Data Acquisition Method: Leach-Burn-Leach Analysis of Irradiated Fuel Compacts Using a Soxhlet Extractor in the 3525 Hot Cell*. AGR-CHAR-DAM-37, Revision 4. Oak Ridge: Oak Ridge National Laboratory.

Kercher, Andrew K., and John D. Hunn. 2006. *Results from ORNL Characterization of Nominal 350 µm LEUCO Kernels (LEU03) from the BWXT G73V-20-69303 Composite*. ORNL/TM-2006/552, Revision 0. Oak Ridge: Oak Ridge National Laboratory.

Kercher, Andrew K., Brian C. Jolly, Fred C. Montgomery, Chinthaka M. Silva, and John D. Hunn. 2011. *Data Compilation for AGR-3/4 Designed-to-Fail (DTF) Fuel Particle Batch LEU03-07DTF*. ORNL/TM-2011/109, Revision 0. Oak Ridge: Oak Ridge National Laboratory.

Lowden, Richard A. 2006. *Fabrication of Baseline and Variant Particle Fuel for AGR-1*. ORNL/CF-2006/02, Revision 0. Oak Ridge: Oak Ridge National Laboratory.

Ludwig, Scott B., and Allen G. Croff. 2002. *ORIGEN2.2—Isotope Generation and Depletion Code Matrix Exponential Method*. Oak Ridge: Oak Ridge National Laboratory.

Petti, David A., Richard R. Hobbins, James M. Kendall, and John J. Saurwein. 2005. *Technical Program Plan for the Advanced Gas Reactor Fuel Development and Qualification Program*. INL/EXT-05-00465, Revision 1. Idaho Falls: Idaho National Laboratory.

Stempien, John D., Francine J. Rice, Phil L. Winston, and Jason M. Harp. 2016. *AGR-3/4 Irradiation Test Train Disassembly and Component Metrology First Look Report.* INL/EXT-16-38005, Revision 1. Idaho Falls: Idaho National Laboratory.

Stempien, John D. 2017. *Radial Deconsolidation and Leach-Burn-Leach of AGR-3/4 Compact 3-3, 12-1, and 12-3.* INL/EXT-17-43182, Revision 0. Idaho Falls: Idaho National Laboratory.

Stempien, John D., Paul A. Demkowicz, Jason M. Harp, and Philip L. Watson. 2018a. *AGR-3/4 Experiment Preliminary Mass Balance.* INL/EXT-18-46049, Revision 0. Idaho Falls: Idaho National Laboratory.

Stempien, John D., Paul A. Demkowicz, Edward L. Reber, and Cad L. Christensen. 2018b. "Preliminary Results from the First Round of Post-Irradiation Heating Tests of Fuel Compacts from the AGR-3/4 Irradiation." *Proc. 9th International Topical Meeting on High Temperature Reactor Technology (HTR-2018)*. Warsaw, October 8–10, 2018.

Stempien, John D. 2021. *AGR-3/4 Post-Irradiation Examination*. INL/MIS-21-63208, Revision 0. Idaho Falls: Idaho National Laboratory.

Stempien, John D., Paul A. Demkowicz, Edward L. Reber, and Cad L. Christensen. 2021. "Reirradiation and Heating Testing of AGR-3/4 TRISO Fuels." *Proc. 10th International Topical Meeting on High Temperature Reactor Technology (HTR-2021)*. Yogyakarta, June 2–4, 2021.

Sterbentz, James W. 2015. *JMOCUP As-Run Daily Depletion Calculation for the AGR-3/4 TRISO Particle Experiment in ATR Northeast Flux Trap.* ECAR-2753, Revision 1. Idaho Falls: Idaho National Laboratory.

X-5 Monte Carlo Team. 2003. *MCNP—A General Monte Carlo N-Particle Transport Code.* Version 5, Volume I (LA-UR-03-1987) and Volume II (LA-CP-03-0245). Los Alamos: Los Alamos National Laboratory.

APPENDIX A. DLBL DATA

APPENDIX A. DLBL DATA

The tables in this appendix document the DLBL data for select actinides and fission products (both radionuclides and stable nuclides). Data is provided for each primary leach solution in terms of compact fraction and particle equivalents, as described in Section 2. Appendix B contains the calculated inventory data used to convert the measured values to compact fraction. Particle equivalents were calculated from the compact fraction by multiplying by an average number of particles per compact of 1918.

In some cases, stable and radioactive isotopes of the same element were reported. The compact fraction data for ^{133}Cs and ^{137}Cs tended to agree closely, while ^{134}Cs was often lower. The ^{140}Ce compact fraction tended to track with, but somewhat exceed that of ^{144}Ce, and the same was true for ^{153}Eu compared with ^{154}Eu and ^{155}Eu. It is possible that ^{133}Cs and ^{153}Eu data were elevated by isobaric interferences. The stable ^{109}Ag nuclide provided some indication of silver behavior in the absence of measurable ^{110m}Ag, which had gone through too many half-lives prior to analysis. However previous comparisons have indicated a typically poor agreement between these two isotopes (Hunn et al. 2013).

Appendix Table A-1. Exposed U and Pu detected by DLBL of AGR-3/4 Compact 1-3 Segment 1

DLBL Step	^{235}U	^{236}U	^{238}U	^{239}Pu	^{240}Pu
Deconsolidation acid	3.67E-6 (0.007)	2.38E-5 (0.046)	6.06E-5 (0.116)	5.09E-5 (0.098)	1.35E-4 (0.259)
Preburn leach 1	3.47E-7 (0.0007)	1.41E-6 (0.0027)	4.02E-6 (0.0077)	4.20E-6 (0.0081)	1.30E-5 (0.025)
Preburn leach 2	2.21E-7 (0.0004)	7.99E-7 (0.0015)	2.32E-6 (0.0045)	1.75E-6 (0.0034)	6.01E-6 (0.012)
Postburn leach 1	4.56E-7 (0.0009)	1.65E-6 (0.0032)	4.91E-6 (0.0094)	3.45E-6 (0.0066)	1.05E-5 (0.020)
Postburn leach 2	3.00E-7 (0.0006)	5.63E-7 (0.0011)	1.71E-6 (0.0033)	9.55E-7 (0.0018)	3.88E-6 (0.0074)
Total	5.00E-6 (0.0096)	2.82E-5 (0.054)	7.35E-5 (0.141)	6.12E-5 (0.117)	1.68E-4 (0.323)

Note: Values are reported as compact inventory fractions and particle equivalents (in parentheses).

Appendix Table A-2. Exposed U and Pu detected by DLBL of AGR-3/4 Compact 1-3 Segment 2

DLBL Step	^{235}U	^{236}U	^{238}U	^{239}Pu	^{240}Pu
Deconsolidation acid	1.38E-5 (0.026)	2.00E-5 (0.038)	4.37E-5 (0.084)	2.10E-5 (0.040)	4.63E-5 (0.089)
Preburn leach 1	4.34E-6 (0.0083)	2.02E-5 (0.039)	5.96E-5 (0.114)	4.40E-5 (0.084)	1.22E-4 (0.234)
Preburn leach 2	3.99E-7 (0.0008)	1.48E-6 (0.0028)	4.53E-6 (0.0087)	3.61E-6 (0.0069)	1.09E-5 (0.021)
Postburn leach 1	2.34E-6 (0.0045)	3.33E-6 (0.0064)	6.41E-6 (0.012)	4.04E-6 (0.0077)	8.29E-6 (0.016)
Postburn leach 2	2.86E-7 (0.0005)	2.77E-6 (0.0053)	4.63E-6 (0.0089)	3.34E-6 (0.0064)	9.68E-6 (0.019)
Total	2.11E-5 (0.041)	4.77E-5 (0.092)	1.19E-4 (0.228)	7.61E-5 (0.146)	1.97E-4 (0.378)

Note: Values are reported as compact inventory fractions and particle equivalents (in parentheses).

Appendix Table A-3. Exposed U and Pu detected by DLBL of AGR-3/4 Compact 1-3 Segment 3

DLBL Step	^{235}U	^{236}U	^{238}U	^{239}Pu	^{240}Pu
Deconsolidation acid	2.97E-3 (5.696)	2.98E-3 (5.714)	2.91E-3 (5.590)	1.56E-3 (3.000)	1.42E-3 (2.722)
Preburn leach 1	1.08E-5 (0.021)	1.18E-5 (0.023)	1.63E-5 (0.031)	3.11E-5 (0.060)	3.33E-5 (0.064)
Preburn leach 2	2.88E-7 (0.0006)	9.38E-7 (0.0018)	2.93E-6 (0.0056)	2.41E-6 (0.0046)	6.10E-6 (0.012)
Postburn leach 1	8.04E-7 (0.0015)	2.22E-6 (0.0043)	7.91E-6 (0.015)	7.09E-6 (0.014)	1.77E-5 (0.034)
Postburn leach 2	5.92E-8 (0.0001)	<3.6E-7 <(0.0007)	9.01E-7 (0.0017)	6.87E-7 (0.0013)	<2.8E-6 <(0.0054)
Total	2.98E-3 (5.719)	2.99E-3 (5.742)	2.94E-3 (5.644)	1.61E-3 (3.079)	1.48E-3 (2.832)

Note: Values are reported as compact inventory fractions and particle equivalents (in parentheses).

Appendix Table A-4. Exposed U and Pu detected by DLBL of AGR-3/4 Compact 1-3 Segment 4

DLBL Step	^{235}U	^{236}U	^{238}U	^{239}Pu	^{240}Pu
Deconsolidation acid	6.91E-3 (13.249)	6.95E-3 (13.322)	7.34E-3 (14.088)	7.20E-3 (13.805)	7.05E-3 (13.528)
Preburn leach 1	9.27E-5 (0.178)	9.35E-5 (0.179)	1.01E-4 (0.194)	1.76E-4 (0.338)	1.58E-4 (0.303)
Preburn leach 2	1.13E-5 (0.022)	1.22E-5 (0.023)	1.43E-5 (0.027)	1.67E-5 (0.032)	1.77E-5 (0.034)
Postburn leach 1	3.24E-5 (0.062)	3.39E-5 (0.065)	3.77E-5 (0.072)	2.17E-4 (0.416)	2.15E-4 (0.413)
Postburn leach 2	3.59E-7 (0.0007)	6.98E-7 (0.0013)	1.76E-6 (0.0034)	2.99E-6 (0.0057)	4.75E-6 (0.0091)
Total	7.04E-3 (13.511)	7.09E-3 (13.591)	7.50E-3 (14.385)	7.61E-3 (14.597)	7.45E-3 (14.287)

Note: Values are reported as compact inventory fractions and particle equivalents (in parentheses).

Appendix Table A-5. Exposed U and Pu detected by DLBL of AGR-3/4 Compact 4-3 Segment 1

DLBL Step	^{235}U	^{236}U	^{238}U	^{239}Pu	^{240}Pu
Deconsolidation acid	2.58E-4 (0.496)	2.53E-4 (0.486)	2.50E-4 (0.479)	5.45E-5 (0.105)	5.56E-5 (0.107)
Preburn leach 1	2.03E-5 (0.039)	1.98E-5 (0.038)	1.97E-5 (0.038)	5.51E-6 (0.011)	6.06E-6 (0.012)
Preburn leach 2	9.37E-7 (0.0018)	9.00E-7 (0.0017)	1.08E-6 (0.0021)	7.83E-7 (0.0015)	<1.1E-6 <(0.0021)
Postburn leach 1	7.78E-6 (0.015)	1.45E-5 (0.028)	6.05E-5 (0.116)	2.45E-5 (0.047)	3.68E-5 (0.071)
Postburn leach 2	1.54E-6 (0.0029)	2.31E-6 (0.0044)	7.89E-6 (0.015)	4.57E-6 (0.0088)	5.79E-6 (0.011)
Total	2.89E-4 (0.554)	2.91E-4 (0.558)	3.39E-4 (0.650)	8.99E-5 (0.172)	1.04E-4 (0.200)

Note: Values are reported as compact inventory fractions and particle equivalents (in parentheses).

Appendix Table A-6. Exposed U and Pu detected by DLBL of AGR-3/4 Compact 4-3 Segment 2

DLBL Step	^{235}U	^{236}U	^{238}U	^{239}Pu	^{240}Pu
Deconsolidation acid	4.10E-3 (7.855)	3.97E-3 (7.615)	3.88E-3 (7.449)	3.24E-3 (6.219)	3.33E-3 (6.387)
Preburn leach 1	4.76E-5 (0.091)	4.66E-5 (0.089)	5.06E-5 (0.097)	1.12E-4 (0.214)	1.15E-4 (0.221)
Preburn leach 2	9.21E-7 (0.0018)	9.48E-7 (0.0018)	1.39E-6 (0.0027)	2.08E-6 (0.004)	2.28E-6 (0.0044)
Postburn leach 1	1.66E-5 (0.032)	1.67E-5 (0.032)	1.68E-5 (0.032)	4.47E-5 (0.086)	4.91E-5 (0.094)
Postburn leach 2	4.33E-7 (0.0008)	3.62E-7 (0.0007)	1.75E-6 (0.0034)	1.73E-6 (0.0033)	1.92E-6 (0.0037)
Total	4.16E-3 (7.980)	4.04E-3 (7.739)	3.95E-3 (7.585)	3.40E-3 (6.526)	3.50E-3 (6.710)

Note: Values are reported as compact inventory fractions and particle equivalents (in parentheses).

Appendix Table A-7. Exposed U and Pu detected by DLBL of AGR-3/4 Compact 4-3 Segment 3

DLBL Step	^{235}U	^{236}U	^{238}U	^{239}Pu	^{240}Pu
Deconsolidation acid	1.48E-3 (2.836)	1.41E-3 (2.706)	1.37E-3 (2.626)	8.62E-4 (1.653)	8.67E-4 (1.663)
Preburn leach 1	4.13E-5 (0.079)	4.07E-5 (0.078)	4.05E-5 (0.078)	4.41E-5 (0.085)	4.51E-5 (0.086)
Preburn leach 2	1.24E-6 (0.0024)	1.20E-6 (0.0023)	2.04E-6 (0.0039)	1.95E-6 (0.0037)	2.44E-6 (0.0047)
Postburn leach 1	7.73E-4 (1.482)	7.10E-4 (1.361)	6.67E-4 (1.279)	6.60E-4 (1.266)	6.61E-4 (1.268)
Postburn leach 2	4.37E-6 (0.0084)	4.06E-6 (0.0078)	4.14E-6 (0.0079)	5.88E-6 (0.011)	5.78E-6 (0.011)
Total	2.30E-3 (4.408)	2.17E-3 (4.156)	2.08E-3 (3.995)	1.57E-3 (3.018)	1.58E-3 (3.033)

Note: Values are reported as compact inventory fractions and particle equivalents (in parentheses).

Appendix Table A-8. Exposed U and Pu detected by DLBL of AGR-3/4 Compact 4-3 Segment 4

DLBL Step	^{235}U	^{236}U	^{238}U	^{239}Pu	^{240}Pu
Deconsolidation acid	9.44E-3 (18.110)	8.98E-3 (17.224)	8.67E-3 (16.636)	7.85E-3 (15.053)	7.95E-3 (15.252)
Preburn leach 1	1.22E-4 (0.234)	1.15E-4 (0.221)	1.17E-4 (0.225)	3.78E-4 (0.724)	3.95E-4 (0.757)
Preburn leach 2	6.13E-6 (0.012)	5.74E-6 (0.011)	6.18E-6 (0.012)	2.42E-5 (0.046)	2.55E-5 (0.049)
Postburn leach 1	7.33E-4 (1.406)	6.88E-4 (1.319)	6.67E-4 (1.280)	9.43E-4 (1.809)	9.58E-4 (1.837)
Postburn leach 2	3.51E-6 (0.0067)	3.31E-6 (0.0063)	3.49E-6 (0.0067)	7.52E-6 (0.014)	7.81E-6 (0.015)
Total	1.03E-2 (19.768)	9.79E-3 (18.782)	9.47E-3 (18.159)	9.20E-3 (17.647)	9.34E-3 (17.910)

Note: Values are reported as compact inventory fractions and particle equivalents (in parentheses).

Appendix Table A-9. Exposed U and Pu detected by DLBL of AGR-3/4 Compact 10-1 Segment 1

DLBL Step	^{235}U	^{236}U	^{238}U	^{239}Pu	^{240}Pu
Deconsolidation acid	2.37E-5 (0.045)	2.66E-5 (0.051)	3.05E-5 (0.058)	1.61E-5 (0.031)	1.73E-5 (0.033)
Preburn leach 1	6.95E-7 (0.0013)	1.03E-6 (0.002)	2.68E-6 (0.0051)	2.04E-6 (0.0039)	2.68E-6 (0.0051)
Preburn leach 2	3.54E-7 (0.0007)	5.65E-7 (0.0011)	1.73E-6 (0.0033)	1.41E-6 (0.0027)	2.18E-6 (0.0042)
Postburn leach 1	1.30E-5 (0.025)	1.25E-5 (0.024)	1.36E-5 (0.026)	4.61E-5 (0.088)	6.82E-5 (0.131)
Postburn leach 2	2.38E-7 (0.0005)	<2.2E-7 <(0.0004)	4.79E-7 (0.0009)	9.88E-7 (0.0019)	1.57E-6 (0.003)
Total	3.79E-5 (0.073)	4.07E-5 (0.078)	4.90E-5 (0.094)	6.66E-5 (0.128)	9.19E-5 (0.176)

Note: Values are reported as compact inventory fractions and particle equivalents (in parentheses).

Appendix Table A-10. Exposed U and Pu detected by DLBL of AGR-3/4 Compact 10-1 Segment 2

DLBL Step	^{235}U	^{236}U	^{238}U	^{239}Pu	^{240}Pu
Deconsolidation acid	4.10E-4 (0.786)	4.18E-4 (0.802)	3.85E-4 (0.737)	1.44E-4 (0.276)	1.39E-4 (0.266)
Preburn leach 1	5.24E-6 (0.010)	5.37E-6 (0.010)	6.54E-6 (0.013)	3.53E-6 (0.0068)	4.14E-6 (0.0079)
Preburn leach 2	1.45E-7 (0.0003)	2.26E-7 (0.0004)	3.71E-7 (0.0007)	7.39E-7 (0.0014)	<1.2E-6 <(0.0022)
Postburn leach 1	1.27E-5 (0.024)	1.28E-5 (0.025)	1.36E-5 (0.026)	4.89E-5 (0.094)	8.40E-5 (0.161)
Postburn leach 2	1.66E-7 (0.0003)	<2.1E-7 <(0.0004)	4.58E-7 (0.0009)	8.21E-7 (0.0016)	1.37E-6 (0.0026)
Total	4.28E-4 (0.821)	4.37E-4 (0.837)	4.06E-4 (0.778)	1.98E-4 (0.380)	2.28E-4 (0.437)

Note: Values are reported as compact inventory fractions and particle equivalents (in parentheses).

Appendix Table A-11. Exposed U and Pu detected by DLBL of AGR-3/4 Compact 10-1 Segment 3

DLBL Step	^{235}U	^{236}U	^{238}U	^{239}Pu	^{240}Pu
Deconsolidation acid	3.38E-4 (0.648)	3.45E-4 (0.662)	3.20E-4 (0.613)	1.36E-4 (0.260)	1.30E-4 (0.250)
Preburn leach 1	1.36E-5 (0.026)	1.38E-5 (0.026)	1.67E-5 (0.032)	1.29E-5 (0.025)	1.54E-5 (0.030)
Preburn leach 2	1.42E-7 (0.0003)	<2.1E-7 <(0.0004)	6.29E-7 (0.0012)	<3.8E-7 <(0.0007)	<1.1E-6 <(0.0021)
Postburn leach 1	1.07E-5 (0.020)	1.15E-5 (0.022)	1.23E-5 (0.024)	4.43E-5 (0.085)	7.49E-5 (0.144)
Postburn leach 2	2.82E-6 (0.0054)	2.74E-6 (0.0053)	3.21E-6 (0.0062)	1.13E-5 (0.022)	2.03E-5 (0.039)
Total	3.65E-4 (0.701)	3.73E-4 (0.715)	3.53E-4 (0.677)	2.04E-4 (0.391)	2.41E-4 (0.462)

Note: Values are reported as compact inventory fractions and particle equivalents (in parentheses).

Appendix Table A-12. Exposed U and Pu detected by DLBL of AGR-3/4 Compact 10-1 Segment 4

DLBL Step	^{235}U	^{236}U	^{238}U	^{239}Pu	^{240}Pu
Deconsolidation acid	9.10E-3 (17.455)	8.95E-3 (17.162)	9.54E-3 (18.290)	7.12E-3 (13.651)	6.73E-3 (12.916)
Preburn leach 1	2.63E-4 (0.504)	2.59E-4 (0.497)	2.48E-4 (0.475)	4.27E-4 (0.819)	5.15E-4 (0.988)
Preburn leach 2	4.57E-6 (0.0088)	4.78E-6 (0.0092)	5.41E-6 (0.010)	1.06E-5 (0.020)	1.38E-5 (0.026)
Postburn leach 1	2.36E-4 (0.452)	2.35E-4 (0.451)	2.25E-4 (0.431)	2.17E-3 (4.167)	2.84E-3 (5.446)
Postburn leach 2	3.44E-6 (0.0066)	3.43E-6 (0.0066)	3.40E-6 (0.0065)	2.57E-5 (0.049)	3.52E-5 (0.068)
Total	9.61E-3 (18.426)	9.45E-3 (18.126)	1.00E-2 (19.213)	9.75E-3 (18.707)	1.01E-2 (19.444)

Note: Values are reported as compact inventory fractions and particle equivalents (in parentheses).

Appendix Table A-13. Exposed U and Pu detected by DLBL of AGR-3/4 Compact 10-2 Segment 1

DLBL Step	^{235}U	^{236}U	^{238}U	^{239}Pu	^{240}Pu
Deconsolidation acid	6.21E-6 (0.012)	7.56E-6 (0.014)	3.68E-5 (0.071)	1.52E-5 (0.029)	2.13E-5 (0.041)
Preburn leach 1	6.06E-7 (0.0012)	8.64E-7 (0.0017)	5.15E-6 (0.0099)	3.21E-6 (0.0061)	5.09E-6 (0.0098)
Preburn leach 2	2.15E-7 (0.0004)	2.88E-7 (0.0006)	1.18E-6 (0.0023)	1.03E-6 (0.002)	1.54E-6 (0.003)
Postburn leach 1	8.91E-6 (0.017)	9.07E-6 (0.017)	1.26E-5 (0.024)	4.25E-5 (0.082)	6.53E-5 (0.125)
Postburn leach 2	2.22E-7 (0.0004)	3.46E-7 (0.0007)	2.35E-6 (0.0045)	2.13E-6 (0.0041)	2.94E-6 (0.0056)
Total	1.62E-5 (0.031)	1.81E-5 (0.035)	5.80E-5 (0.111)	6.41E-5 (0.123)	9.62E-5 (0.184)

Note: Values are reported as compact inventory fractions and particle equivalents (in parentheses).

Appendix Table A-14. Exposed U and Pu detected by DLBL of AGR-3/4 Compact 10-2 Segment 2

DLBL Step	^{235}U	^{236}U	^{238}U	^{239}Pu	^{240}Pu
Deconsolidation acid	6.05E-5 (0.116)	5.82E-5 (0.112)	8.42E-5 (0.162)	1.97E-5 (0.038)	1.99E-5 (0.038)
Preburn leach 1	9.41E-7 (0.0018)	1.10E-6 (0.0021)	3.42E-6 (0.0066)	2.13E-6 (0.0041)	2.81E-6 (0.0054)
Preburn leach 2	1.29E-7 (0.0002)	<2.2E-7 <(0.0004)	4.90E-7 (0.0009)	6.41E-7 (0.0012)	<1.2E-6 <(0.0024)
Postburn leach 1	1.78E-5 (0.034)	1.79E-5 (0.034)	1.97E-5 (0.038)	7.97E-5 (0.153)	1.38E-4 (0.264)
Postburn leach 2	8.66E-8 (0.0002)	<2.3E-7 <(0.0004)	4.02E-7 (0.0008)	7.91E-7 (0.0015)	<1.3E-6 <(0.0024)
Total	7.94E-5 (0.152)	7.71E-5 (0.148)	1.08E-4 (0.208)	1.03E-4 (0.198)	1.60E-4 (0.307)

Note: Values are reported as compact inventory fractions and particle equivalents (in parentheses).

Appendix Table A-15. Exposed U and Pu detected by DLBL of AGR-3/4 Compact 10-2 Segment 3

DLBL Step	^{235}U	^{236}U	^{238}U	^{239}Pu	^{240}Pu
Deconsolidation acid	2.36E-3 (4.535)	2.22E-3 (4.260)	2.23E-3 (4.286)	1.31E-3 (2.510)	1.04E-3 (2.002)
Preburn leach 1	1.61E-5 (0.031)	1.63E-5 (0.031)	2.20E-5 (0.042)	2.53E-5 (0.049)	2.26E-5 (0.043)
Preburn leach 2	1.01E-6 (0.0019)	9.83E-7 (0.0019)	1.85E-6 (0.0036)	2.02E-6 (0.0039)	2.45E-6 (0.0047)
Postburn leach 1	1.03E-5 (0.020)	1.01E-5 (0.019)	1.06E-5 (0.020)	5.05E-5 (0.097)	7.81E-5 (0.150)
Postburn leach 2	2.65E-7 (0.0005)	4.40E-7 (0.0008)	1.78E-6 (0.0034)	1.56E-6 (0.003)	2.37E-6 (0.0046)
Total	2.39E-3 (4.588)	2.25E-3 (4.313)	2.27E-3 (4.356)	1.39E-3 (2.662)	1.15E-3 (2.204)

Note: Values are reported as compact inventory fractions and particle equivalents (in parentheses).

Appendix Table A-16. Exposed U and Pu detected by DLBL of AGR-3/4 Compact 10-2 Segment 4

DLBL Step	^{235}U	^{236}U	^{238}U	^{239}Pu	^{240}Pu
Deconsolidation acid	7.73E-3 (14.824)	7.19E-3 (13.796)	7.29E-3 (13.991)	6.33E-3 (12.137)	6.03E-3 (11.564)
Preburn leach 1	6.87E-5 (0.132)	6.46E-5 (0.124)	6.53E-5 (0.125)	4.75E-4 (0.911)	6.34E-4 (1.216)
Preburn leach 2	2.38E-6 (0.0046)	2.44E-6 (0.0047)	3.25E-6 (0.0062)	1.97E-5 (0.038)	2.80E-5 (0.054)
Postburn leach 1	4.72E-5 (0.091)	4.51E-5 (0.087)	4.57E-5 (0.088)	1.50E-3 (2.873)	2.25E-3 (4.317)
Postburn leach 2	6.81E-7 (0.0013)	7.17E-7 (0.0014)	1.66E-6 (0.0032)	6.47E-5 (0.124)	9.87E-5 (0.189)
Total	7.85E-3 (15.053)	7.31E-3 (14.013)	7.41E-3 (14.213)	8.39E-3 (16.083)	9.04E-3 (17.341)

Note: Values are reported as compact inventory fractions and particle equivalents (in parentheses).

Appendix Table A-17. Typically tracked beta/gamma-emitting fission products detected by DLBL of AGR-3/4 Compact 1-3 Segment 1

DLBL Step	^{90}Sr	^{106}Ru	^{110m}Ag	^{125}Sb	^{134}Cs	^{137}Cs	^{144}Ce	^{154}Eu	^{155}Eu
Deconsolidation acid	2.79E-5 (0.053)	<1.2E-4 <(0.240)	<6.9E-2 <(133.106)	<8.7E-5 <(0.167)	1.45E-4 (0.278)	2.15E-4 (0.413)	<4.3E-5 <(0.083)	1.06E-4 (0.203)	4.82E-5 (0.093)
Preburn leach 1	2.60E-6 (0.005)	<4.8E-5 <(0.091)	<5.1E-2 <(97.791)	<2.4E-5 <(0.045)	8.96E-6 (0.017)	9.87E-6 (0.019)	<1.5E-5 <(0.030)	<1.1E-5 <(0.020)	2.65E-5 (0.051)
Preburn leach 2	1.09E-6 (0.0021)	<2.8E-5 <(0.054)	<3.3E-2 <(62.738)	<1.2E-5 <(0.023)	3.94E-6 (0.0076)	3.67E-6 (0.007)	<8.5E-6 <(0.016)	<5.7E-6 <(0.011)	<9.2E-6 <(0.018)
Postburn leach 1	3.87E-6 (0.0074)	<1.1E-4 <(0.207)	<8.4E-2 <(160.591)	<6.1E-5 <(0.118)	2.54E-4 (0.486)	1.32E-4 (0.253)	1.74E-5 (0.033)	1.76E-4 (0.338)	1.10E-4 (0.210)
Postburn leach 2	8.33E-7 (0.0016)	<4.1E-5 <(0.078)	<3.8E-2 <(73.748)	<1.8E-5 <(0.035)	1.10E-5 (0.021)	7.83E-6 (0.015)	<1.2E-5 <(0.023)	<7.4E-6 <(0.014)	<1.4E-5 <(0.027)
Total	3.63E-5 (0.070)	0.00E+0 (0.000)	0.00E+0 (0.000)	0.00E+0 (0.000)	4.22E-4 (0.810)	3.68E-4 (0.707)	1.74E-5 (0.033)	2.82E-4 (0.541)	1.84E-4 (0.354)

Note 1: Chemical separation and beta analysis were used to measure ^{90}Sr; other nuclides were measured by gamma spectrometry.
Note 2: Values are reported as compact inventory fractions and particle equivalents (in parentheses).
Note 3: A less-than value indicates that the concentration in the leachate was below the minimum detectable limit; these values are not included in the totals.

Appendix Table A-18. Typically tracked beta/gamma-emitting fission products detected by DLBL of AGR-3/4 Compact 1-3 Segment 2

DLBL Step	^{90}Sr	^{106}Ru	^{110m}Ag	^{125}Sb	^{134}Cs	^{137}Cs	^{144}Ce	^{154}Eu	^{155}Eu
Deconsolidation acid	2.04E-5 (0.039)	<1.5E-4 <(0.286)	<7.1E-2 <(135.984)	<9.1E-5 <(0.175)	2.01E-4 (0.385)	2.88E-4 (0.552)	4.87E-5 (0.093)	5.69E-5 (0.109)	<5.0E-5 <(0.095)
Preburn leach 1	2.83E-5 (0.054)	7.58E-5 (0.145)	<8.7E-2 <(167.255)	<5.5E-5 <(0.105)	1.98E-5 (0.038)	6.25E-5 (0.120)	1.01E-4 (0.193)	8.71E-5 (0.167)	5.00E-5 (0.096)
Preburn leach 2	2.64E-6 (0.0051)	<5.2E-5 <(0.100)	<6.4E-2 <(123.207)	<2.4E-5 <(0.045)	2.37E-6 (0.0045)	5.64E-6 (0.011)	1.00E-5 (0.019)	<9.6E-6 <(0.019)	<2.4E-5 <(0.046)
Postburn leach 1	4.47E-6 (0.0086)	<1.1E-4 <(0.209)	<8.5E-2 <(163.366)	<6.5E-5 <(0.124)	1.55E-4 (0.297)	8.40E-5 (0.161)	<3.7E-5 <(0.070)	2.22E-4 (0.427)	1.04E-4 (0.199)
Postburn leach 2	2.21E-6 (0.0042)	<6.0E-5 <(0.116)	<5.8E-2 <(111.926)	<2.8E-5 <(0.053)	5.40E-6 (0.010)	5.62E-6 (0.011)	<1.8E-5 <(0.035)	<1.1E-5 <(0.022)	<2.7E-5 <(0.053)
Total	5.81E-5 (0.111)	7.58E-5 (0.145)	0.00E+0 (0.000)	0.00E+0 (0.000)	3.83E-4 (0.735)	4.46E-4 (0.855)	1.59E-4 (0.306)	3.67E-4 (0.703)	1.54E-4 (0.295)

Note 1: Chemical separation and beta analysis were used to measure ^{90}Sr; other nuclides were measured by gamma spectrometry.
Note 2: Values are reported as compact inventory fractions and particle equivalents (in parentheses).
Note 3: A less-than value indicates that the concentration in the leachate was below the minimum detectable limit; these values are not included in the totals.

Appendix Table A-19. Typically tracked beta/gamma-emitting fission products detected by DLBL of AGR-3/4 Compact 1-3 Segment 3

DLBL Step	^{90}Sr	^{106}Ru	^{110m}Ag	^{125}Sb	^{134}Cs	^{137}Cs	^{144}Ce	^{154}Eu	^{155}Eu
Deconsolidation acid	1.82E-3 (3.500)	6.74E-4 (1.293)	<2.6E-1 <(501.431)	<3.6E-4 <(0.683)	2.66E-3 (5.107)	3.52E-3 (6.757)	2.31E-3 (4.422)	1.74E-3 (3.333)	1.88E-3 (3.603)
Preburn leach 1	8.23E-6 (0.016)	7.97E-5 (0.153)	<4.4E-2 <(84.431)	<2.5E-5 <(0.049)	1.35E-5 (0.026)	2.15E-5 (0.041)	1.96E-5 (0.038)	1.24E-5 (0.024)	<1.6E-5 <(0.031)
Preburn leach 2	1.68E-6 (0.0032)	<3.6E-5 <(0.070)	<4.4E-2 <(83.443)	5.13E-5 (0.098)	3.77E-6 (0.0072)	5.84E-6 (0.011)	<1.1E-5 <(0.022)	<6.8E-6 <(0.013)	<1.3E-5 <(0.025)
Postburn leach 1	7.45E-6 (0.014)	<1.0E-4 <(0.191)	<8.8E-2 <(168.247)	2.07E-4 (0.397)	1.04E-4 (0.199)	5.92E-5 (0.114)	<3.2E-5 <(0.062)	2.56E-4 (0.492)	1.46E-4 (0.279)
Postburn leach 2	6.05E-7 (0.0012)	<5.0E-5 <(0.097)	<5.9E-2 <(112.843)	<2.0E-5 <(0.038)	3.05E-6 (0.0058)	2.13E-6 (0.0041)	<1.5E-5 <(0.028)	<9.1E-6 <(0.017)	<2.2E-5 <(0.042)
Total	1.84E-3 (3.534)	7.54E-4 (1.446)	0.00E+0 (0.000)	2.58E-4 (0.495)	2.79E-3 (5.344)	3.61E-3 (6.927)	2.32E-3 (4.459)	2.01E-3 (3.848)	2.02E-3 (3.882)

Note 1: Chemical separation and beta analysis were used to measure ^{90}Sr; other nuclides were measured by gamma spectrometry.
Note 2: Values are reported as compact inventory fractions and particle equivalents (in parentheses).
Note 3: A less-than value indicates that the concentration in the leachate was below the minimum detectable limit; these values are not included in the totals.

Appendix Table A-20. Typically tracked beta/gamma-emitting fission products detected by DLBL of AGR-3/4 Compact 1-3 Segment 4

DLBL Step	^{90}Sr	^{106}Ru	^{110m}Ag	^{125}Sb	^{134}Cs	^{137}Cs	^{144}Ce	^{154}Eu	^{155}Eu
Deconsolidation acid	9.70E-3 (18.601)	4.88E-3 (9.360)	<3.6E-1 <(699.710)	1.69E-3 (3.246)	3.67E-3 (7.034)	5.06E-3 (9.702)	8.02E-3 (15.387)	5.36E-3 (10.279)	6.01E-3 (11.532)
Preburn leach 1	1.12E-4 (0.215)	1.47E-3 (2.812)	<1.0E-1 <(200.303)	1.49E-3 (2.859)	3.64E-4 (0.697)	4.89E-4 (0.938)	9.90E-5 (0.190)	8.68E-5 (0.167)	8.43E-5 (0.162)
Preburn leach 2	1.52E-5 (0.029)	1.75E-4 (0.336)	<4.7E-2 <(89.401)	6.33E-4 (1.214)	1.47E-5 (0.028)	1.94E-5 (0.037)	2.97E-5 (0.057)	<1.1E-5 <(0.021)	<2.1E-5 <(0.040)
Postburn particle leach 1	7.45E-4 (1.428)	<1.7E-4 <(0.335)	<1.4E-1 <(261.422)	2.49E-3 (4.770)	8.43E-5 (0.162)	8.81E-5 (0.169)	3.72E-4 (0.714)	5.88E-4 (1.129)	6.37E-4 (1.222)
Postburn particle leach 2	6.72E-6 (0.013)	<4.1E-5 <(0.078)	<3.9E-2 <(74.438)	1.57E-4 (0.301)	3.74E-6 (0.0072)	4.75E-6 (0.0091)	<1.6E-5 <(0.031)	<1.0E-5 <(0.020)	<2.6E-5 <(0.051)
Total	1.06E-2 (20.287)	6.52E-3 (12.507)	0.00E+0 (0.000)	6.46E-3 (12.391)	4.13E-3 (7.928)	5.66E-3 (10.856)	8.52E-3 (16.348)	6.03E-3 (11.574)	6.73E-3 (12.915)

Note 1: Chemical separation and beta analysis were used to measure ^{90}Sr; other nuclides were measured by gamma spectrometry.
Note 2: Values are reported as compact inventory fractions and particle equivalents (in parentheses).
Note 3: A less-than value indicates that the concentration in the leachate was below the minimum detectable limit; these values are not included in the totals.

Appendix Table A-21. Typically tracked beta/gamma-emitting fission products detected by DLBL of AGR-3/4 Compact 4-3 Segment 1

DLBL Step	^{90}Sr	^{106}Ru	^{110m}Ag	^{125}Sb	^{134}Cs	^{137}Cs	^{144}Ce	^{154}Eu	^{155}Eu
Deconsolidation acid	1.04E-4 (0.199)	<9.0E-5 <(0.172)	<1.8E-2 <(34.700)	9.11E-5 (0.175)	2.24E-4 (0.429)	3.58E-4 (0.686)	1.43E-4 (0.273)	2.07E-5 (0.040)	2.58E-5 (0.049)
Preburn leach 1	3.99E-4 (0.766)	<4.6E-5 <(0.087)	<1.0E-2 <(19.538)	<3.7E-5 <(0.071)	5.78E-5 (0.111)	7.85E-5 (0.151)	3.64E-5 (0.070)	5.32E-6 (0.010)	1.24E-5 (0.024)
Preburn leach 2	4.36E-5 (0.084)	<2.8E-5 <(0.054)	<8.1E-3 <(15.510)	<2.0E-5 <(0.038)	6.97E-6 (0.013)	9.88E-6 (0.019)	<1.7E-5 <(0.032)	<2.9E-6 <(0.0056)	<1.1E-5 <(0.021)
Postburn leach 1	2.73E-6 (0.0052)	3.44E-5 (0.066)	<8.7E-3 <(16.637)	<1.8E-5 <(0.035)	1.48E-5 (0.028)	3.18E-5 (0.061)	5.05E-5 (0.097)	5.69E-5 (0.109)	6.08E-5 (0.117)
Postburn leach 2	4.45E-6 (0.0085)	<2.1E-5 <(0.040)	<8.4E-3 <(16.138)	<1.3E-5 <(0.026)	4.62E-6 (0.0089)	8.07E-6 (0.015)	<1.3E-5 <(0.026)	<1.7E-6 <(0.0032)	<5.2E-6 <(0.0099)
Total	5.54E-4 (1.062)	3.44E-5 (0.066)	0.00E+0 (0.000)	9.11E-5 (0.175)	3.08E-4 (0.591)	4.86E-4 (0.932)	2.29E-4 (0.440)	8.29E-5 (0.159)	9.90E-5 (0.190)

Note 1: Chemical separation and beta analysis were used to measure ^{90}Sr; other nuclides were measured by gamma spectrometry.
Note 2: Values are reported as compact inventory fractions and particle equivalents (in parentheses).
Note 3: A less-than value indicates that the concentration in the leachate was below the minimum detectable limit; these values are not included in the totals.

Appendix Table A-22. Typically tracked beta/gamma-emitting fission products detected by DLBL of AGR-3/4 Compact 4-3 Segment 2

DLBL Step	^{90}Sr	^{106}Ru	^{110m}Ag	^{125}Sb	^{134}Cs	^{137}Cs	^{144}Ce	^{154}Eu	^{155}Eu
Deconsolidation acid	3.09E-3 (5.922)	1.39E-3 (2.660)	<9.4E-2 <(180.434)	1.80E-3 (3.450)	2.10E-3 (4.020)	2.84E-3 (5.438)	5.51E-3 (10.569)	2.15E-3 (4.130)	2.39E-3 (4.581)
Preburn leach 1	5.89E-5 (0.113)	1.50E-3 (2.881)	<1.6E-2 <(29.891)	1.72E-4 (0.329)	9.57E-5 (0.184)	1.35E-4 (0.258)	1.07E-4 (0.205)	3.39E-5 (0.065)	3.28E-5 (0.063)
Preburn leach 2	5.51E-6 (0.011)	8.87E-5 (0.170)	<7.7E-3 <(14.787)	<1.7E-5 <(0.033)	1.02E-5 (0.020)	1.55E-5 (0.030)	<1.4E-5 <(0.027)	<2.4E-6 <(0.0046)	<7.1E-6 <(0.014)
Postburn leach 1	3.52E-4 (0.676)	<5.6E-5 <(0.108)	<1.7E-2 <(32.010)	<3.7E-5 <(0.071)	6.02E-5 (0.115)	8.17E-5 (0.157)	1.45E-4 (0.278)	1.64E-4 (0.314)	1.97E-4 (0.377)
Postburn leach 2	5.63E-7 (0.0011)	<1.8E-5 <(0.035)	<8.7E-3 <(16.731)	<7.8E-6 <(0.015)	5.47E-7 (0.001)	1.29E-6 (0.0025)	<9.9E-6 <(0.019)	<3.4E-6 <(0.0065)	<4.0E-6 <(0.0077)
Total	3.50E-3 (6.722)	2.98E-3 (5.711)	0.00E+0 (0.000)	1.97E-3 (3.780)	2.26E-3 (4.339)	3.07E-3 (5.885)	5.76E-3 (11.052)	2.35E-3 (4.509)	2.62E-3 (5.021)

Note 1: Chemical separation and beta analysis were used to measure ^{90}Sr; other nuclides were measured by gamma spectrometry.
Note 2: Values are reported as compact inventory fractions and particle equivalents (in parentheses).
Note 3: A less-than value indicates that the concentration in the leachate was below the minimum detectable limit; these values are not included in the totals.

Appendix Table A-23. Typically tracked beta/gamma-emitting fission products detected by DLBL of AGR-3/4 Compact 4-3 Segment 3

DLBL Step	^{90}Sr	^{106}Ru	^{110m}Ag	^{125}Sb	^{134}Cs	^{137}Cs	^{144}Ce	^{154}Eu	^{155}Eu
Deconsolidation acid	2.81E-4 (0.538)	1.45E-4 (0.277)	<2.4E-2 <(46.568)	1.87E-4 (0.358)	1.85E-4 (0.356)	3.88E-4 (0.744)	1.45E-3 (2.781)	2.98E-4 (0.572)	3.83E-4 (0.735)
Preburn leach 1	2.08E-5 (0.040)	1.02E-4 (0.196)	<1.4E-2 <(27.131)	<3.8E-5 <(0.073)	2.31E-5 (0.044)	3.62E-5 (0.069)	9.59E-5 (0.184)	1.50E-5 (0.029)	<1.9E-5 <(0.037)
Preburn leach 2	3.30E-6 (0.0063)	<1.9E-5 <(0.036)	<6.9E-3 <(13.266)	<1.3E-5 <(0.024)	3.59E-6 (0.0069)	5.64E-6 (0.011)	1.05E-5 (0.020)	<2.5E-6 <(0.0047)	<9.6E-6 <(0.018)
Postburn leach 1	9.96E-4 (1.910)	<1.4E-4 <(0.262)	<3.0E-2 <(57.727)	3.24E-4 (0.622)	3.47E-4 (0.666)	4.52E-4 (0.866)	1.21E-3 (2.316)	6.46E-4 (1.240)	7.11E-4 (1.363)
Postburn leach 2	5.73E-6 (0.011)	<1.5E-5 <(0.030)	<5.8E-3 <(11.198)	2.30E-5 (0.044)	3.53E-6 (0.0068)	5.14E-6 (0.0098)	1.21E-5 (0.023)	3.33E-6 (0.0064)	<3.9E-6 <(0.0075)
Total	1.31E-3 (2.506)	2.47E-4 (0.474)	0.00E+0 (0.000)	5.34E-4 (1.024)	5.63E-4 (1.079)	8.86E-4 (1.700)	2.78E-3 (5.325)	9.63E-4 (1.847)	1.09E-3 (2.099)

Note 1: Chemical separation and beta analysis were used to measure ^{90}Sr; other nuclides were measured by gamma spectrometry.
Note 2: Values are reported as compact inventory fractions and particle equivalents (in parentheses).
Note 3: A less-than value indicates that the concentration in the leachate was below the minimum detectable limit; these values are not included in the totals.

Appendix Table A-24. Typically tracked beta/gamma-emitting fission products detected by DLBL of AGR-3/4 Compact 4-3 Segment 4

DLBL Step	^{90}Sr	^{106}Ru	^{110m}Ag	^{125}Sb	^{134}Cs	^{137}Cs	^{144}Ce	^{154}Eu	^{155}Eu
Deconsolidation acid	2.94E-3 (5.631)	2.98E-3 (5.723)	<4.8E-2 <(92.891)	0.00E+0 (0.000)	2.81E-4 (0.539)	7.48E-4 (1.434)	1.50E-2 (28.829)	2.74E-3 (5.247)	3.46E-3 (6.643)
Preburn leach 1	7.06E-4 (1.355)	1.78E-3 (3.413)	<2.1E-2 <(40.336)	7.06E-4 (1.355)	2.84E-5 (0.054)	4.65E-5 (0.089)	3.99E-4 (0.765)	3.82E-4 (0.732)	4.19E-4 (0.804)
Preburn leach 2	1.76E-4 (0.337)	2.25E-4 (0.431)	<1.0E-2 <(19.415)	1.76E-4 (0.337)	6.60E-6 (0.013)	1.02E-5 (0.019)	5.89E-5 (0.113)	9.42E-5 (0.181)	9.57E-5 (0.184)
Postburn particle leach 1	7.72E-3 (14.816)	9.22E-5 (0.177)	<6.8E-2 <(129.809)	7.72E-3 (14.816)	3.07E-4 (0.589)	4.09E-4 (0.784)	2.26E-3 (4.329)	4.55E-3 (8.725)	4.20E-3 (8.049)
Postburn particle leach 2	3.46E-5 (0.066)	2.23E-5 (0.043)	<7.9E-3 <(15.207)	3.46E-5 (0.066)	3.68E-6 (0.0071)	5.36E-6 (0.010)	1.17E-5 (0.022)	2.26E-5 (0.043)	2.80E-5 (0.054)
Total	1.16E-2 (22.205)	5.10E-3 (9.786)	0.00E+0 (0.000)	4.25E-3 (8.157)	6.27E-4 (1.202)	1.22E-3 (2.337)	1.78E-2 (34.059)	7.78E-3 (14.929)	8.20E-3 (15.734)

Note 1: Chemical separation and beta analysis were used to measure ^{90}Sr; other nuclides were measured by gamma spectrometry.
Note 2: Values are reported as compact inventory fractions and particle equivalents (in parentheses).
Note 3: A less-than value indicates that the concentration in the leachate was below the minimum detectable limit; these values are not included in the totals.

Appendix Table A-25. Typically tracked beta/gamma-emitting fission products detected by DLBL of AGR-3/4 Compact 10-1 Segment 1

DLBL Step	^{90}Sr	^{106}Ru	^{110m}Ag	^{125}Sb	^{134}Cs	^{137}Cs	^{144}Ce	^{154}Eu	^{155}Eu
Deconsolidation acid	3.02E-4 (0.579)	<6.2E-5 <(0.119)	<3.8E-2 <(72.172)	<2.5E-5 <(0.047)	1.34E-6 (0.0026)	5.72E-6 (0.011)	2.58E-5 (0.050)	2.81E-4 (0.539)	2.23E-4 (0.429)
Preburn leach 1	4.94E-5 (0.095)	<2.5E-5 <(0.049)	<1.7E-2 <(32.178)	<1.1E-5 <(0.020)	<5.2E-7 <(0.001)	1.31E-6 (0.0025)	<1.3E-5 <(0.026)	8.11E-5 (0.156)	8.49E-5 (0.163)
Preburn leach 2	1.19E-5 (0.023)	<1.8E-5 <(0.034)	<1.2E-2 <(23.838)	6.08E-6 (0.012)	1.67E-7 (0.0003)	8.92E-7 (0.0017)	<8.1E-6 <(0.016)	1.47E-5 (0.028)	1.79E-5 (0.034)
Postburn leach 1	1.12E-3 (2.139)	<6.1E-5 <(0.117)	<4.3E-2 <(82.570)	<2.0E-5 <(0.038)	1.50E-6 (0.0029)	2.94E-6 (0.0056)	<3.1E-5 <(0.059)	1.01E-3 (1.939)	1.08E-3 (2.076)
Postburn leach 2	6.32E-6 (0.012)	<1.6E-5 <(0.031)	<1.1E-2 <(22.030)	<6.2E-6 <(0.012)	<3.7E-7 <(0.0007)	3.97E-7 (0.0008)	<8.5E-6 <(0.016)	5.41E-6 (0.010)	6.65E-6 (0.013)
Total	1.48E-3 (2.847)	0.00E+0 (0.000)	0.00E+0 (0.000)	6.08E-6 (0.012)	3.01E-6 (0.0058)	1.13E-5 (0.022)	2.58E-5 (0.050)	1.39E-3 (2.672)	1.42E-3 (2.714)

Note 1: Chemical separation and beta analysis were used to measure ^{90}Sr; other nuclides were measured by gamma spectrometry.
Note 2: Values are reported as compact inventory fractions and particle equivalents (in parentheses).
Note 3: A less-than value indicates that the concentration in the leachate was below the minimum detectable limit; these values are not included in the totals.

Appendix Table A-26. Typically tracked beta/gamma-emitting fission products detected by DLBL of AGR-3/4 Compact 10-1 Segment 2

DLBL Step	^{90}Sr	^{106}Ru	^{110m}Ag	^{125}Sb	^{134}Cs	^{137}Cs	^{144}Ce	^{154}Eu	^{155}Eu
Deconsolidation acid	3.02E-4 (0.580)	2.13E-4 (0.408)	<2.8E-2 <(52.897)	<2.3E-5 <(0.045)	4.83E-6 (0.0093)	2.06E-5 (0.040)	9.42E-5 (0.181)	2.24E-4 (0.430)	2.36E-4 (0.452)
Preburn leach 1	6.67E-5 (0.128)	5.36E-5 (0.103)	<1.7E-2 <(32.715)	<7.5E-6 <(0.014)	<5.7E-7 <(0.0011)	9.38E-7 (0.0018)	<1.5E-5 <(0.028)	7.29E-5 (0.140)	7.83E-5 (0.150)
Preburn leach 2	8.50E-6 (0.016)	<1.5E-5 <(0.029)	<1.1E-2 <(21.462)	<5.5E-6 <(0.010)	<3.0E-7 <(0.0006)	1.81E-7 (0.0003)	<6.4E-6 <(0.012)	1.22E-5 (0.023)	1.44E-5 (0.028)
Postburn leach 1	1.53E-3 (2.936)	<8.3E-5 <(0.160)	<5.5E-2 <(105.149)	4.57E-5 (0.088)	2.15E-6 (0.0041)	2.25E-6 (0.0043)	<2.8E-5 <(0.053)	1.54E-3 (2.955)	1.58E-3 (3.028)
Postburn leach 2	1.16E-5 (0.022)	<1.8E-5 <(0.035)	<1.4E-2 <(26.081)	<6.1E-6 <(0.012)	<3.8E-7 <(0.0007)	2.55E-7 (0.0005)	<8.6E-6 <(0.017)	1.07E-5 (0.021)	1.25E-5 (0.024)
Total	1.92E-3 (3.683)	2.66E-4 (0.511)	0.00E+0 (0.000)	4.57E-5 (0.088)	6.98E-6 (0.013)	2.42E-5 (0.047)	9.42E-5 (0.181)	1.86E-3 (3.569)	1.92E-3 (3.682)

Note 1: Chemical separation and beta analysis were used to measure ^{90}Sr; other nuclides were measured by gamma spectrometry.
Note 2: Values are reported as compact inventory fractions and particle equivalents (in parentheses).
Note 3: A less-than value indicates that the concentration in the leachate was below the minimum detectable limit; these values are not included in the totals.

Appendix Table A-27. Typically tracked beta/gamma-emitting fission products detected by DLBL of AGR-3/4 Compact 10-1 Segment 3

DLBL Step	^{90}Sr	^{106}Ru	^{110m}Ag	^{125}Sb	^{134}Cs	^{137}Cs	^{144}Ce	^{154}Eu	^{155}Eu
Deconsolidation acid	2.68E-4 (0.514)	1.53E-4 (0.294)	<2.3E-2 <(45.061)	1.83E-5 (0.035)	7.82E-6 (0.015)	3.39E-5 (0.065)	8.47E-5 (0.162)	2.01E-4 (0.385)	2.06E-4 (0.394)
Preburn leach 1	1.00E-5 (0.019)	1.30E-4 (0.249)	<3.1E-2 <(59.503)	<1.6E-5 <(0.030)	7.48E-7 (0.0014)	3.23E-6 (0.0062)	2.11E-5 (0.040)	2.67E-4 (0.511)	2.66E-4 (0.509)
Preburn leach 2	3.57E-7 (0.0007)	<1.5E-5 <(0.029)	<1.3E-2 <(25.519)	<6.2E-6 <(0.012)	<3.4E-7 <(0.0007)	2.15E-7 (0.0004)	<9.1E-6 <(0.017)	6.15E-6 (0.012)	7.40E-6 (0.014)
Postburn leach 1	4.97E-5 (0.095)	<9.8E-5 <(0.188)	<6.9E-2 <(132.026)	<3.1E-5 <(0.059)	<1.7E-6 <(0.0032)	1.94E-6 (0.0037)	<6.0E-5 <(0.116)	1.83E-3 (3.501)	1.91E-3 (3.672)
Postburn leach 2	1.35E-5 (0.026)	<5.2E-5 <(0.100)	<3.1E-2 <(60.200)	<1.4E-5 <(0.027)	<8.9E-7 <(0.0017)	6.22E-7 (0.0012)	<2.7E-5 <(0.052)	4.70E-4 (0.901)	4.74E-4 (0.908)
Total	3.42E-4 (0.655)	2.83E-4 (0.543)	0.00E+0 (0.000)	1.83E-5 (0.035)	8.57E-6 (0.016)	3.99E-5 (0.077)	1.06E-4 (0.203)	2.77E-3 (5.310)	2.87E-3 (5.498)

Note 1: Chemical separation and beta analysis were used to measure ^{90}Sr; other nuclides were measured by gamma spectrometry.
Note 2: Values are reported as compact inventory fractions and particle equivalents (in parentheses).
Note 3: A less-than value indicates that the concentration in the leachate was below the minimum detectable limit; these values are not included in the totals.

Appendix Table A-28. Typically tracked beta/gamma-emitting fission products detected by DLBL of AGR-3/4 Compact 10-1 Segment 4

DLBL Step	^{90}Sr	^{106}Ru	^{110m}Ag	^{125}Sb	^{134}Cs	^{137}Cs	^{144}Ce	^{154}Eu	^{155}Eu
Deconsolidation acid	1.70E-3 (3.255)	4.88E-3 (9.357)	<5.8E-2 <(111.031)	<9.0E-5 <(0.172)	1.45E-4 (0.277)	6.11E-4 (1.171)	4.65E-3 (8.923)	9.48E-4 (1.819)	1.43E-3 (2.752)
Preburn leach 1	1.68E-4 (0.321)	2.12E-3 (4.059)	<4.9E-2 <(94.309)	<4.3E-5 <(0.082)	1.65E-5 (0.032)	6.14E-5 (0.118)	1.48E-3 (2.844)	6.22E-4 (1.193)	7.17E-4 (1.375)
Preburn leach 2	2.04E-5 (0.039)	1.68E-4 (0.322)	<1.7E-2 <(32.182)	<8.2E-6 <(0.016)	3.01E-7 (0.0006)	1.49E-6 (0.0029)	7.96E-5 (0.153)	2.48E-5 (0.048)	3.24E-5 (0.062)
Postburn particle leach 1	5.54E-3 (10.625)	<1.1E-4 <(0.210)	<1.6E-1 <(300.176)	<6.3E-5 <(0.121)	9.63E-6 (0.018)	1.75E-5 (0.034)	1.16E-2 (22.309)	6.24E-3 (11.965)	6.88E-3 (13.189)
Postburn particle leach 2	6.18E-5 (0.119)	1.18E-4 (0.227)	<2.5E-2 <(47.178)	2.45E-5 (0.047)	<7.0E-7 <(0.0013)	9.36E-7 (0.0018)	1.40E-4 (0.269)	7.55E-5 (0.145)	8.45E-5 (0.162)
Total	7.49E-3 (14.359)	7.28E-3 (13.965)	0.00E+0 (0.000)	2.45E-5 (0.047)	1.71E-4 (0.328)	6.92E-4 (1.327)	1.80E-2 (34.498)	7.91E-3 (15.169)	9.15E-3 (17.540)

Note 1: Chemical separation and beta analysis were used to measure ^{90}Sr; other nuclides were measured by gamma spectrometry.
Note 2: Values are reported as compact inventory fractions and particle equivalents (in parentheses).
Note 3: A less-than value indicates that the concentration in the leachate was below the minimum detectable limit; these values are not included in the totals.

Appendix Table A-29. Typically tracked beta/gamma-emitting fission products detected by DLBL of AGR-3/4 Compact 10-2 Segment 1

DLBL Step	^{90}Sr	^{106}Ru	^{110m}Ag	^{125}Sb	^{134}Cs	^{137}Cs	^{144}Ce	^{154}Eu	^{155}Eu
Deconsolidation acid	4.69E-4 (0.900)	<5.5E-5 <(0.106)	<2.8E-2 <(52.952)	8.24E-5 (0.158)	4.18E-6 (0.008)	1.90E-5 (0.036)	4.26E-5 (0.082)	4.57E-4 (0.877)	5.20E-4 (0.998)
Preburn leach 1	9.42E-5 (0.181)	<2.7E-5 <(0.051)	<1.4E-2 <(26.510)	<1.3E-5 <(0.026)	1.15E-6 (0.0022)	3.56E-6 (0.0068)	<1.6E-5 <(0.030)	1.96E-4 (0.375)	2.06E-4 (0.394)
Preburn leach 2	1.00E-5 (0.019)	<1.2E-5 <(0.023)	<7.9E-3 <(15.079)	<5.9E-6 <(0.011)	4.46E-7 (0.0009)	1.17E-6 (0.0022)	<5.3E-6 <(0.010)	2.58E-5 (0.049)	3.31E-5 (0.064)
Postburn leach 1	6.36E-4 (1.219)	<4.6E-5 <(0.088)	<2.8E-2 <(54.579)	<1.6E-5 <(0.031)	1.10E-5 (0.021)	1.60E-5 (0.031)	2.62E-5 (0.050)	8.91E-4 (1.709)	9.63E-4 (1.848)
Postburn leach 2	3.18E-6 (0.0061)	<1.3E-5 <(0.025)	<7.5E-3 <(14.411)	<6.9E-6 <(0.013)	7.25E-7 (0.0014)	1.50E-6 (0.0029)	<6.2E-6 <(0.012)	<1.5E-6 <(0.0028)	<4.5E-6 <(0.0087)
Total	1.21E-3 (2.325)	0.00E+0 (0.000)	0.00E+0 (0.000)	8.24E-5 (0.158)	1.75E-5 (0.034)	4.13E-5 (0.079)	6.88E-5 (0.132)	1.57E-3 (3.011)	1.72E-3 (3.304)

Note 1: Chemical separation and beta analysis were used to measure ^{90}Sr; other nuclides were measured by gamma spectrometry.
Note 2: Values are reported as compact inventory fractions and particle equivalents (in parentheses).
Note 3: A less-than value indicates that the concentration in the leachate was below the minimum detectable limit; these values are not included in the totals.

Appendix Table A-30. Typically tracked beta/gamma-emitting fission products detected by DLBL of AGR-3/4 Compact 10-2 Segment 2

DLBL Step	^{90}Sr	^{106}Ru	^{110m}Ag	^{125}Sb	^{134}Cs	^{137}Cs	^{144}Ce	^{154}Eu	^{155}Eu
Deconsolidation acid	4.68E-4 (0.897)	<4.6E-5 <(0.088)	<2.2E-2 <(41.298)	3.66E-5 (0.070)	1.17E-5 (0.022)	4.46E-5 (0.086)	2.62E-5 (0.050)	3.93E-4 (0.753)	4.04E-4 (0.775)
Preburn leach 1	8.54E-5 (0.164)	<3.0E-5 <(0.058)	<1.8E-2 <(34.220)	1.72E-5 (0.033)	9.12E-7 (0.0018)	2.76E-6 (0.0053)	<1.2E-5 <(0.024)	2.31E-4 (0.443)	2.42E-4 (0.464)
Preburn leach 2	1.06E-5 (0.020)	<1.8E-5 <(0.034)	<1.1E-2 <(20.854)	<8.6E-6 <(0.016)	<4.8E-7 <(0.0009)	4.89E-7 (0.0009)	<8.0E-6 <(0.015)	1.69E-5 (0.032)	2.40E-5 (0.046)
Postburn leach 1	1.80E-3 (3.455)	<1.3E-4 <(0.254)	<8.5E-2 <(163.896)	<5.4E-5 <(0.104)	1.00E-5 (0.019)	1.57E-5 (0.030)	5.33E-5 (0.102)	2.30E-3 (4.420)	2.46E-3 (4.712)
Postburn leach 2	2.61E-6 (0.005)	<1.2E-5 <(0.024)	<9.0E-3 <(17.307)	<5.4E-6 <(0.010)	<3.0E-7 <(0.0006)	1.96E-7 (0.0004)	<8.2E-6 <(0.016)	3.91E-6 (0.0075)	9.58E-6 (0.018)
Total	2.37E-3 (4.542)	0.00E+0 (0.000)	0.00E+0 (0.000)	5.39E-5 (0.103)	2.27E-5 (0.043)	6.38E-5 (0.122)	7.95E-5 (0.152)	2.95E-3 (5.657)	3.14E-3 (6.016)

Note 1: Chemical separation and beta analysis were used to measure ^{90}Sr; other nuclides were measured by gamma spectrometry.
Note 2: Values are reported as compact inventory fractions and particle equivalents (in parentheses).
Note 3: A less-than value indicates that the concentration in the leachate was below the minimum detectable limit; these values are not included in the totals.

Appendix Table A-31. Typically tracked beta/gamma-emitting fission products detected by DLBL of AGR-3/4 Compact 10-2 Segment 3

DLBL Step	^{90}Sr	^{106}Ru	^{110m}Ag	^{125}Sb	^{134}Cs	^{137}Cs	^{144}Ce	^{154}Eu	^{155}Eu
Deconsolidation acid	8.92E-4 (1.711)	2.77E-4 (0.530)	<3.4E-2 <(65.618)	1.25E-4 (0.240)	1.12E-4 (0.216)	4.69E-4 (0.900)	6.53E-4 (1.253)	5.99E-4 (1.149)	8.22E-4 (1.576)
Preburn leach 1	1.36E-4 (0.260)	1.04E-4 (0.199)	<2.5E-2 <(47.334)	2.31E-5 (0.044)	1.37E-6 (0.0026)	5.98E-6 (0.011)	<1.6E-5 <(0.031)	4.94E-4 (0.948)	5.01E-4 (0.961)
Preburn leach 2	1.70E-5 (0.033)	<2.4E-5 <(0.046)	<1.4E-2 <(26.840)	1.19E-5 (0.023)	3.70E-7 (0.0007)	9.84E-7 (0.0019)	<1.2E-5 <(0.024)	5.70E-5 (0.109)	5.81E-5 (0.111)
Postburn leach 1	1.18E-3 (2.270)	<5.7E-5 <(0.109)	<3.8E-2 <(73.137)	<2.0E-5 <(0.039)	3.48E-6 (0.0067)	5.14E-6 (0.0099)	4.32E-5 (0.083)	1.43E-3 (2.750)	1.50E-3 (2.877)
Postburn leach 2	6.93E-6 (0.013)	<2.0E-5 <(0.039)	<1.2E-2 <(23.294)	<9.6E-6 <(0.018)	1.02E-6 (0.002)	2.40E-6 (0.0046)	6.37E-6 (0.012)	9.41E-6 (0.018)	1.31E-5 (0.025)
Total	2.24E-3 (4.288)	3.80E-4 (0.729)	0.00E+0 (0.000)	1.60E-4 (0.307)	1.19E-4 (0.228)	4.84E-4 (0.928)	7.03E-4 (1.348)	2.59E-3 (4.975)	2.89E-3 (5.551)

Note 1: Chemical separation and beta analysis were used to measure ^{90}Sr; other nuclides were measured by gamma spectrometry.
Note 2: Values are reported as compact inventory fractions and particle equivalents (in parentheses).
Note 3: A less-than value indicates that the concentration in the leachate was below the minimum detectable limit; these values are not included in the totals.

Appendix Table A-32. Typically tracked beta/gamma-emitting fission products detected by DLBL of AGR-3/4 Compact 10-2 Segment 4

DLBL Step	^{90}Sr	^{106}Ru	^{110m}Ag	^{125}Sb	^{134}Cs	^{137}Cs	^{144}Ce	^{154}Eu	^{155}Eu
Deconsolidation acid	1.93E-3 (3.701)	4.09E-3 (7.846)	<4.3E-2 <(81.624)	1.34E-3 (2.579)	2.35E-4 (0.451)	9.57E-4 (1.835)	4.43E-3 (8.498)	1.12E-3 (2.155)	1.86E-3 (3.565)
Preburn leach 1	3.78E-4 (0.724)	4.30E-3 (8.251)	<4.1E-2 <(78.109)	4.02E-4 (0.771)	2.37E-5 (0.046)	8.07E-5 (0.155)	1.60E-3 (3.068)	9.79E-4 (1.879)	1.02E-3 (1.955)
Preburn leach 2	2.27E-5 (0.044)	1.53E-4 (0.294)	<4.1E-2 <(79.254)	9.47E-5 (0.182)	5.64E-7 (0.0011)	2.58E-6 (0.005)	7.94E-5 (0.152)	4.64E-5 (0.089)	4.64E-5 (0.089)
Postburn particle leach 1	3.53E-3 (6.762)	<1.1E-4 <(0.216)	<6.3E-2 <(120.589)	1.63E-3 (3.129)	4.57E-6 (0.0088)	8.40E-6 (0.016)	4.79E-3 (9.184)	4.55E-3 (8.721)	4.62E-3 (8.856)
Postburn particle leach 2	2.12E-5 (0.041)	<1.9E-5 <(0.036)	<9.6E-3 <(18.331)	1.32E-4 (0.252)	6.76E-7 (0.0013)	1.65E-6 (0.0032)	1.45E-4 (0.279)	2.78E-5 (0.053)	2.31E-5 (0.044)
Total	5.88E-3 (11.272)	8.55E-3 (16.391)	0.00E+0 (0.000)	3.60E-3 (6.913)	2.65E-4 (0.508)	1.05E-3 (2.014)	1.10E-2 (21.181)	6.72E-3 (12.898)	7.56E-3 (14.508)

Note 1: Chemical separation and beta analysis were used to measure ^{90}Sr; other nuclides were measured by gamma spectrometry.
Note 2: Values are reported as compact inventory fractions and particle equivalents (in parentheses).
Note 3: A less-than value indicates that the concentration in the leachate was below the minimum detectable limit; these values are not included in the totals.

Appendix Table A-33. Exposed inventory of stable nuclides of interest detected by DLBL of AGR-3/4 Compact 1-3 Segment 1

DLBL Step	^{105}Pd	^{109}Ag	^{133}Cs	^{139}La	^{140}Ce	^{141}Pr	^{146}Nd	^{152}Sm	^{153}Eu	^{156}Gd
Deconsolidation acid	<1.1E-4 <(0.216)	2.01E-3 (3.848)	1.78E-4 (0.342)	2.14E-4 (0.410)	1.17E-4 (0.225)	6.35E-5 (0.122)	6.33E-5 (0.121)	4.94E-5 (0.095)	4.58E-4 (0.878)	8.95E-4 (1.716)
Preburn leach 1	<1.4E-4 <(0.259)	4.77E-4 (0.915)	<4.1E-6 <(0.0079)	3.35E-5 (0.064)	1.82E-4 (0.350)	2.53E-5 (0.049)	2.54E-5 (0.049)	<4.1E-5 <(0.079)	<8.2E-5 <(0.157)	3.61E-4 (0.692)
Preburn leach 2	<1.4E-4 <(0.269)	<2.4E-4 <(0.460)	<4.3E-6 <(0.0082)	8.81E-6 (0.017)	1.25E-4 (0.239)	2.00E-5 (0.038)	1.99E-5 (0.038)	<4.3E-5 <(0.082)	<8.5E-5 <(0.163)	<3.4E-4 <(0.652)
Postburn particle leach 1	<1.5E-4 <(0.288)	1.62E-3 (3.108)	9.53E-5 (0.183)	1.48E-5 (0.028)	1.58E-4 (0.302)	2.54E-5 (0.049)	2.55E-5 (0.049)	5.08E-5 (0.097)	2.18E-4 (0.418)	4.30E-4 (0.825)
Postburn particle leach 2	<1.4E-4 <(0.274)	3.27E-4 (0.628)	<4.3E-6 <(0.0083)	<4.2E-6 <(0.0081)	1.05E-4 (0.202)	5.58E-6 (0.011)	<7.3E-6 <(0.014)	<4.3E-5 <(0.083)	<8.7E-5 <(0.166)	<3.5E-4 <(0.664)
Total	0.00E+0 (0.000)	4.43E-3 (8.498)	2.74E-4 (0.525)	2.71E-4 (0.519)	6.87E-4 (1.318)	1.40E-4 (0.268)	1.34E-4 (0.257)	1.00E-4 (0.192)	6.75E-4 (1.295)	1.69E-3 (3.233)

Note 1: Values are reported as compact inventory fractions and particle equivalents (in parentheses).
Note 2: A less-than value indicates that the concentration in the leachate was below the minimum detectable limit; these values are not included in the totals.

Appendix Table A-34. Exposed inventory of stable nuclides of interest detected by DLBL of AGR-3/4 Compact 1-3 Segment 2

DLBL Step	^{105}Pd	^{109}Ag	^{133}Cs	^{139}La	^{140}Ce	^{141}Pr	^{146}Nd	^{152}Sm	^{153}Eu	^{156}Gd
Deconsolidation acid	<1.3E-4 <(0.245)	3.61E-1 (691.849)	2.67E-4 (0.512)	1.37E-4 (0.263)	7.02E-5 (0.135)	4.50E-5 (0.086)	4.17E-5 (0.080)	<3.9E-5 <(0.075)	3.93E-4 (0.754)	4.52E-4 (0.867)
Preburn leach 1	<1.4E-4 <(0.274)	1.47E-1 (281.179)	4.66E-5 (0.089)	8.35E-5 (0.160)	2.37E-4 (0.455)	1.07E-4 (0.205)	1.09E-4 (0.208)	8.26E-5 (0.158)	6.62E-4 (1.270)	1.14E-3 (2.191)
Preburn leach 2	<1.4E-4 <(0.264)	2.00E-2 (38.436)	<4.2E-6 <(0.008)	1.02E-5 (0.020)	1.50E-4 (0.287)	9.52E-6 (0.018)	9.70E-6 (0.019)	<4.2E-5 <(0.080)	<8.3E-5 <(0.160)	<3.3E-4 <(0.641)
Postburn particle leach 1 [a]	<1.4E-4 <(0.259)	9.78E-3 (18.758)	8.25E-5 (0.158)	1.11E-5 (0.021)	3.96E-4 (0.759)	2.00E-5 (0.038)	1.92E-5 (0.037)	5.02E-5 (0.096)	2.42E-4 (0.464)	8.85E-4 (1.698)
Postburn particle leach 2 [a]	<1.4E-4 <(0.274)	1.97E-3 (3.772)	1.22E-5 (0.023)	6.43E-6 (0.012)	1.62E-4 (0.310)	1.18E-5 (0.023)	1.11E-5 (0.021)	<4.3E-5 <(0.083)	<8.7E-5 <(0.166)	<3.5E-4 <(0.664)
Total	0.00E+0 (0.000)	5.39E-1 (1033.994)	4.08E-4 (0.783)	2.48E-4 (0.476)	1.01E-3 (1.947)	1.93E-4 (0.370)	1.90E-4 (0.365)	1.33E-4 (0.255)	1.30E-3 (2.487)	2.48E-3 (4.756)

Note 1: Values are reported as compact inventory fractions and particle equivalents (in parentheses).
Note 2: A less-than value indicates that the concentration in the leachate was below the minimum detectable limit; these values are not included in the totals.

Appendix Table A-35. Exposed inventory of stable nuclides of interest detected by DLBL of AGR-3/4 Compact 1-3 Segment 3

DLBL Step	^{105}Pd	^{109}Ag	^{133}Cs	^{139}La	^{140}Ce	^{141}Pr	^{146}Nd	^{152}Sm	^{153}Eu	^{156}Gd
Deconsolidation acid	<1.6E-4 <(0.307)	3.23E-3 (6.196)	3.40E-3 (6.525)	2.28E-3 (4.371)	2.12E-3 (4.074)	2.23E-3 (4.270)	1.91E-3 (3.673)	2.01E-3 (3.861)	2.04E-3 (3.904)	5.45E-3 (10.453)
Preburn leach 1	<2.8E-4 <(0.538)	2.33E-2 (44.775)	2.59E-5 (0.050)	2.57E-5 (0.049)	1.46E-4 (0.280)	1.69E-5 (0.032)	1.71E-5 (0.033)	<4.3E-5 <(0.082)	<8.5E-5 <(0.163)	4.08E-4 (0.783)
Preburn leach 2	<1.4E-4 <(0.259)	3.60E-3 (6.904)	1.28E-5 (0.024)	7.49E-6 (0.014)	1.56E-4 (0.300)	6.33E-6 (0.012)	<6.9E-6 <(0.013)	<4.1E-5 <(0.079)	<8.2E-5 <(0.157)	<3.3E-4 <(0.629)
Postburn particle leach 1	<1.4E-4 <(0.259)	1.64E-3 (3.152)	7.16E-5 (0.137)	1.64E-4 (0.315)	1.33E-4 (0.254)	3.01E-5 (0.058)	2.83E-4 (0.543)	5.85E-5 (0.112)	3.01E-4 (0.578)	4.82E-4 (0.924)
Postburn particle leach 2	<1.4E-4 <(0.259)	<2.3E-4 <(0.444)	4.81E-6 (0.0092)	<4.0E-6 <(0.0077)	2.35E-5 (0.045)	<4.4E-6 <(0.0084)	<6.9E-6 <(0.013)	<4.1E-5 <(0.079)	<8.2E-5 <(0.157)	<3.3E-4 <(0.629)
Total	0.00E+0 (0.000)	3.18E-2 (61.027)	3.52E-3 (6.745)	2.48E-3 (4.750)	2.58E-3 (4.953)	2.28E-3 (4.372)	2.22E-3 (4.248)	2.07E-3 (3.973)	2.34E-3 (4.482)	6.34E-3 (12.160)

Note 1: Values are reported as compact inventory fractions and particle equivalents (in parentheses).
Note 2: A less-than value indicates that the concentration in the leachate was below the minimum detectable limit; these values are not included in the totals.

Appendix Table A-36. Exposed inventory of stable nuclides of interest detected by DLBL of AGR-3/4 Compact 1-3 Segment 4

DLBL Step	^{105}Pd	^{109}Ag	^{133}Cs	^{139}La	^{140}Ce	^{141}Pr	^{146}Nd	^{152}Sm	^{153}Eu	^{156}Gd
Deconsolidation acid	1.74E-4 (0.334)	9.69E-3 (18.585)	4.61E-3 (8.851)	7.55E-3 (14.486)	7.52E-3 (14.425)	7.35E-3 (14.105)	6.33E-3 (12.139)	6.74E-3 (12.934)	6.19E-3 (11.867)	1.67E-2 (32.090)
Preburn leach 1	<1.4E-4 <(0.264)	3.24E-3 (6.218)	4.59E-4 (0.880)	1.23E-4 (0.237)	2.74E-4 (0.526)	9.93E-5 (0.190)	8.69E-5 (0.167)	9.39E-5 (0.180)	1.24E-4 (0.239)	5.51E-4 (1.057)
Preburn leach 2	<1.5E-4 <(0.288)	7.72E-4 (1.480)	2.38E-5 (0.046)	3.12E-5 (0.060)	1.57E-4 (0.300)	2.45E-5 (0.047)	2.03E-5 (0.039)	<4.6E-5 <(0.088)	<9.1E-5 <(0.175)	<3.6E-4 <(0.699)
Postburn particle leach 1	2.43E-3 (4.668)	2.36E-4 (0.453)	9.28E-5 (0.178)	1.62E-4 (0.311)	6.19E-4 (1.188)	3.53E-4 (0.676)	2.80E-4 (0.536)	4.85E-4 (0.930)	7.17E-4 (1.376)	1.56E-3 (2.987)
Postburn particle leach 2	1.03E-3 (1.973)	<2.2E-4 <(0.428)	8.40E-6 (0.016)	3.97E-6 (0.0076)	2.61E-4 (0.501)	7.11E-6 (0.014)	6.85E-6 (0.013)	<4.0E-5 <(0.076)	<7.9E-5 <(0.151)	<3.2E-4 <(0.606)
Total	3.64E-3 (6.975)	1.39E-2 (26.735)	5.20E-3 (9.971)	7.87E-3 (15.102)	8.83E-3 (16.940)	7.84E-3 (15.032)	6.72E-3 (12.894)	7.32E-3 (14.045)	7.03E-3 (13.481)	1.88E-2 (36.134)

Note 1: Values are reported as compact inventory fractions and particle equivalents (in parentheses).
Note 2: A less-than value indicates that the concentration in the leachate was below the minimum detectable limit; these values are not included in the totals.

Appendix Table A-37. Exposed inventory of stable nuclides of interest detected by DLBL of AGR-3/4 Compact 4-3 Segment 1

DLBL Step	^{105}Pd	^{109}Ag	^{133}Cs	^{139}La	^{140}Ce	^{141}Pr	^{146}Nd	^{152}Sm	^{153}Eu	^{156}Gd
Deconsolidation acid	<4.8E-5 <(0.093)	1.11E-3 (2.120)	3.60E-4 (0.691)	3.62E-3 (6.939)	1.26E-4 (0.242)	3.12E-4 (0.599)	8.76E-5 (0.168)	5.34E-5 (0.103)	1.26E-4 (0.242)	2.36E-4 (0.452)
Preburn leach 1	<5.0E-5 <(0.096)	2.91E-4 (0.558)	7.55E-5 (0.145)	1.57E-4 (0.300)	6.64E-5 (0.127)	3.60E-5 (0.069)	2.60E-5 (0.050)	<1.9E-5 <(0.037)	<2.3E-5 <(0.043)	6.71E-5 (0.129)
Preburn leach 2	<5.2E-5 <(0.100)	7.34E-5 (0.141)	1.11E-5 (0.021)	5.26E-6 (0.010)	9.58E-6 (0.018)	2.04E-6 (0.0039)	<2.9E-6 <(0.0055)	<2.0E-5 <(0.038)	<2.3E-5 <(0.045)	<5.2E-5 <(0.100)
Postburn particle leach 1	<5.4E-5 <(0.104)	1.22E-4 (0.234)	3.25E-5 (0.062)	1.01E-4 (0.193)	8.20E-5 (0.157)	5.02E-5 (0.096)	4.74E-5 (0.091)	6.67E-5 (0.128)	8.82E-5 (0.169)	1.98E-4 (0.381)
Postburn particle leach 2	<5.0E-5 <(0.096)	1.04E-4 (0.199)	9.79E-6 (0.019)	4.80E-6 (0.0092)	1.51E-5 (0.029)	3.32E-6 (0.0064)	3.09E-6 (0.0059)	<1.9E-5 <(0.037)	<2.3E-5 <(0.043)	<5.0E-5 <(0.096)
Total	0.00E+0 (0.000)	1.70E-3 (3.252)	4.89E-4 (0.939)	3.89E-3 (7.452)	2.99E-4 (0.574)	4.04E-4 (0.775)	1.64E-4 (0.315)	1.20E-4 (0.230)	2.14E-4 (0.411)	5.01E-4 (0.961)

Note 1: Values are reported as compact inventory fractions and particle equivalents (in parentheses).
Note 2: A less-than value indicates that the concentration in the leachate was below the minimum detectable limit; these values are not included in the totals.

Appendix Table A-38. Exposed inventory of stable nuclides of interest detected by DLBL of AGR-3/4 Compact 4-3 Segment 2

DLBL Step	^{105}Pd	^{109}Ag	^{133}Cs	^{139}La	^{140}Ce	^{141}Pr	^{146}Nd	^{152}Sm	^{153}Eu	^{156}Gd
Deconsolidation acid	<1.1E-4 <(0.215)	5.00E-3 (9.582)	2.74E-3 (5.255)	6.26E-3 (12.007)	3.06E-1 (586.133)	3.34E-3 (6.405)	2.70E-3 (5.181)	2.88E-3 (5.530)	2.63E-3 (5.053)	4.20E-3 (8.048)
Preburn leach 1	2.54E-4 (0.486)	7.03E-4 (1.349)	1.31E-4 (0.251)	1.28E-4 (0.246)	1.26E-2 (24.176)	7.12E-5 (0.136)	6.05E-5 (0.116)	5.27E-5 (0.101)	5.48E-5 (0.105)	1.42E-4 (0.273)
Preburn leach 2	<5.3E-5 <(0.102)	<5.8E-5 <(0.112)	1.46E-5 (0.028)	5.72E-6 (0.011)	1.11E-3 (2.124)	3.79E-6 (0.0073)	3.10E-6 (0.0059)	<2.0E-5 <(0.039)	<2.4E-5 <(0.046)	<5.3E-5 <(0.102)
Postburn particle leach 1 [a]	9.50E-5 (0.182)	<5.7E-5 <(0.110)	7.70E-5 (0.148)	1.53E-4 (0.294)	1.43E-2 (27.421)	1.02E-4 (0.195)	8.61E-5 (0.165)	1.49E-4 (0.285)	2.04E-4 (0.391)	2.32E-4 (0.444)
Postburn particle leach 2 [a]	<5.1E-5 <(0.098)	1.10E-4 (0.210)	3.40E-6 (0.0065)	1.39E-5 (0.027)	1.04E-3 (1.986)	3.48E-6 (0.0067)	<2.8E-6 <(0.0054)	<2.0E-5 <(0.038)	<2.3E-5 <(0.044)	<5.1E-5 <(0.098)
Total	3.48E-4 (0.668)	5.81E-3 (11.141)	2.97E-3 (5.688)	6.56E-3 (12.584)	3.35E-1 (641.841)	3.52E-3 (6.750)	2.85E-3 (5.468)	3.08E-3 (5.916)	2.89E-3 (5.549)	4.57E-3 (8.766)

Note 1: Values are reported as compact inventory fractions and particle equivalents (in parentheses).
Note 2: A less-than value indicates that the concentration in the leachate was below the minimum detectable limit; these values are not included in the totals.

Appendix Table A-39. Exposed inventory of stable nuclides of interest detected by DLBL of AGR-3/4 Compact 4-3 Segment 3

DLBL Step	^{105}Pd	^{109}Ag	^{133}Cs	^{139}La	^{140}Ce	^{141}Pr	^{146}Nd	^{152}Sm	^{153}Eu	^{156}Gd
Deconsolidation acid	<5.4E-5 <(0.104)	1.99E-3 (3.824)	3.67E-4 (0.704)	2.39E-3 (4.586)	6.17E-4 (1.184)	9.04E-4 (1.734)	7.09E-4 (1.360)	7.45E-4 (1.428)	4.48E-4 (0.860)	9.92E-4 (1.903)
Preburn leach 1	<5.2E-5 <(0.100)	3.03E-4 (0.580)	3.55E-5 (0.068)	1.46E-4 (0.280)	1.08E-4 (0.206)	6.86E-5 (0.132)	5.75E-5 (0.110)	3.07E-5 (0.059)	<2.3E-5 <(0.045)	1.05E-4 (0.202)
Preburn leach 2	<5.9E-5 <(0.113)	<6.5E-5 <(0.125)	6.47E-6 (0.012)	1.37E-5 (0.026)	1.82E-5 (0.035)	7.99E-6 (0.015)	6.47E-6 (0.012)	<2.3E-5 <(0.043)	<2.7E-5 <(0.051)	<5.9E-5 <(0.113)
Postburn particle leach 1	1.02E-3 (1.949)	5.44E-4 (1.044)	4.53E-4 (0.870)	<1.7E-6 <(0.0034)	7.66E-4 (1.469)	7.59E-4 (1.456)	6.29E-4 (1.206)	7.63E-4 (1.463)	7.88E-4 (1.511)	1.01E-3 (1.941)
Postburn particle leach 2	<5.4E-5 <(0.104)	<6.0E-5 <(0.114)	5.78E-6 (0.011)	<1.7E-8 (0.000)	1.05E-5 (0.020)	5.45E-6 (0.010)	4.29E-6 (0.0082)	<2.1E-5 <(0.040)	<2.4E-5 <(0.047)	<5.4E-5 <(0.104)
Total	1.02E-3 (1.949)	2.84E-3 (5.448)	8.68E-4 (1.665)	2.55E-3 (4.892)	1.52E-3 (2.914)	1.75E-3 (3.348)	1.41E-3 (2.696)	1.54E-3 (2.950)	1.24E-3 (2.371)	2.11E-3 (4.045)

Note 1: Values are reported as compact inventory fractions and particle equivalents (in parentheses).
Note 2: A less-than value indicates that the concentration in the leachate was below the minimum detectable limit; these values are not included in the totals.

Appendix Table A-40. Exposed inventory of stable nuclides of interest detected by DLBL of AGR-3/4 Compact 4-3 Segment 4

DLBL Step	^{105}Pd	^{109}Ag	^{133}Cs	^{139}La	^{140}Ce	^{141}Pr	^{146}Nd	^{152}Sm	^{153}Eu	^{156}Gd
Deconsolidation acid	9.51E-5 (0.182)	3.37E-3 (6.460)	7.08E-4 (1.357)	8.14E-3 (15.613)	7.69E-3 (14.744)	7.72E-3 (14.801)	6.55E-3 (12.568)	6.50E-3 (12.458)	3.47E-3 (6.663)	8.68E-3 (16.650)
Preburn leach 1	1.02E-3 (1.954)	7.33E-4 (1.406)	4.66E-5 (0.089)	3.33E-4 (0.638)	3.55E-4 (0.681)	2.40E-4 (0.460)	1.92E-4 (0.367)	1.85E-4 (0.354)	4.53E-4 (0.868)	4.42E-4 (0.847)
Preburn leach 2	1.17E-4 (0.225)	7.31E-5 (0.140)	1.15E-5 (0.022)	6.21E-5 (0.119)	7.44E-5 (0.143)	4.44E-5 (0.085)	3.34E-5 (0.064)	3.21E-5 (0.062)	1.07E-4 (0.205)	8.42E-5 (0.162)
Postburn particle leach 1	6.60E-3 (12.660)	4.37E-4 (0.839)	3.96E-4 (0.760)	1.85E-3 (3.539)	1.95E-3 (3.735)	1.57E-3 (3.015)	1.27E-3 (2.436)	2.08E-3 (3.986)	5.00E-3 (9.599)	3.62E-3 (6.935)
Postburn particle leach 2	4.12E-4 (0.790)	<5.6E-5 <(0.108)	7.32E-6 (0.014)	1.03E-5 (0.020)	2.09E-5 (0.040)	8.79E-6 (0.017)	<8.2E-6 <(0.016)	<2.0E-5 <(0.038)	2.83E-5 (0.054)	<5.1E-5 <(0.098)
Total	8.24E-3 (15.812)	4.61E-3 (8.845)	1.17E-3 (2.243)	1.04E-2 (19.928)	1.01E-2 (19.343)	9.58E-3 (18.378)	8.05E-3 (15.436)	8.79E-3 (16.860)	9.07E-3 (17.390)	1.28E-2 (24.594)

Note 1: Values are reported as compact inventory fractions and particle equivalents (in parentheses).
Note 2: A less-than value indicates that the concentration in the leachate was below the minimum detectable limit; these values are not included in the totals.

Appendix Table A-41. Exposed inventory of stable nuclides of interest detected by DLBL of AGR-3/4 Compact 10-1 Segment 1

DLBL Step	^{105}Pd	^{109}Ag	^{133}Cs	^{139}La	^{140}Ce	^{141}Pr	^{146}Nd	^{152}Sm	^{153}Eu	^{156}Gd
Deconsolidation acid	<6.5E-5 <(0.125)	5.92E-4 (1.136)	5.53E-6 (0.011)	6.31E-4 (1.210)	2.65E-5 (0.051)	5.50E-5 (0.106)	1.50E-5 (0.029)	3.12E-5 (0.060)	2.01E-4 (0.386)	2.10E-4 (0.402)
Preburn leach 1	6.75E-5 (0.129)	5.05E-4 (0.968)	5.29E-6 (0.010)	4.91E-5 (0.094)	5.45E-5 (0.104)	5.36E-6 (0.010)	4.25E-6 (0.0082)	<2.3E-5 <(0.043)	7.69E-5 (0.148)	1.29E-4 (0.247)
Preburn leach 2	<6.3E-5 <(0.120)	1.66E-4 (0.318)	2.88E-6 (0.0055)	5.71E-6 (0.011)	2.36E-5 (0.045)	<2.3E-6 <(0.0044)	<3.5E-6 <(0.0066)	<2.2E-5 <(0.043)	<3.1E-5 <(0.059)	<8.3E-5 <(0.159)
Postburn particle leach 1	<6.0E-5 <(0.116)	9.75E-5 (0.187)	6.22E-6 (0.012)	1.76E-4 (0.338)	1.48E-4 (0.283)	4.22E-5 (0.081)	3.52E-5 (0.068)	1.25E-4 (0.240)	1.05E-3 (2.017)	8.51E-4 (1.633)
Postburn particle leach 2	<6.2E-5 <(0.118)	<7.4E-5 <(0.142)	2.93E-6 (0.0056)	2.61E-6 (0.005)	2.65E-5 (0.051)	<2.2E-6 <(0.0043)	<3.4E-6 <(0.0065)	<2.2E-5 <(0.042)	<3.0E-5 <(0.058)	<8.2E-5 <(0.156)
Total	6.75E-5 (0.129)	1.36E-3 (2.608)	2.29E-5 (0.044)	8.64E-4 (1.658)	2.79E-4 (0.535)	1.03E-4 (0.197)	5.45E-5 (0.105)	1.56E-4 (0.300)	1.33E-3 (2.552)	1.19E-3 (2.282)

Note 1: Values are reported as compact inventory fractions and particle equivalents (in parentheses).
Note 2: A less-than value indicates that the concentration in the leachate was below the minimum detectable limit; these values are not included in the totals.

Appendix Table A-42. Exposed inventory of stable nuclides of interest detected by DLBL of AGR-3/4 Compact 10-1 Segment 2

DLBL Step	^{105}Pd	^{109}Ag	^{133}Cs	^{139}La	^{140}Ce	^{141}Pr	^{146}Nd	^{152}Sm	^{153}Eu	^{156}Gd
Deconsolidation acid	<6.5E-5 <(0.125)	3.41E-4 (0.655)	2.09E-5 (0.040)	3.44E-4 (0.660)	6.96E-5 (0.134)	9.14E-5 (0.175)	7.89E-5 (0.151)	6.23E-5 (0.120)	2.14E-4 (0.411)	2.93E-4 (0.562)
Preburn leach 1	<6.2E-5 <(0.118)	2.73E-4 (0.523)	5.05E-6 (0.0097)	8.74E-4 (1.677)	6.58E-4 (1.262)	3.10E-5 (0.059)	<3.4E-6 <(0.0065)	<2.2E-5 <(0.042)	7.44E-5 (0.143)	5.14E-4 (0.985)
Preburn leach 2	<6.3E-5 <(0.120)	<7.6E-5 <(0.145)	2.97E-6 (0.0057)	3.87E-5 (0.074)	3.93E-4 (0.753)	4.55E-6 (0.0087)	<3.5E-6 <(0.0066)	<2.2E-5 <(0.043)	<3.1E-5 <(0.059)	2.62E-4 (0.502)
Postburn particle leach 1 [a]	7.97E-5 (0.153)	8.49E-5 (0.163)	5.52E-6 (0.011)	1.65E-4 (0.317)	1.74E-4 (0.334)	3.88E-5 (0.075)	2.98E-5 (0.057)	1.22E-4 (0.234)	1.40E-3 (2.683)	1.15E-3 (2.206)
Postburn particle leach 2 [a]	<6.0E-5 <(0.116)	<7.3E-5 <(0.140)	3.18E-6 (0.0061)	6.10E-6 (0.012)	4.39E-5 (0.084)	<2.2E-6 <(0.0042)	<3.3E-6 <(0.0064)	<2.1E-5 <(0.041)	<2.9E-5 <(0.056)	<8.0E-5 <(0.153)
Total	7.97E-5 (0.153)	6.99E-4 (1.340)	3.76E-5 (0.072)	1.43E-3 (2.740)	1.34E-3 (2.567)	1.66E-4 (0.318)	1.09E-4 (0.209)	1.84E-4 (0.353)	1.69E-3 (3.237)	2.22E-3 (4.255)

Note 1: Values are reported as compact inventory fractions and particle equivalents (in parentheses).
Note 2: A less-than value indicates that the concentration in the leachate was below the minimum detectable limit; these values are not included in the totals.

Appendix Table A-43. Exposed inventory of stable nuclides of interest detected by DLBL of AGR-3/4 Compact 10-1 Segment 3

DLBL Step	^{105}Pd	^{109}Ag	^{133}Cs	^{139}La	^{140}Ce	^{141}Pr	^{146}Nd	^{152}Sm	^{153}Eu	^{156}Gd
Deconsolidation acid	<5.3E-5 <(0.102)	1.22E-3 (2.333)	3.47E-5 (0.067)	3.80E-4 (0.730)	5.15E-5 (0.099)	7.82E-5 (0.150)	6.04E-5 (0.116)	6.09E-5 (0.117)	2.34E-4 (0.448)	2.68E-4 (0.514)
Preburn leach 1	<6.2E-5 <(0.118)	3.28E-4 (0.630)	2.14E-5 (0.041)	1.05E-4 (0.201)	1.54E-4 (0.295)	8.36E-6 (0.016)	6.87E-6 (0.013)	2.95E-5 (0.057)	2.67E-4 (0.512)	2.30E-4 (0.442)
Preburn leach 2	<5.9E-5 <(0.114)	<7.1E-5 <(0.137)	<2.1E-6 <(0.004)	2.35E-6 (0.0045)	7.90E-6 (0.015)	<2.2E-6 <(0.0041)	<3.3E-6 <(0.0062)	<2.1E-5 <(0.040)	<2.9E-5 <(0.055)	<7.8E-5 <(0.150)
Postburn particle leach 1	2.22E-4 (0.425)	<7.6E-5 <(0.145)	1.06E-5 (0.020)	1.28E-4 (0.246)	1.04E-4 (0.200)	3.19E-5 (0.061)	2.43E-5 (0.047)	1.73E-4 (0.332)	1.82E-3 (3.489)	1.15E-3 (2.199)
Postburn particle leach 2	<6.0E-5 <(0.116)	<7.3E-5 <(0.140)	4.91E-6 (0.0094)	3.60E-5 (0.069)	3.48E-5 (0.067)	8.25E-6 (0.016)	6.57E-6 (0.013)	4.69E-5 (0.090)	4.77E-4 (0.914)	3.00E-4 (0.575)
Total	2.22E-4 (0.425)	1.54E-3 (2.962)	7.16E-5 (0.137)	6.52E-4 (1.251)	3.52E-4 (0.675)	1.27E-4 (0.243)	9.82E-5 (0.188)	3.10E-4 (0.595)	2.80E-3 (5.364)	1.94E-3 (3.730)

Note 1: Values are reported as compact inventory fractions and particle equivalents (in parentheses).
Note 2: A less-than value indicates that the concentration in the leachate was below the minimum detectable limit; these values are not included in the totals.

Appendix Table A-44. Exposed inventory of stable nuclides of interest detected by DLBL of AGR-3/4 Compact 10-1 Segment 4

DLBL Step	^{105}Pd	^{109}Ag	^{133}Cs	^{139}La	^{140}Ce	^{141}Pr	^{146}Nd	^{152}Sm	^{153}Eu	^{156}Gd
Deconsolidation acid	6.60E-5 (0.127)	1.78E-3 (3.414)	5.65E-4 (1.085)	3.53E-3 (6.764)	3.06E-3 (5.863)	3.29E-3 (6.318)	3.02E-3 (5.784)	2.44E-3 (4.677)	1.41E-3 (2.709)	4.63E-3 (8.876)
Preburn leach 1	<5.9E-5 <(0.114)	4.74E-4 (0.910)	7.26E-5 (0.139)	1.43E-3 (2.750)	1.36E-3 (2.612)	1.26E-3 (2.411)	9.60E-4 (1.842)	9.50E-4 (1.822)	8.08E-4 (1.549)	1.55E-3 (2.980)
Preburn leach 2	<6.4E-5 <(0.123)	8.55E-5 (0.164)	<2.3E-6 <(0.0044)	6.94E-5 (0.133)	6.83E-5 (0.131)	6.00E-5 (0.115)	4.68E-5 (0.090)	4.44E-5 (0.085)	<3.1E-5 <(0.060)	<8.5E-5 <(0.162)
Postburn particle leach 1	1.79E-4 (0.344)	1.07E-4 (0.205)	2.39E-5 (0.046)	1.03E-2 (19.767)	1.02E-2 (19.610)	9.61E-3 (18.440)	7.66E-3 (14.699)	1.04E-2 (20.002)	7.69E-3 (14.759)	1.21E-2 (23.177)
Postburn particle leach 2	<6.5E-5 <(0.125)	<7.8E-5 <(0.150)	3.73E-6 (0.0071)	1.08E-4 (0.207)	1.26E-4 (0.241)	1.01E-4 (0.194)	8.17E-5 (0.157)	1.11E-4 (0.213)	7.93E-5 (0.152)	1.46E-4 (0.279)
Total	2.45E-4 (0.470)	2.45E-3 (4.693)	6.66E-4 (1.277)	1.54E-2 (29.621)	1.48E-2 (28.457)	1.43E-2 (27.478)	1.18E-2 (22.571)	1.40E-2 (26.799)	9.99E-3 (19.169)	1.84E-2 (35.312)

Note 1: Values are reported as compact inventory fractions and particle equivalents (in parentheses).
Note 2: A less-than value indicates that the concentration in the leachate was below the minimum detectable limit; these values are not included in the totals.

Appendix Table A-45. Exposed inventory of stable nuclides of interest detected by DLBL of AGR-3/4 Compact 10-2 Segment 1

DLBL Step	^{105}Pd	^{109}Ag	^{133}Cs	^{139}La	^{140}Ce	^{141}Pr	^{146}Nd	^{152}Sm	^{153}Eu	^{156}Gd
Deconsolidation acid	9.94E-5 (0.191)	1.64E-3 (3.148)	2.03E-5 (0.039)	7.68E-3 (14.731)	5.81E-5 (0.111)	5.04E-4 (0.968)	3.93E-5 (0.075)	5.78E-5 (0.111)	6.81E-4 (1.306)	7.27E-4 (1.394)
Preburn leach 1	2.93E-4 (0.562)	5.19E-4 (0.996)	7.99E-6 (0.015)	1.78E-4 (0.342)	2.66E-5 (0.051)	1.45E-5 (0.028)	4.81E-6 (0.0092)	<2.3E-5 <(0.044)	1.88E-4 (0.360)	1.13E-4 (0.217)
Preburn leach 2	<6.1E-5 <(0.118)	<7.5E-5 <(0.143)	3.79E-6 (0.0073)	5.80E-6 (0.011)	1.40E-5 (0.027)	<2.2E-6 <(0.0043)	<3.4E-6 <(0.0064)	<2.2E-5 <(0.042)	<3.0E-5 <(0.057)	<8.1E-5 <(0.156)
Postburn particle leach 1	1.70E-3 (3.269)	3.71E-4 (0.711)	1.82E-5 (0.035)	1.86E-5 (0.036)	4.63E-4 (0.888)	4.11E-5 (0.079)	3.06E-5 (0.059)	1.24E-4 (0.238)	8.65E-4 (1.660)	7.92E-4 (1.519)
Postburn particle leach 2	1.27E-4 (0.244)	1.01E-4 (0.194)	2.97E-6 (0.0057)	<2.2E-6 <(0.0042)	1.12E-5 (0.021)	<2.4E-6 <(0.0046)	<3.6E-6 <(0.0069)	<2.4E-5 <(0.045)	<3.2E-5 <(0.061)	<8.8E-5 <(0.168)
Total	2.22E-3 (4.265)	2.63E-3 (5.050)	5.33E-5 (0.102)	7.88E-3 (15.120)	5.73E-4 (1.099)	5.60E-4 (1.074)	7.47E-5 (0.143)	1.82E-4 (0.349)	1.73E-3 (3.326)	1.63E-3 (3.130)

Note 1: Values are reported as compact inventory fractions and particle equivalents (in parentheses).
Note 2: A less-than value indicates that the concentration in the leachate was below the minimum detectable limit; these values are not included in the totals.

Appendix Table A-46. Exposed inventory of stable nuclides of interest detected by DLBL of AGR-3/4 Compact 10-2 Segment 2

DLBL Step	^{105}Pd	^{109}Ag	^{133}Cs	^{139}La	^{140}Ce	^{141}Pr	^{146}Nd	^{152}Sm	^{153}Eu	^{156}Gd
Deconsolidation acid	<6.9E-5 <(0.132)	4.31E-4 (0.828)	4.53E-5 (0.087)	8.25E-3 (15.826)	2.96E-5 (0.057)	5.16E-4 (0.990)	1.69E-5 (0.032)	4.30E-5 (0.082)	6.21E-4 (1.191)	5.93E-4 (1.138)
Preburn leach 1	1.13E-4 (0.216)	2.13E-4 (0.408)	5.24E-6 (0.010)	9.50E-5 (0.182)	2.14E-5 (0.041)	8.44E-6 (0.016)	3.52E-6 (0.0068)	<2.2E-5 <(0.043)	1.86E-4 (0.356)	1.05E-4 (0.202)
Preburn leach 2	<6.4E-5 <(0.122)	<7.8E-5 <(0.149)	5.74E-6 (0.011)	6.24E-5 (0.120)	5.53E-5 (0.106)	3.79E-6 (0.0073)	<3.5E-6 <(0.0067)	<2.3E-5 <(0.044)	<3.1E-5 <(0.059)	<8.5E-5 <(0.162)
Postburn particle leach 1 [a]	2.87E-3 (5.499)	3.36E-4 (0.644)	2.18E-5 (0.042)	3.07E-5 (0.059)	3.74E-4 (0.716)	6.86E-5 (0.132)	5.05E-5 (0.097)	2.64E-4 (0.506)	2.22E-3 (4.257)	1.42E-3 (2.730)
Postburn particle leach 2 [a]	7.02E-5 (0.135)	8.29E-5 (0.159)	<2.3E-6 <(0.0044)	<2.2E-6 <(0.0041)	3.36E-6 (0.0064)	<2.4E-6 <(0.0045)	<3.6E-6 <(0.0068)	<2.3E-5 <(0.044)	<3.1E-5 <(0.060)	<8.6E-5 <(0.165)
Total	3.05E-3 (5.850)	1.06E-3 (2.039)	7.80E-5 (0.150)	8.44E-3 (16.187)	4.83E-4 (0.927)	5.97E-4 (1.145)	7.09E-5 (0.136)	3.07E-4 (0.588)	3.03E-3 (5.804)	2.12E-3 (4.070)

Note 1: Values are reported as compact inventory fractions and particle equivalents (in parentheses).
Note 2: A less-than value indicates that the concentration in the leachate was below the minimum detectable limit; these values are not included in the totals.

Appendix Table A-47. Exposed inventory of stable nuclides of interest detected by DLBL of AGR-3/4 Compact 10-2 Segment 3

DLBL Step	^{105}Pd	^{109}Ag	^{133}Cs	^{139}La	^{140}Ce	^{141}Pr	^{146}Nd	^{152}Sm	^{153}Eu	^{156}Gd
Deconsolidation acid	<7.8E-5 <(0.150)	1.08E-3 (2.070)	4.61E-4 (0.884)	1.37E-2 (26.262)	4.56E-4 (0.874)	1.37E-3 (2.621)	4.82E-4 (0.925)	4.35E-4 (0.835)	1.14E-3 (2.188)	1.56E-3 (2.983)
Preburn leach 1	2.55E-4 (0.488)	5.54E-4 (1.063)	9.46E-6 (0.018)	7.41E-5 (0.142)	3.75E-5 (0.072)	1.15E-5 (0.022)	8.23E-6 (0.016)	6.70E-5 (0.129)	3.76E-4 (0.721)	2.56E-4 (0.490)
Preburn leach 2	<6.5E-5 <(0.125)	<7.9E-5 <(0.151)	3.62E-6 (0.007)	1.78E-5 (0.034)	1.37E-5 (0.026)	<2.4E-6 <(0.0045)	<3.6E-6 <(0.0068)	<2.3E-5 <(0.044)	<3.1E-5 <(0.060)	<8.6E-5 <(0.165)
Postburn particle leach 1	1.54E-3 (2.953)	1.29E-4 (0.248)	8.84E-6 (0.017)	1.71E-5 (0.033)	1.80E-4 (0.346)	3.77E-5 (0.072)	2.81E-5 (0.054)	3.37E-4 (0.646)	1.57E-3 (3.010)	9.87E-4 (1.893)
Postburn particle leach 2	1.37E-4 (0.264)	1.30E-4 (0.250)	2.90E-5 (0.056)	1.02E-5 (0.019)	9.05E-5 (0.174)	1.62E-5 (0.031)	1.67E-5 (0.032)	3.25E-5 (0.062)	3.41E-5 (0.065)	1.55E-4 (0.297)
Total	1.93E-3 (3.705)	1.89E-3 (3.631)	5.12E-4 (0.982)	1.38E-2 (26.490)	7.78E-4 (1.492)	1.43E-3 (2.747)	5.35E-4 (1.027)	8.72E-4 (1.672)	3.12E-3 (5.985)	2.95E-3 (5.663)

Note 1: Values are reported as compact inventory fractions and particle equivalents (in parentheses).
Note 2: A less-than value indicates that the concentration in the leachate was below the minimum detectable limit; these values are not included in the totals.

Appendix Table A-48. Exposed inventory of stable nuclides of interest detected by DLBL of AGR-3/4 Compact 10-2 Segment 4

DLBL Step	^{105}Pd	^{109}Ag	^{133}Cs	^{139}La	^{140}Ce	^{141}Pr	^{146}Nd	^{152}Sm	^{153}Eu	^{156}Gd
Deconsolidation acid	1.26E-4 (0.241)	1.70E-3 (3.262)	1.02E-3 (1.951)	1.09E-2 (20.847)	4.15E-3 (7.969)	4.85E-3 (9.302)	3.81E-3 (7.301)	2.78E-3 (5.332)	2.01E-3 (3.854)	5.43E-3 (10.418)
Preburn leach 1	5.10E-4 (0.978)	1.04E-3 (1.987)	9.17E-5 (0.176)	1.61E-3 (3.096)	1.70E-3 (3.268)	1.49E-3 (2.850)	1.24E-3 (2.377)	1.29E-3 (2.476)	1.15E-3 (2.204)	2.07E-3 (3.979)
Preburn leach 2	<6.9E-5 <(0.132)	1.36E-4 (0.261)	4.96E-6 (0.0095)	7.06E-5 (0.135)	8.16E-5 (0.156)	6.27E-5 (0.120)	5.20E-5 (0.100)	5.91E-5 (0.113)	3.51E-5 (0.067)	1.06E-4 (0.204)
Postburn particle leach 1	1.90E-3 (3.643)	3.14E-4 (0.602)	1.32E-5 (0.025)	2.86E-3 (5.486)	6.33E-3 (12.134)	5.59E-3 (10.724)	4.71E-3 (9.039)	7.58E-3 (14.539)	6.02E-3 (11.547)	9.02E-3 (17.299)
Postburn particle leach 2	4.65E-4 (0.891)	1.62E-4 (0.311)	5.60E-6 (0.011)	2.46E-5 (0.047)	1.54E-4 (0.295)	4.82E-5 (0.093)	4.06E-5 (0.078)	4.86E-5 (0.093)	4.26E-5 (0.082)	1.56E-4 (0.299)
Total	3.00E-3 (5.753)	3.35E-3 (6.422)	1.13E-3 (2.172)	1.54E-2 (29.612)	1.24E-2 (23.822)	1.20E-2 (23.088)	9.85E-3 (18.895)	1.18E-2 (22.554)	9.26E-3 (17.753)	1.68E-2 (32.199)

Note 1: Values are reported as compact inventory fractions and particle equivalents (in parentheses).
Note 2: A less-than value indicates that the concentration in the leachate was below the minimum detectable limit; these values are not included in the totals.

Appendix Table A-49. Concentration in each segment from AGR-3/4 Compact 1-3

Nuclide	Segment 1	Segment 2	Segment 3	Segment 4
^{235}U	2.00E-5 (0.038)	5.44E-5 (0.104)	9.06E-3 (17.381)	1.34E-2 (25.639)
^{236}U	1.23E-4 (0.235)	1.23E-4 (0.236)	9.10E-3 (17.454)	1.34E-2 (25.790)
^{238}U	3.15E-4 (0.605)	3.06E-4 (0.587)	8.94E-3 (17.153)	1.42E-2 (27.297)
^{239}Pu	2.68E-4 (0.514)	1.96E-4 (0.376)	4.88E-3 (9.358)	1.44E-2 (27.700)
^{240}Pu	7.27E-4 (1.394)	5.07E-4 (0.973)	4.49E-3 (8.607)	1.41E-2 (27.112)
^{90}Sr	1.49E-4 (0.285)	1.50E-4 (0.287)	5.60E-3 (10.742)	2.01E-2 (38.497)
^{106}Ru	0.00E+0 (0.000)	1.95E-4 (0.374)	2.29E-3 (4.394)	1.24E-2 (23.733)
^{110m}Ag	0.00E+0 (0.000)	0.00E+0 (0.000)	0.00E+0 (0.000)	0.00E+0 (0.000)
^{125}Sb	0.00E+0 (0.000)	0.00E+0 (0.000)	7.85E-4 (1.505)	1.23E-2 (23.514)
^{134}Cs	7.44E-4 (1.427)	9.88E-4 (1.894)	8.47E-3 (16.243)	7.84E-3 (15.045)
^{137}Cs	1.08E-3 (2.069)	1.15E-3 (2.201)	1.10E-2 (21.053)	1.07E-2 (20.600)
^{144}Ce	0.00E+0 (0.000)	4.11E-4 (0.788)	7.07E-3 (13.553)	1.62E-2 (31.023)
^{154}Eu	4.99E-4 (0.958)	9.44E-4 (1.811)	6.10E-3 (11.696)	1.15E-2 (21.963)
^{155}Eu	3.53E-4 (0.676)	3.96E-4 (0.760)	6.15E-3 (11.799)	1.28E-2 (24.508)
^{105}Pd	0.00E+0 (0.000)	0.00E+0 (0.000)	0.00E+0 (0.000)	6.90E-3 (13.237)
^{109}Ag	1.17E-2 (22.455)	1.39E+0 (2663.060)	9.67E-2 (185.484)	2.65E-2 (50.734)
^{133}Cs	8.41E-4 (1.613)	1.05E-3 (2.018)	1.07E-2 (20.502)	9.86E-3 (18.921)
^{139}La	1.21E-3 (2.315)	6.40E-4 (1.227)	7.53E-3 (14.437)	1.49E-2 (28.657)
^{140}Ce	2.00E-3 (3.838)	2.61E-3 (5.013)	7.85E-3 (15.055)	1.68E-2 (32.147)
^{141}Pr	5.13E-4 (0.985)	4.97E-4 (0.953)	6.93E-3 (13.288)	1.49E-2 (28.526)
^{146}Nd	5.12E-4 (0.982)	4.90E-4 (0.940)	6.73E-3 (12.913)	1.28E-2 (24.469)
^{152}Sm	2.33E-4 (0.447)	3.42E-4 (0.656)	6.30E-3 (12.076)	1.39E-2 (26.652)
^{153}Eu	2.16E-3 (4.139)	3.34E-3 (6.406)	7.10E-3 (13.622)	1.33E-2 (25.583)
^{156}Gd	5.92E-3 (11.355)	6.39E-3 (12.248)	1.93E-2 (36.960)	3.58E-2 (68.570)

Note: Values are reported as compact fraction/cm^3 and particle equivalents/cm^3 (in parentheses).

Appendix Table A-50. Concentration in each segment from AGR-3/4 Compact 4-3

Nuclide	Segment 1		Segment 2		Segment 3		Segment 4	
^{235}U	9.26E-04	(1.776)	1.06E-02	(20.279)	6.63E-03	(12.719)	2.47E-02	(47.385)
^{236}U	9.07E-04	(1.739)	1.03E-02	(19.667)	6.25E-03	(11.992)	2.35E-02	(45.019)
^{238}U	8.95E-04	(1.717)	1.00E-02	(19.274)	6.01E-03	(11.528)	2.27E-02	(43.526)
^{239}Pu	2.01E-04	(0.386)	8.65E-03	(16.585)	4.54E-03	(8.710)	2.21E-02	(42.300)
^{240}Pu	2.04E-04	(0.391)	8.89E-03	(17.051)	4.56E-03	(8.752)	2.24E-02	(42.929)
^{90}Sr	1.81E-03	(3.470)	8.91E-03	(17.081)	3.77E-03	(7.231)	2.78E-02	(53.225)
^{106}Ru	0.00E+00	(0.000)	7.57E-03	(14.513)	7.13E-04	(1.367)	1.22E-02	(23.457)
^{110m}Ag	0.00E+00	(0.000)	0.00E+00	(0.000)	0.00E+00	(0.000)	0.00E+00	(0.000)
^{125}Sb	3.02E-04	(0.578)	5.01E-03	(9.605)	1.54E-03	(2.954)	2.07E-02	(39.728)
^{134}Cs	9.55E-04	(1.833)	5.75E-03	(11.027)	1.62E-03	(3.115)	1.50E-03	(2.881)
^{137}Cs	1.48E-03	(2.832)	7.80E-03	(14.954)	2.56E-03	(4.906)	2.92E-03	(5.602)
^{144}Ce	5.92E-04	(1.136)	1.46E-02	(28.085)	8.01E-03	(15.365)	4.26E-02	(81.638)
^{154}Eu	8.62E-05	(0.165)	5.97E-03	(11.459)	2.78E-03	(5.331)	1.87E-02	(35.784)
^{155}Eu	1.27E-04	(0.243)	6.65E-03	(12.761)	3.16E-03	(6.056)	1.97E-02	(37.714)
^{105}Pd	0.00E+00	(0.000)	8.86E-04	(1.698)	2.93E-03	(5.624)	1.98E-02	(37.902)
^{109}Ag	4.87E-03	(9.333)	1.48E-02	(28.312)	8.20E-03	(15.722)	1.11E-02	(21.202)
^{133}Cs	1.48E-03	(2.839)	7.54E-03	(14.455)	2.50E-03	(4.804)	2.80E-03	(5.376)
^{139}La	1.25E-02	(23.998)	1.67E-02	(31.979)	7.36E-03	(14.117)	2.49E-02	(47.768)
^{140}Ce	6.70E-04	(1.284)	8.50E-01	(1631.0)	4.38E-03	(8.409)	2.42E-02	(46.364)
^{141}Pr	1.16E-03	(2.224)	8.94E-03	(17.154)	5.04E-03	(9.660)	2.30E-02	(44.052)
^{146}Nd	3.76E-04	(0.721)	7.24E-03	(13.895)	4.06E-03	(7.781)	1.93E-02	(36.999)
^{152}Sm	1.77E-04	(0.339)	7.84E-03	(15.035)	4.44E-03	(8.513)	2.11E-02	(40.413)
^{153}Eu	4.18E-04	(0.802)	7.35E-03	(14.102)	3.57E-03	(6.841)	2.17E-02	(41.683)
^{156}Gd	1.00E-03	(1.922)	1.16E-02	(22.275)	6.09E-03	(11.673)	3.07E-02	(58.952)

Note: Values are reported as compact fraction/cm^3 and particle equivalents/cm^3 (in parentheses).

Appendix Table A-51. Concentration in each segment from AGR-3/4 Compact 10-1

Nuclide	Segment 1		Segment 2		Segment 3		Segment 4	
^{235}U	8.63E-05	(0.166)	1.30E-03	(2.494)	9.74E-04	(1.869)	2.12E-02	(40.583)
^{236}U	9.84E-05	(0.189)	1.33E-03	(2.543)	9.94E-04	(1.907)	2.08E-02	(39.922)
^{238}U	1.22E-04	(0.234)	1.23E-03	(2.362)	9.41E-04	(1.804)	2.21E-02	(42.317)
^{239}Pu	6.81E-05	(0.131)	6.02E-04	(1.154)	5.44E-04	(1.044)	2.15E-02	(41.203)
^{240}Pu	7.74E-05	(0.148)	6.92E-04	(1.328)	6.42E-04	(1.232)	2.23E-02	(42.826)
^{90}Sr	1.27E-03	(2.430)	5.83E-03	(11.184)	9.11E-04	(1.747)	1.65E-02	(31.627)
^{106}Ru	0.00E+00	(0.000)	8.09E-04	(1.552)	7.55E-04	(1.449)	1.60E-02	(30.758)
^{110m}Ag	0.00E+00	(0.000)	0.00E+00	(0.000)	0.00E+00	(0.000)	0.00E+00	(0.000)
^{125}Sb	2.12E-05	(0.041)	1.39E-04	(0.266)	4.87E-05	(0.093)	5.40E-05	(0.104)
^{134}Cs	5.26E-06	(0.010)	2.12E-05	(0.041)	2.29E-05	(0.044)	3.77E-04	(0.723)
^{137}Cs	2.76E-05	(0.053)	7.36E-05	(0.141)	1.06E-04	(0.204)	1.52E-03	(2.923)
^{144}Ce	9.02E-05	(0.173)	2.86E-04	(0.549)	2.82E-04	(0.541)	3.96E-02	(75.983)
^{154}Eu	1.31E-03	(2.522)	5.65E-03	(10.840)	7.38E-03	(14.161)	1.74E-02	(33.410)
^{155}Eu	1.14E-03	(2.185)	5.83E-03	(11.182)	7.65E-03	(14.663)	2.01E-02	(38.633)
^{105}Pd	2.36E-04	(0.452)	2.42E-04	(0.464)	5.91E-04	(1.134)	5.40E-04	(1.036)
^{109}Ag	4.41E-03	(8.453)	2.12E-03	(4.070)	4.12E-03	(7.900)	5.39E-03	(10.337)
^{133}Cs	4.78E-05	(0.092)	1.14E-04	(0.219)	1.91E-04	(0.366)	1.47E-03	(2.812)
^{139}La	2.39E-03	(4.592)	4.34E-03	(8.320)	1.74E-03	(3.335)	3.40E-02	(65.241)
^{140}Ce	3.65E-04	(0.700)	4.07E-03	(7.797)	9.39E-04	(1.800)	3.27E-02	(62.678)
^{141}Pr	2.11E-04	(0.404)	5.03E-04	(0.966)	3.38E-04	(0.648)	3.16E-02	(60.520)
^{146}Nd	6.74E-05	(0.129)	3.30E-04	(0.633)	2.62E-04	(0.502)	2.59E-02	(49.712)
^{152}Sm	1.09E-04	(0.209)	5.59E-04	(1.072)	8.28E-04	(1.587)	3.08E-02	(59.024)
^{153}Eu	9.72E-04	(1.864)	5.13E-03	(9.830)	7.46E-03	(14.305)	2.20E-02	(42.219)
^{156}Gd	1.18E-03	(2.265)	6.74E-03	(12.923)	5.19E-03	(9.947)	4.06E-02	(77.776)

Note: Values are reported as compact fraction/cm^3 and particle equivalents/cm^3 (in parentheses).

Appendix Table A-52. Concentration in each segment from AGR-3/4 Compact 10-2

Nuclide	Segment 1		Segment 2		Segment 3		Segment 4	
^{235}U	2.19E-05	(0.042)	2.00E-04	(0.383)	7.60E-03	(14.578)	1.94E-02	(37.119)
^{236}U	2.71E-05	(0.052)	1.94E-04	(0.372)	7.15E-03	(13.706)	1.80E-02	(34.554)
^{238}U	1.34E-04	(0.257)	2.72E-04	(0.522)	7.22E-03	(13.840)	1.83E-02	(35.049)
^{239}Pu	6.06E-05	(0.116)	2.59E-04	(0.497)	4.41E-03	(8.460)	2.07E-02	(39.660)
^{240}Pu	8.68E-05	(0.167)	4.03E-04	(0.773)	3.65E-03	(7.004)	2.23E-02	(42.761)
^{90}Sr	1.78E-03	(3.423)	5.95E-03	(11.416)	7.10E-03	(13.624)	1.45E-02	(27.796)
^{106}Ru	0.00E+00	(0.000)	0.00E+00	(0.000)	1.21E-03	(2.317)	2.11E-02	(40.419)
^{110m}Ag	0.00E+00	(0.000)	0.00E+00	(0.000)	0.00E+00	(0.000)	0.00E+00	(0.000)
^{125}Sb	2.56E-04	(0.492)	1.35E-04	(0.260)	5.08E-04	(0.975)	8.89E-03	(17.047)
^{134}Cs	1.80E-05	(0.034)	5.70E-05	(0.109)	3.77E-04	(0.723)	6.53E-04	(1.252)
^{137}Cs	7.39E-05	(0.142)	1.60E-04	(0.307)	1.54E-03	(2.950)	2.59E-03	(4.967)
^{144}Ce	1.33E-04	(0.255)	2.00E-04	(0.383)	2.23E-03	(4.285)	2.72E-02	(52.231)
^{154}Eu	2.11E-03	(4.051)	7.41E-03	(14.219)	8.24E-03	(15.809)	1.66E-02	(31.805)
^{155}Eu	2.36E-03	(4.531)	7.88E-03	(15.121)	9.20E-03	(17.638)	1.87E-02	(35.776)
^{105}Pd	1.22E-03	(2.343)	7.67E-03	(14.703)	6.14E-03	(11.772)	7.40E-03	(14.187)
^{109}Ag	6.72E-03	(12.897)	2.67E-03	(5.125)	6.02E-03	(11.537)	8.26E-03	(15.836)
^{133}Cs	9.98E-05	(0.191)	1.96E-04	(0.376)	1.63E-03	(3.121)	2.79E-03	(5.356)
^{139}La	2.45E-02	(46.940)	2.12E-02	(40.687)	4.39E-02	(84.175)	3.81E-02	(73.022)
^{140}Ce	3.07E-04	(0.589)	1.21E-03	(2.329)	2.47E-03	(4.740)	3.06E-02	(58.745)
^{141}Pr	1.62E-03	(3.098)	1.50E-03	(2.878)	4.55E-03	(8.728)	2.97E-02	(56.935)
^{146}Nd	1.37E-04	(0.263)	1.78E-04	(0.342)	1.70E-03	(3.262)	2.43E-02	(46.595)
^{152}Sm	1.80E-04	(0.345)	7.71E-04	(1.479)	2.77E-03	(5.312)	2.90E-02	(55.617)
^{153}Eu	2.70E-03	(5.185)	7.61E-03	(14.590)	9.91E-03	(19.017)	2.28E-02	(43.779)
^{156}Gd	2.61E-03	(5.014)	5.33E-03	(10.230)	9.38E-03	(17.993)	4.14E-02	(79.401)

Note: Values are reported as compact fraction/cm^3 and particle equivalents/cm^3 (in parentheses).

APPENDIX B. CALCULATED INVENTORIES

APPENDIX B. CALCULATED INVENTORIES

The tables in this appendix provide the calculated inventories for select actinides and fission products (both radionuclides and stable nuclides) that were used to calculate values reported herein (i.e., compact fraction and M/C as described in Section 2). Calculated inventories were estimated via physics depletion calculations using the Oak Ridge Isotope Generation and Depletion (ORIGEN2) code (Croff 1983, Ludwig and Croff 2002), the Monte Carlo N-Particle Transport (MCNP) code (X-5 Monte Carlo Team 2003), and Jim Sterbentz's MCNP-ORIGEN2 coupled utility program (JMOCUP) and software extraction modules (Sterbentz 2015).

Appendix Table B-1. Calculated inventories of select actinides one year after EOL

Compact	Value	^{235}U	^{236}U	^{238}U	^{239}Pu	^{240}Pu
AGR-3/4 1-3	moles/compact	2.4390E-04	2.5120E-05	1.4797E-03	1.6574E-05	3.2220E-06
AGR-3/4 1-3	µg/compact	5.7327E+04	5.9295E+03	3.5224E+05	3.9620E+03	7.7345E+02
AGR-3/4 4-3	moles/compact	1.0825E-04	4.5250E-05	1.4278E-03	2.0830E-05	7.9350E-06
AGR-3/4 4-3	µg/compact	2.5444E+04	1.0681E+04	3.3989E+05	4.9795E+03	1.9048E+03
AGR-3/4 10-1	moles/compact	1.4272E-04	4.0680E-05	1.4421E-03	2.1840E-05	7.5480E-06
AGR-3/4 10-1	µg/compact	3.3545E+04	9.6023E+03	3.4329E+05	5.2209E+03	1.8119E+03
AGR-3/4 10-2	moles/compact	1.4433E-04	4.0420E-05	1.4443E-03	2.1030E-05	7.1650E-06
AGR-3/4 10-2	µg/compact	3.3924E+04	9.5410E+03	3.4382E+05	5.0273E+03	1.7200E+03

Appendix Table B-2. Calculated inventories of select stable nuclides one year after EOL

Compact	Value	^{105}Pd	^{109}Ag	^{133}Cs	^{139}La	^{140}Ce
AGR-3/4 1-3	moles/compact	1.5228E-06	1.7137E-07	7.8990E-06	7.7630E-06	7.4520E-06
AGR-3/4 1-3	µg/compact	1.5975E+02	1.8663E+01	1.0498E+03	1.0783E+03	1.0426E+03
AGR-3/4 4-3	moles/compact	3.8730E-06	6.7890E-07	1.6466E-05	1.7122E-05	1.6692E-05
AGR-3/4 4-3	µg/compact	4.0630E+02	7.3935E+01	2.1884E+03	2.3784E+03	2.3353E+03
AGR-3/4 10-1	moles/compact	3.2180E-06	5.1500E-07	1.4306E-05	1.4560E-05	1.4119E-05
AGR-3/4 10-1	µg/compact	3.3758E+02	5.6086E+01	1.9013E+03	2.0225E+03	1.9753E+03
AGR-3/4 10-2	moles/compact	3.1680E-06	5.0220E-07	1.4170E-05	1.4422E-05	1.3983E-05
AGR-3/4 10-2	µg/compact	3.3234E+02	5.4692E+01	1.8833E+03	2.0033E+03	1.9563E+03

Appendix Table B-2 (continued). Calculated inventories of select stable nuclides one year after EOL

Compact	Value	^{141}Pr	^{146}Nd	^{152}Sm	^{153}Eu	^{156}Gd
AGR-3/4 1-3	moles/compact	7.0190E-06	4.2880E-06	6.9060E-07	3.4460E-07	8.4500E-08
AGR-3/4 1-3	µg/compact	9.8903E+02	6.2568E+02	1.0492E+02	5.2697E+01	1.3175E+01
AGR-3/4 4-3	moles/compact	1.5457E-05	1.0124E-05	1.4001E-06	1.1828E-06	5.2270E-07
AGR-3/4 4-3	µg/compact	2.1780E+03	1.4772E+03	2.1270E+02	1.8088E+02	8.1500E+01
AGR-3/4 10-1	moles/compact	1.3154E-05	8.4220E-06	1.2543E-06	9.0680E-07	3.2730E-07
AGR-3/4 10-1	µg/compact	1.8535E+03	1.2289E+03	1.9055E+02	1.3867E+02	5.1033E+01
AGR-3/4 10-2	moles/compact	1.3029E-05	8.3330E-06	1.2282E-06	9.0150E-07	3.2170E-07
AGR-3/4 10-2	µg/compact	1.8359E+03	1.2159E+03	1.8659E+02	1.3786E+02	5.0160E+01

Appendix Table B-3. Calculated inventories of select radionuclides one day after EOL

Compact	Value	^{85}Kr	^{90}Sr	^{106}Ru	^{110m}Ag	^{125}Sb
AGR-3/4 1-3	moles/compact	2.9250E-07	6.4020E-06	5.2420E-07	4.8200E-10	4.5960E-08
AGR-3/4 1-3	Bq/compact	3.5972E+08	2.9414E+09	6.8116E+09	9.3237E+06	2.2038E+08
AGR-3/4 1-3	Bq/particle	1.8754E+05	1.5336E+06	3.5514E+06	4.8611E+03	1.1490E+05
AGR-3/4 4-3	moles/compact	6.1760E-07	1.3430E-05	1.8892E-06	5.1900E-09	1.1785E-07
AGR-3/4 4-3	Bq/compact	7.5950E+08	6.1705E+09	2.4549E+10	1.0039E+08	5.6511E+08
AGR-3/4 4-3	Bq/particle	3.9599E+05	3.2171E+06	1.2799E+07	5.2343E+04	2.9463E+05
AGR-3/4 10-1	moles/compact	5.3150E-07	1.1575E-05	1.4339E-06	3.1980E-09	9.7240E-08
AGR-3/4 10-1	Bq/compact	6.5362E+08	5.3182E+09	1.8633E+10	6.1861E+07	4.6628E+08
AGR-3/4 10-1	Bq/particle	3.4078E+05	2.7728E+06	9.7146E+06	3.2253E+04	2.4311E+05
AGR-3/4 10-2	moles/compact	5.2720E-07	1.1484E-05	1.4039E-06	3.0590E-09	9.5750E-08
AGR-3/4 10-2	Bq/compact	6.4833E+08	5.2764E+09	1.8243E+10	5.9172E+07	4.5914E+08
AGR-3/4 10-2	Bq/particle	3.3802E+05	2.7510E+06	9.5113E+06	3.0851E+04	2.3938E+05

Appendix Table B-3 (continued). Calculated inventories of select radionuclides one day after EOL

Compact	Value	^{134}Cs	^{137}Cs	^{144}Ce	^{154}Eu	^{155}Eu
AGR-3/4 1-3	moles/compact	2.3820E-07	7.2280E-06	3.0460E-06	3.3590E-08	1.9020E-08
AGR-3/4 1-3	Bq/compact	1.5257E+09	3.1785E+09	5.1652E+10	5.1659E+07	5.2933E+07
AGR-3/4 1-3	Bq/particle	7.9545E+05	1.6572E+06	2.6930E+07	2.6934E+04	2.7598E+04
AGR-3/4 4-3	moles/compact	1.4243E-06	1.6316E-05	6.3020E-06	1.8404E-07	6.7270E-08
AGR-3/4 4-3	Bq/compact	9.1227E+09	7.1750E+09	1.0686E+11	2.8304E+08	1.8721E+08
AGR-3/4 4-3	Bq/particle	4.7564E+06	3.7409E+06	5.5717E+07	1.4757E+05	9.7609E+04
AGR-3/4 10-1	moles/compact	9.5820E-07	1.3787E-05	5.4700E-06	1.3193E-07	4.9880E-08
AGR-3/4 10-1	Bq/compact	6.1373E+09	6.0628E+09	9.2756E+10	2.0290E+08	1.3882E+08
AGR-3/4 10-1	Bq/particle	2.7096E+06	3.1610E+06	4.8361E+07	1.0579E+05	7.2376E+04
AGR-3/4 10-2	moles/compact	9.4420E-07	1.3648E-05	5.4230E-06	1.2945E-07	4.8980E-08
AGR-3/4 10-2	Bq/compact	6.0476E+09	6.0017E+09	9.1959E+10	1.9908E+08	1.3631E+08
AGR-3/4 10-2	Bq/particle	3.1531E+06	3.1292E+06	4.7945E+07	1.0380E+05	7.1070E+04